Illinois U Library

VOLUME 46 [J. CELL. AND COMP. PHYSIOL.] NUMBER 3

JOURNAL OF CELLULAR AND COMPARATIVE PHYSIOLOGY

BOARD OF EDITORS

ARTHUR K. PARPART, Managing Editor
Princeton University

W. R. AMBERSON
University of Maryland

D. W. BRONK
The Rockefeller Institute

M. H. JACOBS
University of Pennsylvania

H. F. BLUM
National Cancer Institute

L. B. FLEXNER
University of Pennsylvania

D. MARSLAND
New York University

F. BRINK
The Rockefeller Institute

E. N. HARVEY
Princeton University

D. MAZIA
University of California

DECEMBER 1955

PUBLISHED BIMONTHLY BY
THE WISTAR INSTITUTE OF ANATOMY AND BIOLOGY
WOODLAND AVENUE AND THIRTY-SIXTH STREET, PHILADELPHIA 4, PA.

Entered as second-class matter February 19, 1932, at the post office at Philadelphia, Pa., under Act of March 3, 1879. Acceptance for mailing at special rate of postage provided for in section 1103, Act of October 3, 1917, authorized on July 2, 1918

Price, $7.50 per volume, Domestic; $8.00 per volume, Foreign

Has YOUR

Subscription Expired?

This is the closing number of

JOURNAL OF CELLULAR
AND
COMPARATIVE PHYSIOLOGY

to be published in 1955, and with it most subscriptions expire.

If you have not already renewed, do so now, so that 1956 numbers as published will reach you promptly.

Send subscriptions direct or through your agent to

THE WISTAR INSTITUTE
OF ANATOMY AND BIOLOGY
Woodland Avenue and 36th Street
Philadelphia 4, Pa.

A STATISTICAL THEORY OF MONOSYNAPTIC INPUT-OUTPUT RELATIONS

WILFRID RALL
Physiology Department, Medical School, University of Otago
Dunedin, New Zealand

EIGHT FIGURES

INTRODUCTION

This paper is concerned with the theoretical input-output relations which may be deduced for certain simplified models of a monosynaptic reflex pathway. In particular, it is concerned with theoretical relations found to be consistent with the experimental input-output results obtained for the monosynaptic reflex pathway of gastrocnemius nerve in the cat spinal cord (Rall, '55; cf. preliminary reports Rall, '51, '54).

The general features of such an input-output situation may be summarized in a few sentences. A single-shock stimulus produces an approximately synchronous input volley of impulses in a certain number of the several hundred afferent fibers stimulated. Some, but not all, of these afferent fibers distribute large numbers of presynaptic terminations directly to motoneurons of the pathway. The intensity of synaptic excitation so delivered to any one of these motoneurons depends upon the number (and perhaps the arrangement, cf. Lorente de Nó, '38; Lloyd, '45) of such active terminals received by it. The fact, that reflex discharge of any motoneuron requires an input volley involving several afferent fibers, shows that spatial summation of the excitation produced by the active terminals must be an essential feature of the process. As a result of variations in the distribution of such synaptic excitation, the various motoneurons may be expected to represent many different intensities of spatially summed excitation. The size of the monosynaptic reflex

JOURNAL OF CELLULAR AND COMPARATIVE PHYSIOLOGY, VOL. 46, NO. 3
DECEMBER 1955

output volley resulting from a given input volley is determined by the number of these motoneurons receiving at least a threshold intensity of such spatially summed excitation.

It has been found that a rather simple set of assumptions is sufficient to provide a theoretical model having input-output relations which fit those obtained experimentally; these assumptions are:

1 The number of synaptic knobs activated synchronously over the motoneuron pool represents effective input magnitude.
2 The distribution of these knobs over the motoneurons in the pool is random in terms of either (a) individual knobs, or (b) knob clusters.
3 The threshold for reflex discharge of a motoneuron may be defined in terms of either (a) the number of its knobs which must be active together upon it, irrespective of their location on its surface, or (b) a local density of active knobs corresponding to some number of knobs which must be active together within the area of some one of several possible discrete zones on the surface of the motoneuron.
4 The distribution of motoneurons with respect to their threshold values is random in the sense of being normal and independent of active knob distribution.

The possibility of interpreting the monosynaptic input-output relation in terms of "the statistical chances for effective summation" was recognized by Lloyd ('45). Statistical formulations of synaptic input-output problems have usually been concerned primarily with problems of temporal summation rather than spatial summation (cf. reviews by Householder and Landahl, '45; Rashevsky, '48; and Shimbel, '50). The present paper has, in common with that of Rosenblueth, Wiener, Pitts and Garcia Ramos ('49), the object of formulating a statistical theory designed specifically to account for synchronous monosynaptic input-output relations in terms of pure spatial summation. Although these two formulations are based upon similar considerations of elementary probability theory, there are significant differences between them (cf. Discussion), both in the assumptions made and in the conclusions reached.

Part I of the present paper defines a theoretical model of the monosynaptic reflex pathway and formulates its mathematical consequences. Part II presents the resulting families of input-output curves and compares them with experimental results; it also includes theoretical results relevant to post-tetanic potentiation and to facilitation between monosynaptic synergists. The implications of these results for hypotheses concerning spatial summation and motoneuron threshold are discussed in part III.

PART I

CONSTRUCTION OF THEORETICAL MODEL

A. Distribution of monosynaptic knobs

Monosynaptic knob. The designation, monosynaptic knob, is used to refer to those synaptic knobs which belong to the monosynaptic pathway. It is known that a significant proportion of the synaptic knobs distributed to mammalian motoneurons must belong to other pathways. The monosynaptic knobs are probably in the minority.

The monosynaptic fraction, γ. Let the symbol, γ, represent the unknown ratio between the number of monosynaptic knobs and the total number of synaptic knobs ending on the entire motoneuron pool. In some of the calculations a value of $\frac{1}{5}$ will be assumed for purposes of illustration.

Assumption of randomness in knob distribution. Two different assumptions will be considered. (a) Assume the distribution of individual monosynaptic knobs to be random in the sense that any synaptic knob chosen arbitrarily anywhere over the motoneuron pool has the same *a priori* probability of being a monosynaptic knob; this probability must then be given by the fraction γ. (b) Assume that all the synaptic knobs are distributed in clusters, and that any arbitrarily chosen cluster has the same *a priori* probability of being a monosynaptic knob cluster; this probability is also given by the fraction, γ, if the average number of knobs per cluster is assumed to be the same for monosynaptic clusters as for other clusters.

Number of synaptic knobs per motoneuron. Assume, initially, that every motoneuron has the same number of synaptic knobs. Let this number be N. Below it will be noted that a modified definition of N and γ will permit some variability in the number of synaptic knobs on a motoneuron without changing the essential results of the theory.

Number of monosynaptic knobs on a motoneuron. This number, in view of the overall monosynaptic fraction, γ, may be expected to have a most probable value of γN. However, any given motoneuron may receive, as a consequence of the random knob distribution, a number of monosynaptic knobs significantly larger or smaller than this mean value.

Binomial distribution of motoneurons. With the assumption (a) of random *individual* knob distribution, it is assumed that each of the N synaptic knobs on a motoneuron is subject to the same probability binomial, namely, an *a priori* probability, γ, of being monosynaptic, and an *a priori* probability, $1-\gamma$, of not being monosynaptic. When this probability binomial is compounded N times, one obtains an expression (the binomial, or Bernoullian distribution) which gives the probability corresponding to each possible number of monosynaptic knobs on a motoneuron. Since the same distribution of probabilities applies to each of a large number of motoneurons, it may be expected that the population of motoneurons should exhibit the corresponding binomial frequency distribution of motoneurons with respect to the number of monosynaptic knobs received.

The properties of such binomial frequency distributions are well known and discussions of them may be found in standard textbooks on the theory of statistics. With N large and γ not too small, as in the case here, the binomial distribution may be approximated quite well with the *normal (Gaussian)* distribution having the same *mean* and *variance.* The distribution considered here has a *mean* equal to γN, and a *variance* equal to $\gamma(1\text{-}\gamma)$N. Thus, for example, if N equals 500 knobs and γ equals $\frac{1}{5}$, the mean number of monosynaptic knobs per motoneuron is 100, and the *variance* is 80, implying a *standard deviation* (square root of *variance)* equal to approximately 9 monosynaptic knobs. In this example, therefore, a *normal* distribution implies that about $\frac{2}{3}$ of the motoneuron population would consist of motoneurons receiving more than 91 but less than 109 monosynaptic knobs each; motoneurons in about $\frac{1}{6}$ of the population would receive 91 or fewer monosynaptic knobs each, and those in another $\frac{1}{6}$ of the population would receive 109 or more monosynaptic knobs each.

At this point it may be noted that the number, N, need not be interpreted as the number of synaptic knobs per motoneuron. A more general model of the monosynaptic pathway may be obtained by letting N represent a number of loci (or elements of surface area) spaced fairly equally over each motoneuron. It could be assumed that only a fraction, such as 4/5, of all the loci on the pool are occupied by synaptic knobs of any kind, and that the *a priori* probability that any locus is occupied by a knob is equal to this fraction. Then the number of synaptic knobs on a motoneuron would also become a variable with respect to which the motoneuron population exhibits a binomial frequency distribution. In this way, the model would include variation between motoneurons with respect to their knob number, and also provide for non-uniform distributions of synaptic knobs on each motoneuron surface. If γ is re-interpreted as the probability that any given *locus* is occupied by a monosynaptic knob, the resulting binomial frequency distribution of motoneurons with respect to monosynaptic knob number would be the same as before.

With the assumption (b) of a random distribution in terms of knob clusters, probability considerations lead to a slightly different binomial distribution of the motoneurons. If, for simplicity, all clusters are assumed to consist of the same number of knobs, c, the *mean* of the binomial distribution will be γN/c monosynaptic clusters, or γN monosynaptic knobs, as before. The *variance* of this distribution will be $\gamma(1\text{-}\gamma)$N/c, in terms of clusters; this must, however, be multiplied by c^2 to express the *variance* in terms of knobs instead of clusters, giving $\gamma(1-\gamma)cN$. Thus, for example, if N equals 500 knobs, γ equals $\frac{1}{5}$, and c equals 4 knobs per cluster, the mean value per motoneuron is 25 monosynaptic clusters, or 100 monosynaptic knobs, as before; however, the *variance* is 20 in terms of clusters, or 320 in terms of knobs, implying a *standard deviation* equal to approximately 18 monosynaptic knobs (twice as great as before).

Both the general expressions and the illustrative examples make it clear that the variability between motoneurons, with respect to the number of monosynaptic knobs received, is greater when the knobs are distributed in clusters than when they (the same number of knobs) are distributed as individuals.

B. Distribution of monosynaptic input

The effective (monosynaptic) input delivered by an input volley to the motoneuron pool is assumed to be proportional to the number of monosynaptic knobs activated by the input volley.

The monosynaptic input fraction, β. Let the symbol, β, represent the ratio between the number of monosynaptic knobs activated by a given volley and the total number of monosynaptic knobs distributed over the motoneuron pool.

Assumption of randomness. The distribution of active knobs (or knob clusters) is assumed to be random in the sense that any monosynaptic knob (or cluster), chosen arbitrarily anywhere over the motoneuron pool, has the same *a priori* probability of being among those activated by a given input volley; this probability must be given by the fraction, β.

The variable, n. Let n represent the number of active monosynaptic knobs on a motoneuron. This number may be expected to have a most probable value of $\beta\gamma N$. However, any given motoneuron may receive, as a consequence of the random knob distribution, a number, n, which is significantly larger or smaller than this most probable value.

Distribution of motoneurons with respect to n. Consider first a particular motoneuron having γN monosynaptic knobs.

The probability distribution of n for such a motoneuron is obtained by compounding, γN times, the probability binomial, β that a monosynaptic knob is active, and $1-\beta$ that a monosynaptic knob is not active. The resulting binomial probability distribution has a mean of $\beta\gamma N$ and a *variance* of $\beta(1-\beta)\gamma N$. This *variance,* it may be noted, is zero when β equals unity, which is consistent with the fact that the total number of monosynaptic knobs on any particular motoneuron is fixed.

When the whole population of motoneurons is considered, the frequency distribution of n depends upon the variability in monosynaptic knob number as well as the variability considered just above. The resultant *variance,* equal to $\beta\gamma(1-\beta\gamma)N$, may be obtained directly by compounding, N times, the probability binomial, $\beta\gamma$ that a knob is both monosynaptic and active, and $1-\beta\gamma$ that a knob is not activated by the input volley. This result may also be interpreted as the sum of two independent variances: (i) the *variance,* $\beta(1-\beta)\gamma N$ of the previous paragraph, which would result if all the motoneurons had the same number of monosynaptic knobs, and (ii) the *variance,* $\beta^2\gamma(1-\gamma)N$, which represents the *variance,* $\gamma(1-\gamma)N$ in monosynaptic knob number, rescaled relative to a mean of $\beta\gamma N$ instead of γN.

The result is that the population of motoneurons is distributed with respect to n, about a mean value, $\bar{n}$, and with a *variance,* σ_n^2, the values of which are given by the expressions,

$$\bar{n} = \beta\gamma N \qquad (1),$$

and

$$\sigma_n^2 = \beta\gamma(1-\beta\gamma)N \qquad (2a).$$

As a numerical example, if N equals 500 knobs, γ equals $\frac{1}{5}$, and β equals 0.75, the mean of n is 75 active monosynaptic knobs per motoneuron, and the *variance* is approximately 64, implying a *standard deviation* of 8 active monosynaptic knobs; this may be compared with the mean value of 100 and the *standard deviation* of 9 active monosynaptic knobs when β equals unity.

If the same analysis is carried out for a random distribution of knob clusters with all clusters composed of the same number of knobs, c, the resulting *variance* in terms of active monosynaptic knobs is found to equal $\beta\gamma(1\text{-}\beta\gamma)cN$. This result can be applied more generally to clusters of variable size, if it is assumed that the *a priori* probability, $\beta\gamma$, is completely independent of cluster size. Then, if $\bar{c}$ represents the weighted mean value for the number of knobs in a cluster,

$$\sigma_n^2 = \beta\gamma(1\text{-}\beta\gamma)\bar{c}N \qquad (2b).$$

C. Synaptic thresholds of motoneurons

To determine how many motoneurons will be discharged by any given monosynaptic input, it is obviously necessary to define the synaptic threshold of a motoneuron, and to consider its variability.

Dependence upon spatial summation. Two different assumptions will be considered. (a) Assume that the synaptic excitation delivered to a motoneuron by a synaptic knob is the same regardless of its position on the neuron or its distance from other active knobs; then the excitation due to activity in several such knobs would be simply additive, and the threshold for discharge of a given motoneuron may be defined by the requirement that the number of active monosynaptic knobs, n, must exceed a threshold number, h, on that motoneuron. (b) Assume that effective spatial summation depends upon a fairly high density of active synaptic knobs over some portion (or zone) of the motoneuron surface; then the synaptic threshold might be defined in terms of a threshold number of knobs which must be active together within the area of some one of several possible zones on the surface of the motoneuron.

It has been found that these two definitions of synaptic threshold lead to very similar input-output relations. Since, however, it is simpler to derive the relations according to assumption (a) above, this assumption will be used in the following sections; the derivation based upon assumption (b) is given as an Appendix.

Variability of synaptic thresholds. The synaptic threshold of each motoneuron may be expected to fluctuate with time; also, the motoneurons may be expected to differ among themselves in temporal average values of these thresholds. The present model does not explore the effects of temporal fluctuation; it is intended for comparison with experimental input-output relations obtained when temporal fluctuation was reduced by anesthesia and average experimental output values were obtained for each stimulus strength.

However, differences *among motoneurons* are assumed for the synaptic thresholds of the model. Such differences could arise from several sources. One is provided by possible differences in the intrinsic excitability of the motoneurons. Another is provided by differences in the amount of facilitation or inhibition delivered to the various motoneurons by synaptic knobs representing internuncial background activity in the spinal cord. Also, actual spinal motoneurons are known to differ in their surface area, and even if their knob number were approximately proportional to their surface area, one might expect variation from such proportionality; this would correspond, in the simpler model, to an additional source of variation in synaptic threshold values.

The magnitude of these various sources of difference in synaptic threshold is unknown in actual monosynaptic pathways; however, it seems reasonable to suppose that their effects are distributed independently of each other. Thus, it will be assumed that these effects may be lumped together and treated as one *normally* distributed variability in the h values of the motoneuron population, having a *variance*, σ_h^2, of unknown magnitude. It will also be assumed that the differences between motoneurons, in respect to their synaptic thresholds (h values), are statistically independent of their differences, in respect to their active monosynaptic knob numbers (n values).

D. Distribution of motoneurons with respect to n-h

The definitions and assumptions made in the previous sections are sufficient to define a distribution of the motoneurons with respect to their values of n-h. The significance of this distribution is that all of the motoneurons having n-h values greater than zero (for any particular input magnitude) would, by definition, discharge reflexly, while those having n-h values less than or equal to zero would not discharge reflexly. Hence, knowledge of this distribution makes possible a calculation of the fraction of the model motoneuron population which would discharge reflexly in response to any given input magnitude.

By making explicit, for the model, the quite reasonable assumption, that the distribution of motoneurons with respect to their h values is statistically independent of their distribution with respect to their n values, it follows (from statistical theory) that the distribution of these same motoneurons with respect to their n-h values must have a *variance* equal to the sum of the variances of the separate distributions. Thus, using the earlier result for the *variance* of n values (equations 2a and 2b), the *variance* of n-h values, about a mean of $\bar{n} - \bar{h}$, may be written,

$$\sigma^2 = \beta\gamma(1\text{-}\beta\gamma)\bar{c}N + \sigma_h{}^2 \tag{3}$$

where $\sigma_h{}^2$ represents the synaptic threshold *variance.* As before, $\beta\gamma N = \bar{n}$, while $\bar{c}$ represents the mean number of knobs per cluster, including, of course, the case where this is equal to one (cf. equations 2a and 2b).

It may be noted that this combined *variance* is perfectly valid, whether or not the component distributions are assumed to be *normal.* However, since the *binomial* distribution with respect to n values is approximately *normal,* and the distribution with respect to h values is assumed to be *normal,* and since these two distributions are assumed to be statistically independent, it follows (from statistical theory) that the distribution with respect to n-h values is essentially *normal.* With such a *normal* distribution, it is a simple procedure to calculate the portion of the motoneuron population in which n values exceed h values, for any given set of values of $\bar{n}$, $\bar{h}$ and σ^2; this procedure is illustrated in section (E) below.

This distribution of motoneurons, with respect to n-h values, provides a specific and precise model of the now familiar qualitative notion of the various grades of subliminal and supraliminal synaptic excitation represented by the various motoneurons in a reflexly excited motoneuron pool (cf. Denny-Brown and Sherrington, '28, pages 179–180), with the qualification that only the spatial aspect of summation is included here.

Knob variability. In the model, as defined so far, all of the monosynaptic knobs have been treated as equal in the amount of synaptic excitation each delivers when active. This simplification is satisfactory in many respects; however, the consequences of assuming variability between knobs will be considered briefly.

One consequence is that the *effective* values of n, h and n-h would no longer be confined to integers; these variables would become continuous, except, perhaps, for the smallest values of n. This would give physical meaning to the use of a continuous distribution function. Of course, the mean values, $\bar{n}$, $\bar{h}$ and $\overline{n\text{-}h}$, can have non-integral values even in the simpler model.

The *variance,* corresponding to the differences between the effective and actual values of n, would have to be taken into account. On the assumption that differences between knobs are independent of their relation to β, and that knob effects are simply additive and independent of location, the *variance* in effective n value would be simply additive to that given in equation (3). Assuming simple linear addition of different knob effects, such that the combined effect of 15 average knobs would be equivalent to that of 10 superior knobs (which happen to be 1.5 times as effective as an average knob), it follows that the additional *variance,* for groups of n knobs, is n times the *variance* in individual knob effects. Thus, the *variance,* additional to equation (3) would be proportional to $\beta\gamma N$.

The magnitude, in actual monosynaptic pathways, of variability in knob effect, is unknown. A histological study of variability in knob size has been reported by Haggar and Barr ('50); they found, for motoneurons in the region of the cat spinal cord which contains the gastrocnemius motoneurons, that the mean profile area of a knob is 0.85 square micra, with a standard deviation of 0.58; thus, the *variance* in knob profile area is equal to $(0.58/0.85)^2$, or approximately 0.47, when these areas are expressed in terms of a scale on which the average profile area is unity. Although this provides a quantitative measure of knob variability, there are reasons to suspect that this might be quite different from the unknown variability in the excitatory effects of monosynaptic knobs: (i) with the mechanism of synaptic transmission still unknown, it is impossible to assess the relative importance of (a) geometric factors such as knob area, knob volume, contact area with cell body, or distance of knob from cell body, and (b) non-geometric factors such as differences in metabolic and/or electrical properties of knobs; (ii) even if knob size is the principal factor in knob effect, (a) the monosynaptic knobs, being a minority of the knob population, could easily have a significantly different variability than is found for the population as a whole, and (b) the size variability of such small and possibly labile structures could be different in a histological preparation than it is in living tissue.

Error from assuming normality. The insignificance of the error, introduced by assuming a *normal* distribution of n-h, has been verified by numerical calculation in several special cases; details will not be given here. The method takes account of skewness by calculation of the third *moment* of the combined distribution, and by using this to obtain a ''Gram-Charlier Type-A'' series expression for the combined distribution. Even when one includes the relatively large skewness found by Haggar and Barr ('50), for distribution of knob profile areas, the series expression for the combined distribution leads to results which differ, by a negligible correction term, from those obtained with a *normal* distribution.

E. Relation of output to input

Given a *normal* distribution of motoneurons with respect to n-h values, the fraction of the motoneuron population having positive n-h values may be calculated from the values of $\bar{n}$, $\bar{h}$, and σ, together with a table of the areas under a normal distribution curve. An illustration, in terms of such areas, is provided by figure 1-A, for three different values of β. The particular assumptions in this example are: $\gamma N = 100$, $\bar{h} = 80$, and $\sigma = 20$ when $\beta = 1$. For simplicity of graphical presentation, the threshold distribution is not shown separately; only the mean synaptic threshold value is shown, and the combined variability of n and h is shown as a single normal distribution of n about $\bar{n}$. In other words, the *variance* shown for n values actually represents the *variance* of n-h values.

With a maximum input volley, $\beta = 1$, $n = 100$ and $\bar{n}$-$h = 20$; with $\sigma = 20$, this means that $\bar{n}$ exceeds $\bar{h}$ by an amount equal to the standard deviation of n-h values; hence, the fraction of the motoneuron population having n values greater than their h values, indicated by the cross-hatched portion of the area under the lowermost *normal* curve shown in figure 1-A, is given as 0.84 in the appropriate mathematical tables. If the input value, β, were reduced from 1 to 0.8, the mean value of n would equal the mean value of h, and the fraction of the motoneuron population for which n exceeds h would be exactly one half; this result is independent of σ. In figure 1-A the *normal* distributions for β values of 0.5 and 0.75 are shown with only slightly smaller variance than for the case of maximum input. As indicated in the figure, the corresponding fractional pool discharge values are 0.05 and 0.40; the three pairs of input-output values of figure 1-A are shown plotted in figure 1-B, with intermediate values indicated by the continuous curve. The shape of this curve agrees well with that

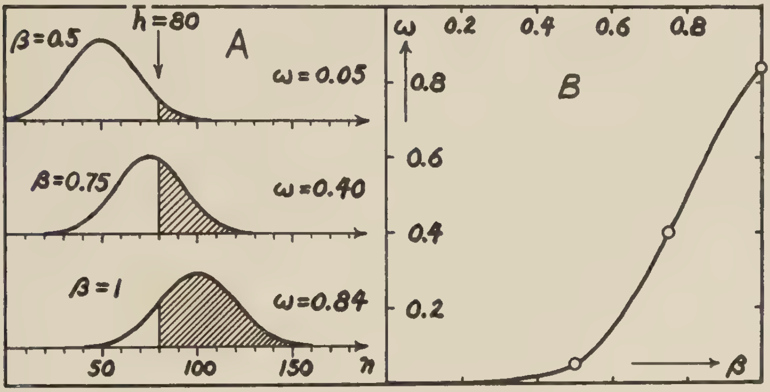

Fig. 1 Illustration of method used to obtain fractional pool discharge from the normal distribution of motoneurons with respect to n-h values.

of the experimentally derived curves of Lloyd ('45), and of Rall ('55).

Dependence of σ upon β. A value of $\sigma = 20$, when $\beta = 1$ and $\gamma N = 100$, could arise from several different combinations of the terms in equation (3). Three such combinations will be considered here, with $\gamma = 1/5$ in each case.

Let $\bar{c} = 1$; then $\gamma(1 - \gamma)\bar{c}N = 80$, and a synaptic threshold variance of 320 is required to make $\sigma = 20$ for $\beta = 1$. Then, $\beta = 0.5$ implies a combined variance of 365, or $\sigma = 19.1$; with $\bar{h} = 80$, a fractional pool discharge value of 0.06 is implied for half-maximum input.

Let $\bar{c} = 2$; then $\gamma(1 - \gamma)\bar{c}N = 160$, and a synaptic threshold variance of 240 is required to make $\sigma = 20$ for $\beta = 1$. Then, $\beta = 0.5$ implies a combined variance of 330, or $\sigma = 18.2$; with $\bar{h} = 80$, a fractional pool discharge value of 0.05 is implied for half-maximum input. This case is illustrated in figure 1-A.

Let $\bar{c} = 5$; then $\gamma(1 - \gamma)\bar{c}N = 400$, and a zero synaptic threshold variance is required to make $\sigma = 20$ for $\beta = 1$. Then, $\beta = 0.5$ implies a combined variance of 225, or $\sigma = 15$; with $\bar{h} = 80$, a fractional pool discharge value of only 0.02 is implied for half-maximum input.

The σ values, obtained above for half-maximum input, all lie between the two extreme values, 14.1 and 20, which correspond to the extreme assumptions, (i) that σ is proportional to the square root of β, and (ii) that σ is independent of β. It is a perfectly general result, that the dependence of σ upon β, implied by equation (3), must lie somewhere between these two extreme relations. The addition of knob variability would merely weight this dependence more toward a proportionality with square root of β.

Explicit recognition of these extremes is useful because the difference in the theoretical input-output results obtained for the two extremes is found to be quite small in some respects. For such cases, the relative magnitudes assumed for different sources of variability are obviously not critical.

PART II

RESULTS

A. Families of input-output curves in terms of theoretical parameters

Various families of input-output curves may be obtained by considering several values of one theoretical parameter while the values of the other theoretical parameters are held constant. A particular family, corresponding to 4 equally spaced values of h, is illustrated in the lower left-hand corner of figure 2. It has been assumed that σ is independent of β, and that the values of γ, N and σ are the same for all members of this family. For the value, $\gamma N = 100$, a value of $\sigma = 20$, together with $\bar{h}$ values of 60, 80, 100 and 120, would satisfy this family of curves. However this particular set of values is not unique; for any given value of γN, it can be shown, that a value of $\sigma = \gamma N/5$, together with $\bar{h}$ values of 3σ, 4σ, 5σ, and 6σ, would also satisfy this family of curves. This is a consequence of the fundamental fact, that each input-output curve is determined by the values of only two independent theoretical parameters, such as $\gamma N/\sigma$ and h/σ. A demonstration of this fact follows, together with a development of its consequences for other families of input-output curves.

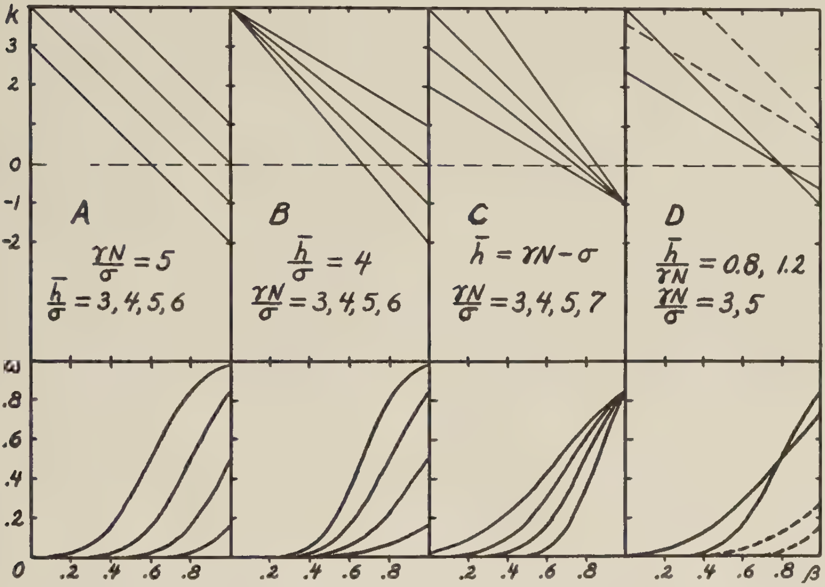

Fig. 2 Four families of input-output curves. Values assumed for the theoretical parameters are stated in center of figure. Lower part of figure shows curves relating output (ω) to input (β); upper part of figure shows the corresponding linear relations between k and β.

For any combination of values of β, γ, N, σ and $\bar{h}$, the fractional pool discharge is given by the fraction of the area under a standard *normal* curve for which a critical deviation, $k = (\bar{h} - \bar{n})/\sigma$, is exceeded. The value of this fraction may be defined mathematically as the definite integral, from k to plus infinity, of the standard *normal* density function. This definite integral is a function of k only, and whether one prefers to think in terms of the definite integral, or simply in terms of tabulated values of areas under the *normal* curve, the significance of this is, that any particular value of k is sufficient to specify, uniquely, a particular value of fractional pool discharge. From this, it follows that each input-output curve (or family of such curves) corresponds uniquely to a particular k versus β relation (or family of such relations). Thus, the dependence of input-output families upon the values of theoretical parameters may be investigated indirectly in terms of the simpler k versus β relations.

Using the relation, $\bar{n} = \beta\gamma N$ (equation 1), the critical deviation, k, may be written,

$$k = \bar{h}/\sigma - \beta(\gamma N/\sigma) \qquad (4).$$

With the slightly simplifying assumption that σ is independent of β, equation (4) defines a linear relation between k and β. This depends, of course, also upon assuming h, γ and N to be independent of β; there is, however, no reason to assume otherwise. An advantage of this linearity is that the dependence of the k versus β relation, upon only two independent theoretical parameters, is made obvious; also, the families of k versus β relations are very simple. Since only two points, or one point and a slope, are required to determine a straight line, the members of any family of straight lines, for which the value of one parameter is the same, must either (a) all be parallel to each other, or (b) all intersect in a common point. Four different families of this kind are illustrated in the upper half of figure 2; the corresponding families of input-output curves are illustrated in the lower half of the same figure.

The values of the theoretical parameters assumed in constructing the families of figure 2 are shown in the middle portion of the figure. It may be recalled that γN, the average number of monosynaptic knobs per motoneuron, represents a structural constant of the monosynaptic pathway; hence, for any given pathway, γN is not a variable, and both $\bar{h}$ and σ may be expressed relative to γN.

In the case of family (A), σ is constant relative to γN, and there are 4 values of $\bar{h}$ relative to σ, or to γN. The k versus β family consists of parallel straight lines. The input-output family consists of curves which differ from each other simply by translation with respect to their β coördinates; in other words, for any output value, the difference in the β value of neighboring curves is always the same (0.2 in this case). These curves are all segments of the sigmoid curve obtained from stepwise integration of *normal* distribution functions having the same standard deviation; they differ in the (cut-off) point, where the integration stops with attainment of maximum input. It may be noted that such input-output curves are nearly linear over the range of output values from 0.2 to 0.8 of total pool discharge. The relation between the members of this family of curves resembles closely the relation found in the experimentally derived family of input-output curves reported elsewhere (Rall, '55, '51). A plot of this experimentally derived family, in terms of k versus β values, is given below, in figure 4, and will be discussed in the next section.

Family (B), in figure 2, differs from family (A) in that σ does not remain constant relative to γN. Here, $\bar{h}$ and σ are assumed to vary together in direct proportion; the constant theoretical parameter is the ratio, $\bar{h}/\sigma$. As shown in figure 2-B, the k versus β family consists of straight lines which intersect at the k intercept for $\beta = 0$. Correspondingly, the input-output family consists of curves which tend to focus at a common threshold input value. As in family (A), these curves are segments of the *normal* distribution integration curve, but, here, each curve corresponds to a different standard deviation. For convenience in comparison, the intercept values at $\beta = 1$, have been matched in families (A) and (B).

In contrast with family (B), family (C) has been constructed to provide a comparison of different $\gamma N/\sigma$ values with a constant intercept value for $\beta = 1$. As in family (B), these curves are segments of the *normal* distribution integration curve, each with a different standard deviation. This family of curves is useful for evaluating the fit of a particular theoretical curve to a set of experimental points in which the maximum output value is the most accurately known.

Both (B) and (C) illustrate the effect of changing σ relative to γN; however, in neither case is the value of $\bar{h}$ constant relative to γN. This requirement is met in (D), for two values of $\bar{h}$. In both cases, the pair of k versus β lines intersect at a point defined by $k = 0$ and $\beta = \bar{h}/\gamma N$. Similarly, the two pairs of input-output curves intersect at a point defined by 0.5 output and $\beta = \bar{h}/\gamma N$. These curves are also segments of the *normal* distribution integration curve; two standard deviations are represented.

Returning to a consideration of type-(A) families, figure 3-A illustrates the way in which the members of such a family of curves differ from each other, when the points, representing the same fraction of maximum output of each curve, are compared. The comparison is aided, in figure 3-A by the 4 dashed-line curves which connect the points representing 75%, 50%, 30%, and 10% of the maximum output on each curve. It is obvious that the members of such a family of curves would not superimpose as a single curve when each is scaled relative to its maximum value. Experimental families of curves with which such superimposition is successful, may be expected to resemble family (B) of figure 2 more closely than family (A).

A theoretical family of curves can be constructed to intersect at any desired point; such a point may lie inside or outside the normal range of input and output. If the desired point is specified by $\beta = \beta^*$ and $k = k^*$, the requirement that this point be common to all members of a family of curves is satisfied by the following relation,

$$h = \sigma k^* + \gamma N \beta^* \qquad (5).$$

When this relation is satisfied, it implies that $\bar{h}$ is linearly related to σ, with a slope equal to k^*. For a family of curves intersecting at a small value of output, the value of k^* must be positive, and equation (5) implies a minimum value of h corresponding to a minimum value of σ; it does not predict that a single minimum value of $\bar{h}$ could account for the intersection of a family of curves at a common reflex threshold.

Although equation (5) implies a definite relation between $\bar{h}$ and σ, it may be noted that the theoretical model, as defined in Part I, does not provide such a relation; it only provides a relation between σ and the *variance* of synaptic thresholds (equation 3). Remembering that synaptic thresholds, as defined, include differences between motoneurons, in respect to the background of internuncial inhibition and facilitation they receive, it seems reasonable to suppose that a positive correlation between $\bar{h}$ and σ (as implied by positive k^* values in equation 5), could arise from changes in the magnitude of inhibitory background distributed randomly over the pool; similarly, a negative correlation between $\bar{h}$ and σ (as implied by negative k^* values in equation 5), could arise from changes in the magnitude of facilitatory background distributed randomly over the pool. If changes in the magnitude of facilitation or inhibition are not distributed randomly over the pool, the relation between σ and h would depend upon the

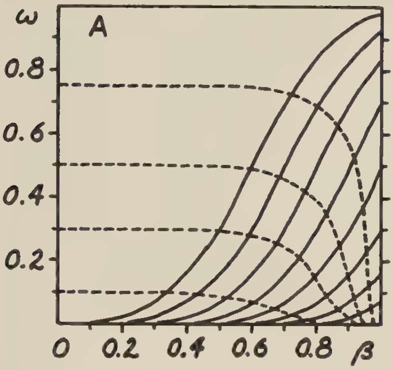

Figure 3a

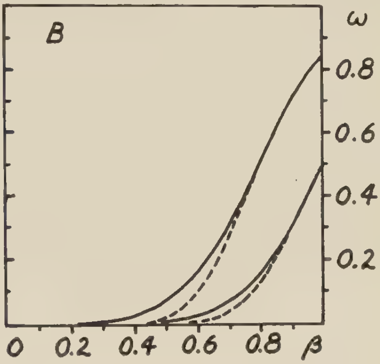

Figure 3b

Fig. 3a Family of input-output curves with $\gamma N/\sigma = 5$, and $\bar{h}/\sigma$ values from 3 to 6.5 in steps of 0.5. Each dashed-line curve is a locus of points representing a certain percentage (10%, 30%, 50% or 75%) of the maximum output value obtained in each input-output curve.

Fig. 3b Affect of assuming σ proportional to the square root of β. Dashed-line curves assume $\sigma = (\gamma N/5)\sqrt{\beta}$, while continuous curves assume $\sigma = \gamma N/5$.

pattern of such distribution. In the special case where $\bar{h}$ is changed without changing σ, we return to a family of type (A), in figure 2.

Effect of assuming σ proportional to square root of β. The simplifying assumption, that σ is independent of β, has been used in most of the considerations so far. The resulting errors may be evaluated by considering the consequences of the simple, and overcompensating assumption, that σ is proportional to the square root of β. If we write, $\sigma = \sigma_m (\beta)^{\frac{1}{2}}$, equation (4) becomes,

$$k = (\bar{h}/\sigma_m)(\beta)^{-\frac{1}{2}} - (\gamma N/\sigma_m)(\beta)^{+\frac{1}{2}} \qquad (6).$$

First, it may be noted that the relation between k and β, although not linear, is dependent upon two theoretical parameters, $\bar{h}/\sigma_m$ and $\gamma N/\sigma_m$. Secondly, these k versus β relations do not deviate very significantly from linearity over the range of values, β greater than 0.5; this is illustrated, for example, by the dashed-line curves in figure 4. Finally, the effect on the shape of the input-output curves is illustrated by the dashed-line curves in figure 3-B. The essential change is a reduction in curvature for the smaller input values. This change may be compensated approximately by increasing the value of σ_m. Also, as is indicated by the differences between members of family (C) of figure 2, the effect shown in figure 3-B may be approximated by a smaller value of σ, assumed independent of β.

B. Comparison with experimentally derived input-output family

The points, shown as circles and triangles in figure 4, have been plotted to represent the k and β values which correspond to the family of experimental input-output results reported elsewhere (Rall, '55, figs. 2 and 6; also Rall, '51). The experimental basis for estimation of effective monosynaptic input values and fractional pool discharge values has been discussed in some detail in the experimental report. Here, I simply restate two points: (i) although the relation between β values and actual experimental input volley measurements could not be accurately determined, the *same* estimated relation was used to obtain all of the β values shown in figure 4, and (ii) although the fractional pool discharge values were not precisely known as absolute values, their relative values are accurate, and their absolute values are consistent with the post-tetanic potentiation observed.

Inspection of figure 4 shows that each of the 4 sets of points is reasonably consistent with a linear relation between k and β. The 4 straight lines have all been drawn with the same slope, corresponding to $\sigma = \gamma N/5$. The 4 dashed-line curves were calculated with $\sigma = 0.23\gamma N\sqrt{\beta}$. Although the experimental points agree very slightly better with the dashed-line curves, a calculation of the root-mean-square (r.m.s.) value of the two sets of deviations indicates that the difference between the two fits is not significant (cf. figure legend). Thus, this particular family of experimental results does not provide evidence sufficient to determine the true dependence of σ upon β; it does, however, illustrate the utility of the simplifying assumption that σ is independent of β.

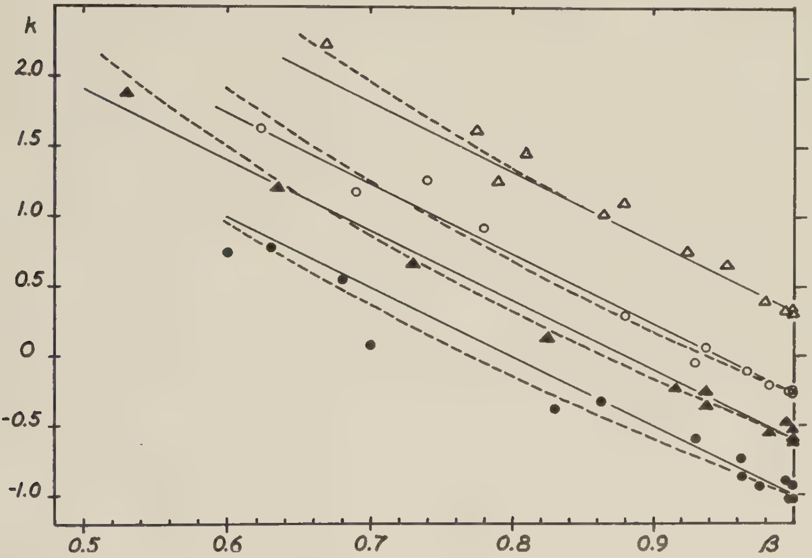

Fig. 4 Comparison of experimental input-output results with theoretical k versus β relations. The straight lines correspond to $\sigma = \gamma N/5$. The dashed lines correspond $\sigma = 0.23\,\gamma N\ \sqrt{\beta}$. With equal weighting, the root-mean-square deviation of the 50 experimental points is 0.114 in terms of k, relative to the straight lines, and 0.098, in terms of k, relative to the dashed-line curves. The difference, 0.016, is not significant when compared with a predicted standard error of 0.015.

Quite apart from the question of linearity, however, a significant feature of figure 4 is provided by the agreement of the experimental points with essentially parallel k versus β slopes; hence, this experimental family resembles a theoretical family of type (A) in figure 2. This implies that the 4 sets of experimental points correspond to 4 different $\bar{h}/\sigma$ values, together with an essentially constant $\gamma N/\sigma$ value. Although it was expected that increased depth of nembutal anesthesia would correspond to an increase in the synaptic thresholds of motoneurons, it was not obvious, *a priori,* that the *variance* of n-h values in the motoneuron pool would remain essentially unchanged (the predictions for tetanic conditioning are considered in the next section). It may be noted that the experimental points in figure 4 are not inconsistent with a slight decrease in σ with increase in $\bar{h}$; such a correlation could result from a decrease of internuncial facilitatory background with increased depth of anesthesia. Further study of the correlation between σ and $\bar{h}$ under these, and other experimental conditions, is required. However, in the case of figure 4, it is a good first approximation, that the differences between the 4 input-output relations can be accounted for in terms of the values of a single theoretical parameter.

A particular relation between β and the experimental measurements of the input volleys had to be assumed in the construction of figure 4; the particular relation used must be regarded as hypothetical. Only approximate, and indirect experimental support was provided by ventral root synaptic potential measurements and monosynaptic facilitation experiments. One safeguard, however, is provided by the fact that the same relation was assumed for all 4 sets of results in figure 4. It is conceivable that the linear aspect of the results in figure 4 could result partly from a fortuitous choice of a particular relation between β and experimental input. It should be added, however, that this particular relation is not unique in yielding approximate linearity between k and β. There are many similar hypothetical relations which would also yield such linearity for values of β greater than 0.6; these similar relations satisfy the requirement that the (1-β) values for any one of them must be proportional with the corresponding (1-β) values of any other, over the range, β greater than 0.6. The resulting slope of the k versus β relations would be slightly different in each case; it seems possible that the $\gamma N/\sigma$ value could be as small as 4 or as large as 7, cf. family (C) in figure 2.

C. Post-tetanic potentiation of output

Since the experimental points shown as filled circles and triangles in figure 4 represent input-output data obtained with tetanic conditioning (cf. Rall, '55, for details), this figure indicates that the effect of tetanic conditioning may be represented as a decrease in the value of $\bar{h}$ while the value of σ remains essentially unchanged. At first glance, this might seem surprising because tetanic conditioning has been shown to enhance the synaptic excitatory effectiveness of the conditioned pathway rather than to increase the excitability of the motoneurons (Lloyd '49; Eccles and Rall, '51). However, it can be shown that an increase in the effect of the active knobs, together with an associated increase in σ is theoretically equivalent to a decrease in $\bar{h}/\sigma$, with the effective value of $\gamma N/\sigma$ unchanged.

The appropriate theoretical treatment of post-tetanic potentiation would seem to involve the assumption that each of the conditioned synaptic knobs is more effective than normal. If the conditioned knobs are, on the average, r times as effective as normal, then the average *effective number* of active knobs per motoneuron will be increased from $\beta\gamma N$ to $r\beta\gamma N$. This, however, is equivalent to a change in the scale on which active knob number is expressed, and consequently, the value of σ must also be increased to $r\sigma$; (strictly, this increase applies only to the *variance* of n values, and not to the *variance* of h values; it is an oversimplification to apply it simply to the variance of n-h values). Thus, when the linear dependence of k upon β (equation 4) is examined, the slope remains the same, and the value of $\bar{h}/\sigma$ is reduced. Thus, in the expression for k,

$$k = (\bar{h} - r\beta\gamma N)/r\sigma = \bar{h}/r\sigma - \beta(\gamma N/\sigma) \qquad (7).$$

This formulation receives quantitative support from the experimental results shown in figure 4, because closely similar r values can account for significantly different factors of output potentiation. For the parallel straight lines, an r value of 1.19 accounts for the shift from open circles to filled circles, while an r value of 1.21 accounts for the shift from open triangles to filled triangles; for the dashed-line curves, the corresponding r values are 1.22 and 1.25. Each pair of r values agrees within two or three per cent; however, the corresponding factors of output potentiation with maximum input volleys, were 1.4 for circles, and 1.95 for the deeper level of anesthesia shown as triangles; when $\beta = 0.8$, the corresponding factors of output potentiation were 2.2 for circles and 3.8 for triangles. This theoretical result thus provides a quantitative basis for explaining the familiar observation that identical tetanic conditioning routines produce larger factors of output potentiation in cases of smaller reflex control levels.

Figure 5 illustrates the theoretical relation between fractional pool discharge (as ordinate) and factor of output potentiation (as abscissa) over a wide range of values represented on a logarithmic scale. The pair of continuous curves differ by an r factor of 1.2; the pair of dashed-line curves differ by an r factor of 1.5, corresponding to more severe tetanic conditioning; both pairs of curves were calculated with $\gamma N/\sigma = 5$ and $\beta = 1$. The points shown as crosses represent experimental values obtained with brief tetanic conditioning and fractional pool discharge estimation, as reported elsewhere (Rall, '55). If this agreement survives further testing, it provides the basis for a simple and convenient method of indirect estimation of fractional pool discharge.

The 4 points, shown as circles and triangles in figure 5, correspond to the 4 levels of output obtained with maximum input in the experiment of figure 4. In that experiment, only the relative values of these output magnitudes were actually measured; the fractional pool discharge values were estimated from the post-tetanic potentiation. Figure 5 shows that these estimated values are consistent, not only with each other, but also with the other experimental points shown as crosses. Test calculations, based upon this criterion of consistency, indicate that the fractional pool discharge values assigned to the circles and triangles are unlikely to err by more than 5%.

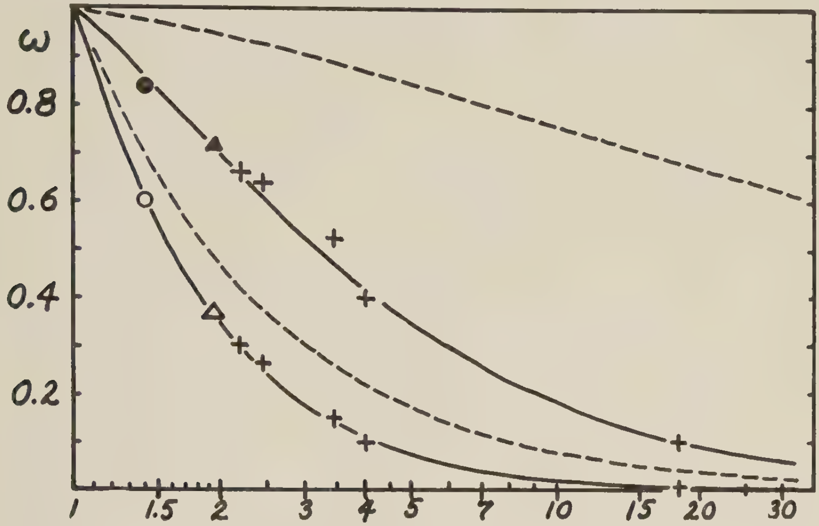

Fig. 5 Post-tetanic potentiation. Relation between fractional pool discharge level (ordinate) and the factor of output potentiation (on logarithmic scale). The continuous curves correspond to r = 1.2; the dashed-line curves correspond to r = 1.5 (see text). For any given factor of output potentiation, the lower curve gives the fractional pool discharge value for the unpotentiated output, and the upper curve gives the fractional pool discharge value for the potentiated output.

An r value of 1.2 appears to correspond to the brief potentiation which follows such brief conditioning as 50 maximal input volleys at a frequency of 400 per sec. (cf. brief tetani of Eccles and Rall, '51). Jefferson and Benson ('53) used much more severe tetanic conditioning; an r value of about 1.5 appears to correspond approximately to some of their results. The fact, that theoretical curves, such as those in figure 5, can be calculated for several different r values, suggests the desirability of further quantitative experimental results, obtained with several different standardized conditioning procedures.

D. Monosynaptic synergy

The fact that monosynaptic synergists display very effective cross-facilitation and little or no cross-discharge (Lloyd, '43b, '46b) has been used as an argument against the simple neuron threshold concept based upon the total number of active knobs distributed anywhere on the neuron surface. It is, therefore, of interest to test the sufficiency of a theoretical treatment of monosynaptic synergy based upon such a simple assumption.

Consider a pair of monosynaptically synergic motoneuron pools, (1) and (2), distinguishable by the fact that motor axons from pool-1 innervate muscle-1, and motor axons from pool-2 innervate muscle-2. When both afferent nerves (which will be designated (1) and (2) according to the muscles from which they arise) conduct maximum afferent volleys together, the average number of active knobs per motoneuron is γN in both pools; assume, for example, $\gamma N = 100$. Assume also, that a maximum volley in afferent nerve-1 activates an average of 90 of these knobs per motoneuron in pool-1, and an average of only 10 knobs per motoneuron of the synergic pool-2. This simple assumption, together with the assumption of a constant value of $\sigma = 20$, implies that the k value, for maximum stimulation of both nerves, must be 0.5 less than the k value for pool-1, when only afferent nerve-1 is stimulated. Resulting pairs of ω values predicted for these two situations at different levels of reflex excitability are: 0.84 and 0.69; 0.60 and 0.40; 0.50 and 0.31; 0.25 and 0.12. Such values are reasonably consistent with experimental findings (unpublished observations of mine; also Jefferson and Benson, '53, pp. 386–387).

With such assumptions, it is possible to predict theoretical input-output relations for various combinations of synergic input. Explicit expressions for the k values in the two pools may be written,

$$k_1\sigma_1 = \bar{h}_1 - (\beta_1\gamma_{11} + \beta_2\gamma_{21})N,$$

and

$$k_2\sigma_2 = \bar{h}_2 - (\beta_2\gamma_{22} + \beta_1\gamma_{12})N \qquad (7),$$

where, if the simplifying assumption of synergic symmetry is made, the numerical values, $N = 500$, $\gamma_{11} = \gamma_{22} = 0.18$, and $\gamma_{21} = \gamma_{12} = 0.02$, may be used for illustration. Together with the numerical assumptions, $\sigma = 20$ and $h = 90$, this system implies input-output relations such as those shown in figure 6.

This figure shows the dependence of fractional discharge in both pools upon the value of β_1, for the three different cases defined by $\beta_2 = 0$, $\beta_2 = 1$, and $\beta_2 = \beta_1$. The case where both inputs are increased together, shown as a dashed-line curve in both pools, is equivalent to the results found earlier when a single homogeneous system was assumed. In pool-1, the two cases $\beta_2 = 0$ and $\beta_2 = 1$, differ simply by translation with respect to the β_1 coordinate; the amount of the translation is 0.11, which is the value of the ratio, γ_{21}/γ_{11}; this represents the effect of a constant amount of facilitation. In pool-2, the case, $\beta_2 = 0$ represents the absence of "cross-discharge," while the case, $\beta_2 = 1$, represents the essentially linear increase produced by graded "cross-facilitation."

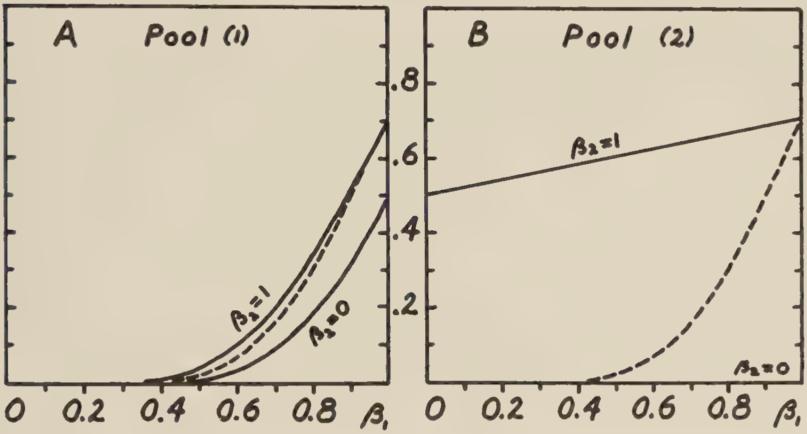

Fig. 6 Simple monosynaptic synergy. In synergic pools (1) and (2), the continuous curves show the dependence of output upon β_1, when $\beta_2 = 0$, and when $\beta_2 = 1$; the dashed-line curve shows the case where $\beta_2 = \beta_1$.

Although the facilitated output in pool-2 increased linearly with β_1, it is important to note that this linearity will be obscured in experiments where the reflex is recorded from a ventral root containing significant representation of both motoneuron pools. This complication is illustrated in figure 7. In (A), two-thirds of the relevant axons are assumed to be a representative sample from pool-1, and one-third from pool-2; in (B), this assumption is reversed. The non-linearity of the relation between facilitated output and β_1 is clearly shown by the theoretical results, in figure 7. This source of non-linearity is of particular significance in experiments which attempt to estimate the relation of β to the experimental

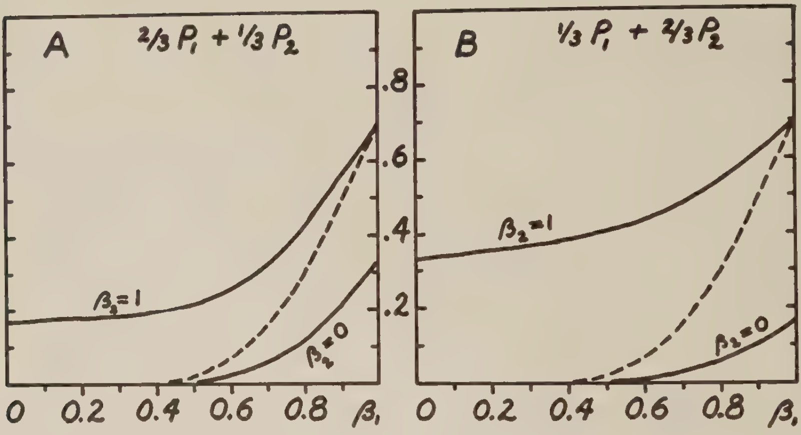

Fig. 7 Synergic input-output relations when both pools are represented in the ventral root. Construction based upon figure 6 (see text).

input volley, from the results of experiments with graded facilitation. The correction indicated for one such experiment (Rall, '55 inset of fig. 4) was based upon these considerations. Obviously, the best solution to this problem is to obtain a reflex measurement which gives the response of only one pool.

Although this very simple model of monosynaptic synergy provides approximate agreement with a number of different experimental results, further testing will be required to investigate the ratio between heterosynaptic and homosynaptic knobs, the possible difference in σ for the distribution of these two groups of knobs, and, finally, the sufficiency of such simple assumptions over a wide range of conditions.

PART III

DISCUSSION

A. Spatial summation and motoneuron threshold

It is a significant feature of these theoretical results, that a simple threshold definition has been shown to be sufficient for the prediction of various relations which were previously assumed to be incompatible with such a simple definition. The assumed insufficiency of a threshold, defined in terms of the *number* of knobs required to be active at the same time on a motoneuron, has been used as an argument in favor of a *zonal* concept of spatial summation and motoneuron threshold (Lorente de Nó, '38, '39; Lloyd, '45, '46a,b). According to this *zonal* concept, threshold stimulation of a motoneuron is assumed to take place whenever all, or at least the majority, of the knobs at a discrete zone of the neuron are activated within a very short interval of time.

Lorente de Nó based his zonal theory partly upon his observation, in the oculomotor preparation, that a large presynaptic volley may be reflexly ineffective, while a few of the impulses contained in this volley, when combined with subliminal afferent impulses from another source, may be capable of producing a reflex discharge. This interesting observation does not seem to be incompatible with the simpler definition of motoneuron threshold. With either threshold definition, it seems sufficient to assume that the first afferent source distributes knobs fairly evenly over a large motoneuron pool, while the second afferent source distributes its knobs preferentially to a small group of motoneurons within the large pool. The difference in the two cases would seem to lie only in whether one assumes that the preferential distribution of knobs must be preferential in a zonal clustering sense, or simply in terms of more knobs per motoneuron of this smaller pool. Lorente de Nó's valuable histological studies of interlacing clusters of synaptic knobs would seem also to be compatible with either threshold definition; the same knob clusters, which contribute to the zonal knob density of a motoneuron, must also contribute to the total knob number on that motoneuron. The form of the relation between "discharge zone" and "excited zone" (Lloyd, '45, '46a) is very similar to the form of the input-output relations given in figures 1 and 2 of the present paper; this form, therefore, does not provide evidence against the simpler threshold definition. Also, the contrast between significant "cross facilitation" and insignificant "cross discharge" between monosynaptic synergists (Lloyd, '46b), does not appear to require the zonal hypothesis for explanation (cf. section D of Results in the present paper).

It should be emphasized that this demonstration of the sufficiency of the simpler threshold definition, in several situations, does not disprove the zonal concept of spatial summation. On the contrary, it seems reasonable to suppose that the group of motoneurons, which happens to receive the largest number of active knobs per motoneuron, would also be the most likely to attain, by chance, a region of high active knob density. In fact, a modified zonal theory, given in the Appendix, indicates that the input-output predictions, based upon chance attainment of high zonal active knob density, are very similar to those based upon the simpler assumption. Thus, the sufficiency of the simpler assumption appears to imply the sufficiency of the modified zonal assumption.

The success of the basic assumption of randomness, in the distribution of monosynaptic knobs, deserves brief comment. This randomness can hold only in the narrow sense of randomness in the details of distribution within a functionally homogeneous reflex system; for example, already in the consideration of monosynaptic synergy, it was necessary to assume that each pool receives a larger portion of its monosynaptic knobs from afferent fibers in its homonymous nerve than from afferent fibers in the synergic nerve. The randomness assumption provides a means of dealing with our ignorance concerning the particular selection of monosynaptic knobs activated as the result of different increments in the strength of electric stimulus to the afferent nerve. The statistical approach is successful because the experiments are concerned with reasonably homogeneous populations of knobs and motoneurons, in which the individuals are not distinguished from each other.

The spatial electrotonic decrement of subliminal synaptic stimulation was also cited by Lorente de Nó ('38, '39; cf. also Eccles, '39, '46, and Lloyd, '45, '46a,b) in support of the zonal concept of spatial summation. He considered the spatial decrement to be so high that effective summation would not take place with impulses delivered to knobs located at distances from each other greater than the distances between the knobs from any fiber. However, a mathematical consideration of passive electrotonic spread on a closed (spherical) membrane surface having the approximate size of a motoneuron soma (Rall, '53; full report in preparation), indicates that the spatial decrement in a distribution of purely passive electrotonus may be expected to disappear with a time constant of the order of one microsecond; consequently, the spatial decrement of passive electrotonus surrounding a sharply focussed local response could be significant only as long as the local response activity continues to draw significant current from surrounding areas. The passive electrotonic potential due to several synchronously active foci would be essentially uniform by the time it reached peak value. Since superimposed passive electrotonic potentials are simply additive, a simple *number* definition of threshold should be expected, if the *activity* of the foci could be assumed to remain unaffected, either by the activity of neighboring foci, or by the electrotonic potential. If one were to assume, for example, that synaptic stimulation becomes critical when peak activity in several foci is superimposed upon an electrotonic potential of critical magnitude, asynchronism between the instants of peak activity would tend to make the *number* of active foci a sufficient criterion of threshold; a dense group of foci would have to be highly synchronous in order to gain a zonal advantage; even then, the uniformly distributed component of electrotonic potential would tend to be larger than the component having spatial decrement. However, if one assumes a mutual enhancement in the intensity of activity in neighboring foci, the advantage of a zone of high density becomes increased. These alternatives are all hypothetical; their significance is that a consideration of spatial decrement does not lead to an unambiguous conclusion for or against the possibility of zonal advantage; however, the extreme zonal assumption, implying no addition in the effects of widely separated foci, would seem to be incompatible with these considerations.

It may be concluded that neither the experimental input-output relations, nor speculations concerning spatial decrement, force the abandonment of the simple *number* concept of spatial summation and motoneuron threshold. Both the simple definition, and a modified zonal definition of threshold (Appendix) have been found sufficient to account for experimental input-output results obtained with populations. Although an extreme zonal concept of spatial summation now appears to be improbable, further evidence will be required to determine whether there are situations in which the simple *number* concept is less sufficient than a modified zonal concept in accounting for experimental observations.

B. The assumptions of an earlier statistical theory

The theory of the present paper was begun independently of that by Rosenblueth et al. ('49); however, since it is being published considerably later, an opportunity is provided for a brief consideration of differences in assumptions.

Rosenblueth et al. defined neuron threshold in terms of the number of active afferent fibers with which a neuron must be in contact. This is not equivalent to a definition in terms of active knob number; for example, one neuron might, by chance, receive only 15 knobs from 10 afferent fibers, while another might receive 50 knobs from 5 afferent fibers. Hence, this threshold definition would seem to correspond neither to the zonal concept nor to the simple number concept of spatial summation and motoneuron threshold.

In order to obtain agreement between their theory and experiment Rosenblueth et al. found it necessary to relax their initial assumption of a constant threshold value for all neurons. Instead of assuming a random threshold variation, however, they used special threshold distributions involving the assumption of as many as *thirty* parameters to ensure an adequate fit; these parameters were "introduced in a very special and restricted way." The necessity for these parameters is at least partly explained by their erroneous assumption, that their maximum experimental output represented complete pool discharge, and their arbitrary assumption, that effective input is a linear function of experimentally measured input from zero up to the input value giving a maximum output value.

Rosenblueth et al. assumed a random distribution of synaptic knobs, meaning "the probability that a given afferent is connected with a specific efferent cell is the same for all afferents and efferents." They added the incompatible assumption, "that each efferent neuron is in contact with the same number, n, of independent afferents." It is known that the segmental monosynaptic pathway represents a non-functional combination of several distinct pathways (Lloyd, '43); hence, their formulation of the randomness condition cannot hold for the entire segmental pathway. However, overlooking this difficulty, the assumption of randomness for such large numbers of afferent fibers would imply that the number of afferent fibers in contact with an efferent neuron is a variable having a Poisson-Exponential distribution with a *mean* and *variance* equal to n. Thus, when they assumed n constant with a value of 29, they neglected a standard deviation of over 5 in the value of n. (It may be added that their assumption of constant n could have been avoided; there is also a Poisson-Exponential distribution, having a *mean* and *variance* equal to nx, for the variable which expresses, in their notation, the number of *active* afferent fibers with which an efferent neuron is in contact).

The 4 basic assumptions of the present paper are stated in the third paragraph of the introduction, and in the summary. An essential difference from the theory of Rosenblueth et al. is provided by the focus of attention upon the number of monosynaptic knobs active on a motoneuron, rather than upon the number of active fibers with which it is connected, and by the assumption that motoneuron thresholds have a simple *normal distribution.* The resulting demonstration, that the values of two independent theoretical parameters suffice to define a very large variety of input-output curves, and that adjustment of the values of one of these parameters is sufficient to provide reasonable agreement with an experimental family of input-output curves, must cast doubt upon the special threshold distributions deduced by Rosenblueth et al.

SUMMARY

A statistical theory of monosynaptic input-output relations has been developed for an abstract model of the monosynaptic reflex pathway. This model is based upon four assumptions:

(1) the number of synaptic knobs activated synchronously over the motoneuron pool represents effective input magnitude;

(2) the distribution of these knobs over the motoneurons in the pool is random in terms of either (a) individual knobs, or (b) knob clusters;

(3) the threshold for reflex discharge of a motoneuron may be defined in terms of either (a) the number of its knobs which must be active together upon it, irrespective of their location on its surface, or (b) a local density of knobs which must be active together within some zone on the surface of the motoneuron;

(4) the distribution of motoneurons with respect to such threshold values is random in the sense of being normal and independent of active knob distribution.

The relation between the effective input magnitude and the resulting monosynaptic reflex output, expressed as fractional motoneuron pool discharge, is found to depend upon the values of only two independent theoretical parameters. These two parameters may conveniently be interpreted as (a), the average motoneuron threshold for monosynaptic excitation, and (b) the standard deviation of the motoneuron population with respect to the distribution of net motoneuron excitation (n–h); both are expressed relative to the overall average number of monosynaptic knobs per motoneuron of the pool.

Families of input-output curves, predicted for different combinations of these two parameters, are illustrated in figure 2; also shown in this figure are the linear relations (k versus β) which correspond to these input-output curves.

Good agreement between an experimental family of input-output results and a theoretical input-output family, is illustrated in figure 4. This agreement indicates that the effect of increased nembutal anesthesia upon the input-output relation is equivalent to an increase in motoneuron thresholds without significant change in the other theoretical parameter.

Post-tetanic potentiation of monosynaptic reflex output is successfully represented in the theory as resulting from an increase in the synaptic excitation delivered by the knobs which have been tetanically conditioned. Good agreement is obtained with the experimental observation, that the same conditioning procedure is responsible for very different factors of output potentiation, at different levels of fractional pool discharge; experimental examples of this are compared with theoretical predictions in figure 5.

A simple theory of monosynaptic synergy is defined and found to provide approximate agreement with experimental observations regarding absence of ''cross-discharge,'' in spite of effective ''cross-facilitation'' between monosynaptic synergists. In this simple theory, it is found sufficient to assume that each of the synergic pools receives the majority of its monosynaptic knobs from its homonymous afferent nerve, and a smaller number of monosynaptic knobs from the synergic afferent nerve.

It is concluded that the simple knob number concept of spatial summation and motoneuron threshold is *no less* sufficient, than is a modified zonal concept, in accounting for experimental input-output results so far obtained with motoneuron populations.

The author wishes to thank the Medical Research Council of New Zealand for the cost of publication.

APPENDIX

Approximate theory for zonal motoneuron thresholds

Suppose that a high local density of active knobs is required for reflex discharge of a motoneuron, and suppose that this threshold requirement may be expressed in terms of a critical *number* of monosynaptic knobs which must be active together within any one of several possible surface zones. Consider, for example, surface zones defined by approximately circular boundaries enclosing surface areas equal to one-fifth the surface of the motoneuron soma and proximal dendrites. Then, the assumption of a completely random distribution of synaptic knobs implies that the most probable number of monosynaptic knobs to be found active together in an arbitrarily chosen zone is equal to $\beta\gamma N/5$; the probability distribution has a *variance* of $\beta\gamma(1-\beta\gamma)N/5$, about this mean. This binomial distribution permits a calculation of the probability, p, that an arbitrarily selected zone receives more than any specifed number, h, of active monosynaptic knobs. Using the *normal* approximation to the binomial distribution, this probability, p, is equal to the definite integral, I(k), of the *normal* distribution function, for zonal $(h\text{-}n)/\sigma$ values from k to infinity. This probability, however, is considerably smaller than the required probability for motoneuron discharge. Reflex discharge of any given motoneuron depends, not upon an arbitrarily selected zone, but upon that particular zone, of all possible zones on that motoneuron, which happens to receive the largest number of active monosynaptic knobs; such a zone may be designated the optimal zone on that motoneuron. It is the probability of success in the optimal zone of an arbitrarily selected motoneuron, which corresponds to average motoneuron discharge probability, and hence, to fractional pool discharge, ω. A rigorous calculation of this probability appears to be a formidable task.

An approximate solution of this problem may be obtained by treating the probability of success in the optimal zone as equivalent to the probability of success in at least one of 15 arbitrarily selected zones. The exact number, 15, is not of critical importance; it simply represents an estimate of the number of significantly different zones to be considered on a motoneuron. It is obvious that 15 zones, each representing a 5th of the surface area, cannot be completely independent of each other; however, a consideration of overlapping areas on a closed surface suggests that three sets of 5 zones could be arranged in such a way that any of these zones would not have more than about one-third of its area in common with any other zone; also, the optimal zone, whatever its orientation, could not have less than about two-thirds of its area in common with one of the 15 significantly different zones. To permit a simple treatment, we make the false assumption that these 15 zones are independent of each other, and thus, each equivalent to an arbitrarily selected zone. Since p is the probability of success in an arbitrarily selected zone, it follows that the probability of failure in 15 such zones is $(1-p)^{15}$. Hence, the probability of success in at least one of 15 zones is equal to the difference, $1-(1-p)^{15}$, or approximately, $1-\exp[-15p]$; where p is very small, these expressions approach a value of 15p.

These expressions correspond, on the assumptions made, to the probability of success in the optimal zone of an arbitrarily selected motoneuron. Since this is equivalent to the probability of reflex discharge of such a motoneuron, it is also equivalent, for the motoneuron population, to the fractional pool discharge.

Figure 8 permits a comparison of the two functions, $I(k)$ and $1-\exp[-15 \cdot I(k)]$, both plotted against the same scale of k values. The two curves possess obvious similarities in form; translation to the right, together with a uniform contraction relative to the k-scale, of the curve on the left, provides a good fit to the curve on the right. In fact, any $I(k)$ value may be obtained, within 0.01, by multiplying its k value by 0.56, and adding 1.70, to obtain the appropriate k value for the curve on the right; for example, $I(k) = 0.84$ corresponds to $k = -1$, which, if multiplied by 0.56 and added to 1.70 gives 1.14, for which k value the curve on the right has an ordinate of 0.85. This generalization means that sets of experimental points, such as those presented in figure 4, which fit a straight line relation between k and β on the simpler theory, where $\omega = I(k)$, must also fit a straight line relation between k and β on the modified zonal theory, where $\omega = 1-\exp[-15\ I(k)]$. However, the slope of the straight line fit will be different; in the case of figure 4, the slope of k versus β would become approximately 2.9 instead of 5, corresponding to $\sigma = 6.9$ if $\gamma N/5 = 20$. Both $\bar{h}$ and σ are larger, relative to $\gamma N/5$ in the zonal theory, than they are, relative to γN in the simple number theory. For example, $\omega = 0.84$ implies that $\bar{h}$ equals 80% of the mean monosynaptic knob number per motoneuron of the simple number theory, while it implies that $\bar{h}$ equals 140% of the mean monosynaptic knob number per zone of the zonal theory. The post-tetanic potentiation of figure 4 implies a factor of increase in knob effectiveness of 1.12 for the zonal theory, compared with 1.2 for the simple number theory. There is a difference between the two theories with regard to ω values greater than 0.5; an increase in σ, while $\bar{h}$ remains constant, would *increase* ω on the zonal theory, whereas it would *decrease* ω on the simple number theory; hence, an experimental means of control over the value of σ might provide a means of distinguishing between the suitability of the two theories.

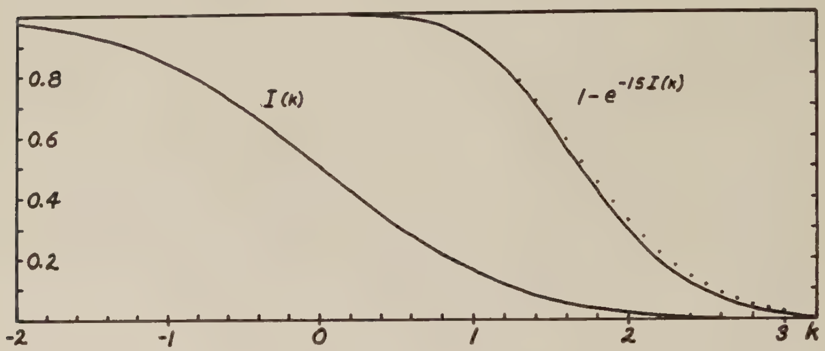

Fig. 8 Comparison of I(k), for simple number theory, with the value of $1 - \exp[-15\,I\,(k)]$, for the modified zonal theory (see text). The dots, shown beside the curve on the right, indicate the maximum correction calculated for skewness of the n-h distribution (using a Gram-Charlier series); the maximum skewness includes both the skewness of the binomial distribution of n values, and the skewness of the knob size distribution found by Haggar and Barr ('50).

LITERATURE CITED

DENNY-BROWN, D. E., AND C. S. SHERRINGTON 1928 Subliminal fringe in spinal flexion. J. Physiol., *66:* 175–180.

ECCLES, J. C. 1939 The spinal cord and reflex action. Ann. Rev. Physiol., *1:* 363–384.

———— 1946 An electrical hypothesis of synaptic and neuromuscular transmission. Ann. N. Y. Acad. Sci., *47:* 429–455.

ECCLES, J. C., AND W. RALL 1951 Effects induced in a monosynaptic reflex path by its activation. J. Neurophysiol., *14:* 353–376.

HAGGAR, R. A., AND M. L. BARR 1950 Quantitative data on the size of synaptic end-bulbs in the cat's spinal cord. J. Comp. Neurol., *93:* 17–35.

HOUSEHOLDER, A. S., AND H. D. LANDAHL 1945 Mathematical biophysics of the central nervous system. The Principia Press, Bloomington, Indiana.

JEFFERSON, A., AND A. BENSON 1953 Some effects of post-tetanic potentiation of monosynaptic responses of spinal cord of cat. J. Neurophysiol., *16:* 281–396.

LLOYD, D. P. C. 1943a Reflex action in relation to pattern and peripheral source of afferent stimulation. J. Neurophysiol., *6:* 111–120.

——— 1943b Neuron patterns controlling transmission of ipsilateral hind limb reflexes in cat. J. Neurophysiol., *6:* 293–316.

——— 1945 On the relation between discharge zone and subliminal fringe in a motoneuron pool supplied by a homogeneous presynaptic pathway. Yale J. Biol. Med., *18:* 117–121.

——— 1946a Principles of nervous and muscular activity. Howell's Textbook of Physiology, 15th ed., 7–77.

——— 1946b Facilitation and inhibition of spinal motoneurons. J. Neurophysiol., *9:* 421–438.

———1949 Post-tetanic potentiation of response in monosynaptic reflex pathways of the spinal cord. J. Gen. Physiol., *33:* 147–170.

LORENTE DE NÓ, R. 1938 Synaptic stimulation as a local process. J. Neurophysiol., *1:* 194–207.

——— 1939 Transmission of impulses through cranial motor nuclei. J. Neurophysiol., *5:* 435–458.

RALL, W. 1951 Input-output relation of a monosynaptic reflex. Proc. Univ. Otago Med. Sch., *29:* 17–18.

——— 1953 Electrotonic theory for a spherical neurone. Proc. Univ. Otago Med. Sch., *31:* 14–15.

——— 1954 Monosynaptic reflex input-output analysis. J. Physiol., *125:* 30–31.

——— 1955 Experimental monosynaptic input-output relations in the mammalian spinal cord. J. Cell. and Comp. Physiol., *46:* 413–438.

RASHEVSKY, N. 1948 Mathematical Biophysics, revised edition. Univ. Chicago Press.

ROSENBLUETH, A., N. WIENER, W. PITTS AND J. GARCIA RAMOS 1949 A statistical analysis of synaptic excitation. J. Cell. and Comp. Physiol., *34:* 173–205.

SHIMBEL, A. 1950 Contributions to the mathematical biophysics of the central nervous system with special reference to learning. Bull. Math. Biophysics, *12:* 241–275.

EXPERIMENTAL MONOSYNAPTIC INPUT-OUTPUT RELATIONS IN THE MAMMALIAN SPINAL CORD

WILFRID RALL
Physiology Department, University of Otago, Dunedin, New Zealand

INTRODUCTION

The input-output relation of a monosynaptic reflex pathway is of special interest for the indirect evidence it provides about spatial summation of synaptic excitation. The first study of such a relation in the mammalian spinal cord is that of Lloyd ('43a, '45).

The general features of such an input-output situation may be summarized in a few sentences. A single-shock stimulus produces an approximately synchronous input volley of impulses in a certain number of the several hundred afferent fibers stimulated. Some, but not all, of these afferent fibers distribute large numbers of presynaptic terminations directly to the motoneurons of the pathway. The intensity of synaptic excitation so delivered to any one of these motoneurons depends upon the number (and perhaps the arrangement, cf. Lorente de Nó, '38; Lloyd, '45) of such active terminals received by it. The fact, that reflex discharge of any motoneuron requires an input volley involving several afferent fibers, shows that spatial summation of the excitation produced by the active terminals must be an essential feature of the process. As a result of variations in the distribution of such synaptic excitation, the various motoneurons may be expected to represent many different intensities of spatially summed excitation. The size of the monosynaptic reflex output volley resulting from a given input volley depends upon the number of these motoneurons with at least a threshold intensity of such spatially summed excitation.

The aim of the present research was to obtain experimental results which would be suitable for testing the adequacy of a statistical input-output theory based upon the assumption of a random distribution of presynaptic terminals, and upon a simple treatment of spatial summation. Consistent with this aim, an attempt has been made to satisfy a combination of 4 requirements not met by the original experiments of Lloyd ('43a), or by the later experiments of Rosenblueth, Wiener, Pitts and Garcia Ramos ('49). These 4 requirements may be stated briefly as follows:

(i) That the input-output results be obtained from a monosynaptic pathway having functional significance,

(ii) That the magnitude of reflex output be expressed as the fraction of the motoneuron pool discharged,

(iii) That the relation between the *effective* input and the experimental input measurement be determined as well as possible, and

(iv) That the experimental relation between the two variables, input and output, be obtained for several different values of a third variable, reflex excitability, thus providing an experimental *family* of input-output relations.

The first requirement was met by restricting stimulation to the nerves of a particular synergic muscle group (triceps surae). If, as in the previous experiments, a segmental reflex is evoked by dorsal root stimulation, the monosynaptic input-output results correspond to a non-functional combination of several different monosynaptic pathways represented in different degrees of incompleteness (cf. Lloyd, '43b).

The second requirement was met approximately by comparing the size of a reflex motor volley with the size of a maximal antidromic motor volley recorded from the same ventral root; observations of post-tetanic potentiation (Lloyd, '49; Eccles and Rall, '51) of the reflex provided contributory evidence.

The third requirement presents special difficulties. Complication of the afferent volley measurement by impulses in cutaneous afferent fibers may be avoided simply by stimulating muscle nerve rather than a dorsal root. Also, with about 15 cm of afferent volley conduction distance from the point of stimulation, the impulses in group II and smaller afferent fibers lag sufficiently behind those in the faster conducting group I fibers to permit a measurement in the dorsal root input record of what corresponds essentially to the group I component of the afferent volley (cf. Brock, Eccles and Rall, '51). However, even this refinement is not sufficient to remove the discrepancy between the input measurement and the magnitude of effective input to the monosynaptic pathway (Rall, '51). The relation between these two variables has therefore been estimated indirectly from evidence such as that provided by the experimental relation of monosynaptic facilitation to the input measurement (cf. Lloyd, '43a, '45).

The 4th requirement was met in a few experiments by adjusting the depth of anesthesia and by means of brief tetanic conditioning. In this way, significantly different input-output relations were obtained from the same pathway.

Short communications of this research have appeared (Rall, '51, '54). A full presentation was completed in 1953 as part of a Ph.D. thesis. A statistical input-output theory found to be consistent with these experimental results will be presented separately (Rall, '55).

METHOD

The experiments were performed upon cats under light pentobarbital (Abbot Nembutal) anesthesia. In most cases, the lumbar cord was isolated from higher levels by cord transection in the mid-thoracic region. After laminectomy (3rd to 7th lumbar vertebrae), the first sacral ventral root (S_1VR) and the 7th lumbar ventral root (L_7VR) were sectioned intradurally.

Stimulating and recording electrodes were of platinum wire; the exposed tissues were protected from drying and insulated electrically by two pools of warmed paraffin oil. The two gastrocnemius nerves, medial branch (GM) and the lateral branch including soleus nerve (GLS), were dissected free for a length of about 20 to 25 mm, cut peripherally, and mounted on electrodes spaced about 15 mm apart. The adequacy of such stimulating conditions, with regard to equal effectiveness for nerve fibers at all positions in the cross-section of the nerve trunk, has been discussed in a recent publication from this laboratory (Brock et al., '51).

The monosynaptic reflex output was recorded monophasically from the central stump of S_1VR (occasionally also L_7VR), which was mounted to provide 15 to 30 mm of insulated length, with one electrode at the crushed end and the other usually 10 to 20 mm more proximally placed on the root; the shorter distance in each case refers to experiments in which approximately equal central and peripheral stumps of S_1VR were used to permit comparison of the reflex motor volley with a maximal antidromic motor volley.

An electrode placed in contact with the (unsevered) dorsal roots was used to record the input volley relative to an indifferent electrode placed on adjacent muscle tissue; this indifferent electrode was usually also grounded to the metal mounting frame. In most of the experiments, S_1DR was raised (about 1 mm) clear of neighboring roots for a length of about 15 mm, and the platinum recording electrode was hooked underneath. Such partial insulation of the dorsal root improved the ratio between the volley measurement and the recorded physiological noise from the spinal cord and neighboring roots. It also resulted in distortion of the normally triphasic record to one of diphasic appearance. Care was required to insure that accumulation of cerebrospinal fluid did not progressively reduce the length of insulated root during an experimental series. The use of two small insulating wedges to define this length served to minimize this difficulty. At the end of each experiment, the dorsal roots were cut and monophasic afferent volleys were recorded for various stimulus strengths.

Two different sets of stimulating and recording apparatus were used. In the earlier experiments the stimulus was a break induction shock synchronized with a single-beam CRO sweep by means of a Lucas pendulum; observations could be repeated manually at about 6 second intervals. With the single beam CRO it was necessary either (i) to record input and output alternately with photographic superimposition of several records of each, or (ii) to record both input and output simultaneously with a single amplifier by connecting one lead of a differential input to the dorsal root electrode and the other lead to the crushed end of the ventral root.

In the later experiments the stimulus was a condenser discharge coupled inductively to the stimulating electrodes; relative stimulus strengths were measured from a "stimulus sample" coupled directly to the CRO amplifier; the stimulator was synchronized with a double-beam CRO sweep which could be set to repeat at regular intervals such as 3 or 6 seconds. Thus, input and output could be recorded simultaneosuly at different amplification, and photographic superimpositions could be made easily. Records obtained in this way are illustrated in figure 1. Such superimposition of several input-output records at each stimulus setting was employed to minimize errors resulting from random fluctuations in reflex output. The sequence of stimulus strengths was designed to reveal any significant drift in afferent or reflex excitability during an experimental series.

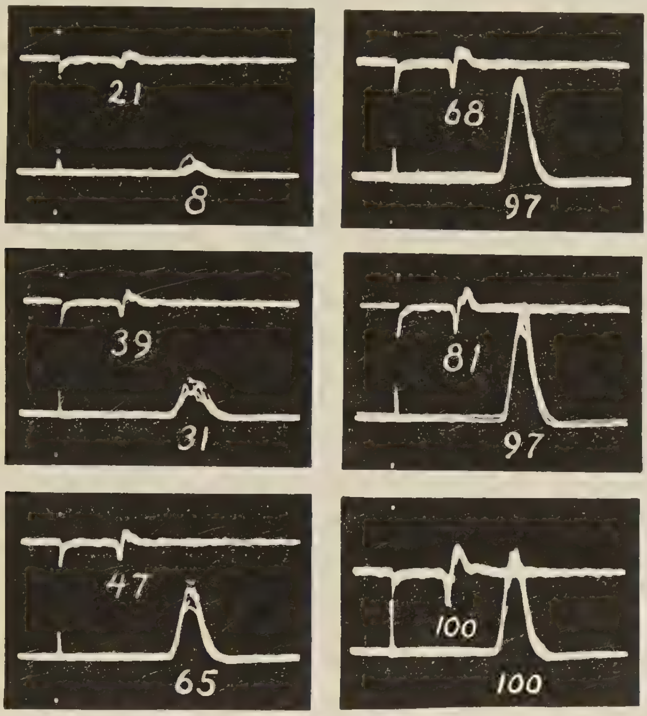

Fig. 1 Specimen input-output records. Each pair of records represents a superimposition of five pairs of cathode ray traces. The upper record in each case shows the ''stimulus sample'' and a diphasic record of the afferent input volley in S_1DR, with a number expressing its diphasic amplitude as a percentage of maximum. The lower record in each case shows the ''stimulus sample'' and a monophasic record of the reflex output volley in S_1VR, with a number expressing its amplitude as a percentage of the maximum of this series. Stimuli were applied to GM nerve, and each was preceded by brief tetanic conditioning.

Deliberate increase in depth of anesthesia, as for example in the experiment of figure 2, was obtained by intravenous injection of about

24 mg nembutal per kilogram of body weight, where the original level had been obtained by means of an initial intraperitoneal injection of 40 mg nembutal per kilogram of body weight.

When post-tetanic potentiation was used to obtain a shift in the input-output relation, it was found more satisfactory to employ a very brief tetanic conditioning of the afferent nerve before each test input volley, than to employ the alternative procedure of a long conditioning tetanus followed by several test input volleys. The conditioning usually consisted of 50 volleys at a frequency of 400 per second; the test input volley was evoked 150 msec. after the last conditioning volley and thus occurred near the peak of the brief early phase of post-tetanic potentiation (cf. Eccles and Rall, '51).

In addition to a number of exploratory experiments performed without simultaneous recording of input and output, there have been 15 preparations which were sufficiently stable to provide one or more satisfactory sets of input-output results.

RESULTS

Experimental input-output relation

It is a general result of all the experiments with reasonably stable reflexes, that the input volley record had to be greater than about 20% of its maximum size before any reflex output was observed, and that the output record reached essentially its maximum size (for a particular input-output series) when the input record was somewhere between 60% and 80% of its maximum size. This general result is illustrated by the specimen records in figure 1, and by each of the 4 sets of experimental input-output results plotted in figure 2.

The experimental points in figure 2 provide a family of 4 input-output relations (input as abscissa, output as ordinate) obtained from the gastrocnemius monosynaptic pathway of a single animal. The differences between the 4 sets of results were produced by using two levels of anesthesia in combination with tetanic conditioning. The points shown as open circles were obtained without tetanic conditioning and at the first level of anesthesia; the other points were obtained as noted in the figure legend.

It is important to note that the relative magnitudes of all the output values in figure 2 are quite accurate because the recording conditions remained unchanged; only the scaling relative to total pool discharge is estimated. Thus, on the basic assumption that the output record is proportional to the number of gastrocnemius motoneurons discharged (which assumption is discussed and approximately justified in the next section), it may be seen from figure 2, that the maximum reflex output must represent considerably less than a total pool discharge in at least three of the 4 experimental series. This means that the characteristic asymptotic approach to

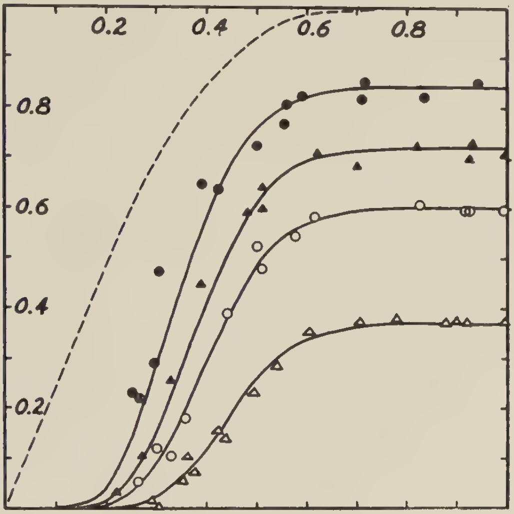

Fig. 2 Four different sets of input-output results obtained with gastrocnemius nerve of a single animal. Each point represents the average of 4 or 5 superimposed input-output records. Abscissae represent diphasic input amplitude in S_1DR, expressed relative to average maximum. Ordinates represent monophasic output amplitude in S_1VR, expressed relative to estimated size of total gastrocnemius pool discharge in S_1VR. Points shown as circles were obtained at the first level of anesthesia; filled circles were obtained with tetanic conditioning; open circles were obtained without tetanic conditioning. Points shown as triangles were obtained at a deeper level of anesthesia; filled triangles were obtained with tetanic conditioning; open triangles were obtained without tetanic conditioning. The dashed-line curve represents the relation of estimated effective input (as ordinate) to the diphasic input amplitude.

output maximum, seen in each case, cannot be due to approaching saturation of pool discharge.

In fact, figure 2 makes it clear that, although the asymptotic approach to output maximum can occur at several different levels of fractional pool discharge, it always occurs over the same range of input values. This fact suggests that afferent impulses in the higher threshold fibers, which contribute to the last 30% of a maximum input record, do not contribute to the excitation of the monosynaptic reflex. The implications of this for threshold distributions of functional subdivisions within group I will be discussed later. However, a specific interpretation is provided by the dashed-line curve in figure 2, which represents a postulated relation between *effective monosynaptic input* and the experimental input measurement. This dashed-line curve implies that the *effective* input is 60% of maximum when the input measurement is 25% of maximum, and that it is 98% of maximum when the measurement is 60% of maximum. This curve has the property (although not uniquely) of being consistent with all 4 of the input-output relations in figure 2. Independent experimental support for this type of relation is considered in a later section.

Comparison of the 4 input-output relations in figure 2 reveals that they are not of identical form; they would not superimpose accurately if each were scaled relative to its maximum output level. This is shown by the fact that lower maximum output level is associated with a higher reflex threshold; also, it may be noted that when the input record is 40% of maximum, the 4 outputs are approximately 32%, 50%, 60% and 75% of their respective maxima.

Experimental output

The monophasic amplitude of the monosynaptic reflex output record from the ventral root was measured. It is assumed that this amplitude is proportional to the *number* of gastrocnemius motoneurons contributing to the monosynaptic reflex discharge. This overall assumption rests upon several subsidiary facts and assumptions which ought to receive explicit mention.

1. The fact that the monosynaptic reflex volley recorded from a ventral root occurs only in gastrocnemius motoneurons when the input volley is restricted to gastrocnemius afferent fibers was established by Lloyd ('43b). It may be noted that the involvement of soleus nerve is implicit in both input and output when whole gastrocnemius nerve is stimulated; in some experiments this was avoided by restriction of stimulation to the medial branch of gastrocnemius nerve. In the case of post-tetanic potentiation, the increased monosynaptic reflex output recorded in S_1VR can have been provided only by gastrocnemius motoneurons, because both the tetanic conditioning and the test stimulation were confined to gastrocnemius nerve (cf. Lloyd, '49; Eccles and Rall, '51).

2. It is assumed that the motor axons in one of the ventral roots provide a representative sample of all the motoneurons in the gastrocnemius motor pool. This assumption has been at least approximately confirmed in the course of the present experiments, by comparison of relative output in the two ventral roots (S_1 and L_7).

3. It is assumed that any given output volley is produced by activity in a sample of motoneurons having a representative axon size distribution. This is assumed because the size of gastrocnemius motor axons is not uniform (Eccles and Sherrington, '30; Rexed and Therman, '48), and because the contribution to the recorded volley, made by an impulse in any given axon, is proportional to the diameter of the axon (Gasser and Grundfest, '39). Since there is at present no known correlation between the reflex excitability of a motoneuron and the size of its axon, it seems best to assume that there is none; if such a correlation is discovered, appropriate correction of measured output values would be required.

4. It has become customary to assume that the monophasic spike amplitude is a valid measure of the size of motor volley obtained in a monosynaptic reflex. In a strict sense, this as-

sumption requires that the impulses of which the volley is composed should be synchronous and of identical form and duration; otherwise, the area under the monophasic spike should be used as the measure of size (cf. the reconstructions of Gasser and Grundfest, '39). These requirements are fairly well met by the monosynaptic reflex volley. Recently, this correlation between spike amplitude and area has been checked experimentally (Rosenblueth et al., '49; Brock et al., '51).

Output as fractional pool discharge

Accepting the output measurement as proportional to the *number* of motoneurons discharged, the next step is to express this as a fraction of the total number of motoneurons in the pool; this fraction corresponds to the form in which predictions of output would be expressed on the basis of a statistical input-output theory.

Experimental estimates of this fraction were made in several animals where the ventral root (S_1VR) had been sectioned near the middle of its intradural length. Monophasic records of the reflex volley in the central stump of S_1VR could be compared with monophasic records of a maximum antidromic motor volley in the peripheral stump of S_1VR. Both motor volleys can involve only gastrocnemius motor axons when stimulation is confined to gastrocnemius nerve, and there can be no doubt that a maximum antidromic motor volley involves the same set of S_1VR axons which would be involved in a complete gastrocnemius pool discharge. However, the validity of the comparison depends upon the degree of equivalence in the recording conditions at the ventral root stumps. Equivalence would require (i) that the electrode spacing be the same on both stumps, (ii) that the distribution of injury current near the two crushed-ends be the same, (iii) that the ventral root be uniform over the length of the two stumps with regard both to axon diameters and to interaxonal conductivity, and (iv) that the degree of synchronism be the same in both volleys. Some uncertainty regarding equivalence would seem to be unavoidable. Thus, even in favorable cases, this comparison should be regarded as providing an estimate rather than a determination of the fractional pool discharge.

The results of applying the above procedure in combination with observation of post-tetanic potentiation have suggested that fractional pool discharge may be estimated indirectly from the factor of output potentiation obtainable with a standard brief tetanic conditioning. It was found in one experiment that a maximum output estimated as 10% of the pool was potentiated by a factor of 4; in another animal, a maximum output estimated as 15% of the pool was potentiated by a factor of 3.5; in a third animal, an estimated 26% of the pool was potentiated by a factor of 2.5; in a 4th animal, an estimated 30% of the pool was potentiated by a factor of 2.2. These results are all for the whole gastrocnemius nerve. When the medial branch (GM) was used separately, the fractional discharge of the GM pool was smaller than the fractional discharge of the whole pool with whole nerve input, as should be expected; also, the smaller GM fractional pool discharge displayed a correspondingly larger factor of post-tetanic potentiation.

These results provide quantitative examples of the familiar observation that post-tetanic potentiation is most dramatic when the reflex is small. Also, by relating the factor of output potentiation to fractional pool discharge, an experimental result is obtained which can be compared with theoretical predictions (Rall, '55, fig. 5).

Although antidromic motor volleys were not recorded in the experiment of figure 2, the scaling of output relative to absolute maximum used in that figure may be seen to be consistent with the results cited above. In figure 2, an output (open triangle maximum) which was potentiated by a factor of 1.95 was scaled as 37% of the pool; this scaling then implies potentiation by a factor of 1.4 for an output scaled as 60% of the pool.

In a few animals, fractional pool discharge for the gastrocnemius reflex was estimated on the other side of the animal. Recording electrodes were placed on gastrocnemius nerve. With ventral roots still intact, dorsal roots (L_6, L_7, S_1, S_2) were cut and mounted on stimulating electrodes, and a maximum monosynaptic reflex volley was recorded peripherally from the nerve. Then the corresponding ventral roots were cut centrally and stimulated to produce a maximum motor volley which could be recorded from gastrocnemius nerve under identical conditions. Results obtained in this way were in essential agreement with those reported above.

Since the time of the above experiments, there have appeared two independent reports of fractional pool discharge estimation. Jefferson and Benson ('53) report unpotentiated fractional pool discharge estimates for spinal cats which are quite similar to those found here with light nembutal anesthesia. They, and also Henneman ('54), have observed potentiated outputs which seem to represent essentially complete pool discharge; these results, however, were obtained with severe tetanic conditioning of one minute duration, as compared with 125 msec. duration in the brief conditioning of the present experiments.

Effective input

It was noted earlier that the results in figure 2 suggest a significant discrepancy between the experimental input measurement and the *effective* input to the monosynaptic pathway. Several problems arise. First, is the problem of defining this effective input. Next is the problem of estimating its relation to the experimental input record. Finally, there is the separate problem of explaining this relation in terms of the size, threshold, and knob distributions of group I afferent fibers. Each of these problems offers difficulties.

Effective input might be defined as a quantity which is directly proportional to the number of synaptic knobs activated over the pool by the input volley. In our ignorance of detailed knob distributions and of spatial summation mechanism, a more appropriate definition is not obvious. However, this quantity cannot be measured directly; it can only be estimated indirectly from the post-synaptic side of the pathway.

One method of doing this is to record the ventral root synaptic potential (cf. Eccles, '46), which may be regarded as a measure of subliminal synaptic excitation of a motoneuron pool as a whole. When the depth of anesthesia is sufficient to prevent reflex discharges, it is also sufficient to block internuncial activity, and the size of the ventral root synaptic potential may be regarded as proportional to pool excitation resulting only from activity in the synaptic terminals of the monosynaptic reflex pathway. Although such synaptic potentials must be recorded at high amplification, and their measurement is complicated by baseline fluctuations, the experimental results plotted in figure 3 do indicate rough agreement between this estimate of *effective* input and the estimate implied by the dashed-line curve of figure 2, reproduced here for comparison.

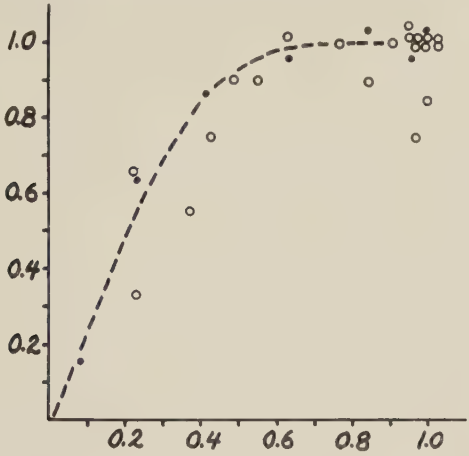

Fig. 3 Ventral root synaptic potentials. Ordinates represent relative amplitude of the ventral root synaptic potential in S_1VR. Abscissae represent the relative size of diphasic input in S_1DR, with stimulation of gastrocnemius nerve. Circles and dots represent two different experiments. The dashed-line curve is from figure 2.

Another method of estimating *effective* input is to record graded monosynaptic facilitation (cf. "excited zone" of Lloyd, '45, '43a). The facilitation obtained with different input volleys in the medial branch (GM) of gastrocnemius nerve may be compared in figure 4 B with the dashed-line curve of figure 2. In this experiment, a reasonably stable control reflex was obtained with the lateral nerve (GLS) by means of brief tetanic conditioning of the GLS nerve prior to each GLS maximum afferent volley; this control level is indicated in figure 4 A by the horizontal dashed-line. In order to avoid any possibility of disynaptic complications (Laporte and Lloyd, '51), the GM afferent volley was made simultaneous with the GLS afferent volley. The open circles in figure 4 A represent facilitated output plotted against the GM input record; the open circles in figure 4 B represent the same results replotted to show relative increase in output above the control level.

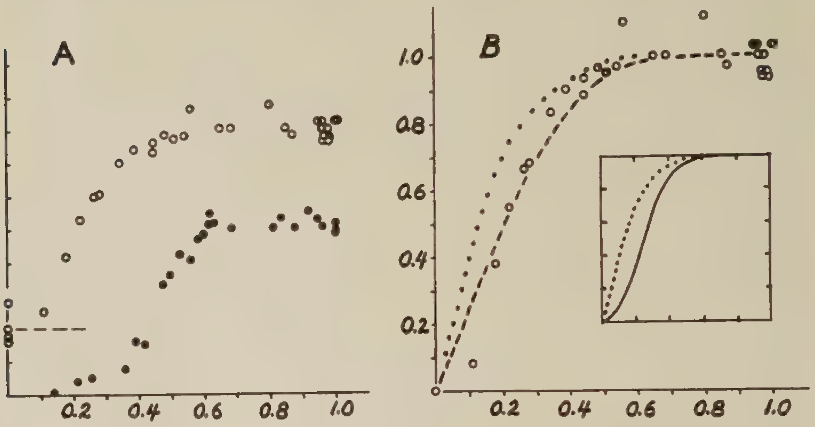

Fig. 4 Monosynaptic facilitation. Abscissae in both (A) and (B) represent the relative size of GM diphasic input records in S$_1$DR. Ordinates of open circles in (A) represent output in S$_1$VR (average of 5 superimposed records) when each GM input was simultaneous with a tetanically conditioned maximum GLS input volley; each abscissal value of this series represents the average of three GM input records obtained separately without complication by a GLS volley. Open circles of (A) are replotted in (B) as relative increment in output versus GM input; the dashed-line curve is the same as in figure 2. Filled circles in (A) represent GM input-output results (each the average of 5 traces) obtained with tetanic conditioning of GM nerve; specimen records of this series are shown in figure 1. The inset is explained in the text.

There are two reasons for expecting some discrepancy between the experimental points in figure 4 B and the dashed-line curve. One is that this particular dashed-line curve corresponds to experimental results from a different animal (fig. 2), and the relation of effective input to experimental input measurement may be expected to vary a little from cat to cat and perhaps also with slight differences in the input recording conditions. This possibility is supported by a comparison of the GM input-output results, shown as filled circles in figure 4 A, with the input-output results shown in figure 2. The asymptotic approach to maximum effective input must have occurred for slightly smaller input records in the experiments of figure 4, than in those of figure 2; a more nearly correct estimate of the effective input in figure 4 is indicated by the dotted curve in figure 4 B.

The other reason for expecting discrepancy in figure 4 B is that the facilitated output volleys recorded in S_1VR represent a combined output in both GM and GLS motoneurons, and the apparent facilitation of such a combined output should not be expected to be directly proportional to the effective GM input magnitude. It seems reasonable to expect the increase in GLS output to be approximately proportional to the effective input delivered by GM afferent fibers to GLS motoneurons, because the control reflex already represents a significant discharge of the GLS motoneuron pool (cf. Lloyd, '45). However, the GM motoneuron pool is only subliminally excited by the GLS control input, and there must still be a threshold requirement of GM input before any GM output occurs; thus the portion of increased output in S_1VR which is due to discharge of GM motoneurons should not be expected to be proportional to the effective GM input.

A quantitative prediction of this discrepancy depends upon a knowledge of the relative representation of the two motoneuron pools in the ventral root, and upon assumptions concerning the reciprocal symmetry in synergic monosynaptic excitation. Using simple assumptions, one prediction of such discrepancy is shown as an inset in figure 4 B; the dotted curve represents the same estimate of effective GM input as the dotted curve in the main figure; the continuous curve represents the relative increment in ventral root output predicted for this effective input. The experimental results in figure 4 may be seen to be consistent with such a predicted discrepancy. A more detailed presentation of facilitation predictions must be given elsewhere in conjunction with a theoretical model of synergic monosynaptic reflex pathways (cf. Rall, '55, fig. 7).

Experimental input record

The most reliable record of an afferent volley is the monophasic record obtained when the dorsal root is severed centrally. Such records have been illustrated and discussed recently (Brock et al., '51). With gastrocnemius nerve it was concluded that the amplitude of the monophasic record may be attributed to impulses in group I fibers; because of a conduction distance of about 15 cm, the impulses in group II fibers were found to contribute, at most, a "hump" to the declining phase of the monophasic record.

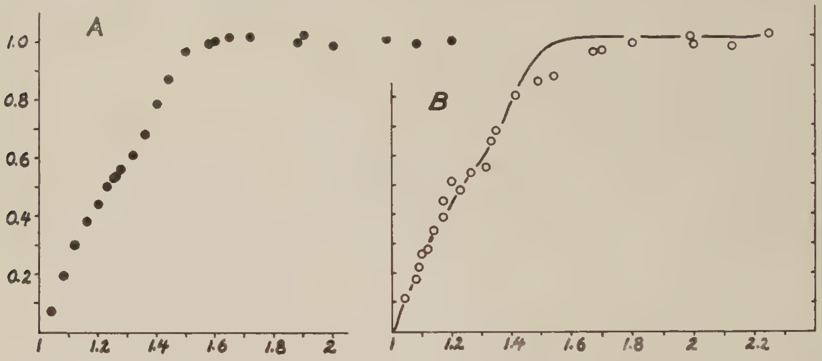

Fig. 5 Comparison of diphasic input record with monophasic afferent volley records. Abscissae in both (A) and (B) represent relative strength of "stimulus sample." Filled circles in (A) and the continuous line in (B) represent monophasic amplitude of records from cut S_1DR. Open circles in (B) represent the diphasic input amplitude of the same input records (from intact S_1DR) used in the facilitation series of figure 4.

Figure 5 permits a comparison between the diphasic amplitude of records obtained from intact dorsal root and the amplitude of monophasic records. The results are for GM nerve of the same animal as in figures 1 and 4. Monophasic amplitudes are plotted against stimulus strength in figure 5 A; the diphasic amplitudes (of the same input records as in the facilitation series of fig. 4) are plotted against stimulus strength in figure 5 B. The two relations agree quite well up to stimulus strengths 1.4 times afferent nerve threshold; however, the monophasic amplitude reaches its maximum value for a stimulus 1.6 times threshold, while the diphasic record is only about 90% of maximum at this stimulus strength. Thus, it seems quite likely that the final 10% of the diphasic input record is due to impulses in group II fibers and that this may correspond to the ''group II hump'' observed in monophasic records (Brock, et al., '51).

This comparison indicates that if the diphasic input values are expressed relative to 90% of maximum, and if the monophasic amplitude is assumed proportional to the size of the afferent volley in group I fibers, then these input values would approximately represent the percentage of a maximum group I volley. This it should be added, would not be directly proportional to the number of group I fibers conducting impulses, because there is known to be an approximately inverse proportionality between the diameter and the threshold to electrical stimulation of these fibers (O'Leary, Heinbecker and Bishop, '35; Erlanger and Gasser, '37), and the diameter of the largest fibers is nearly twice that of the smallest fibers within group I of gastrocnemius nerve (Eccles and Sherrington, '30; O'Leary et al., '35; Rexed and Therman, '48; Lloyd and Chang, '48).

Having reached this point, it should be noted that the 10% discrepancy revealed in figure 5 is not sufficient to account for all of the ineffective input revealed by figures 2, 3 and 4. Asymptotic approach to maximum output for input values between 60% and 80% of diphasic maximum corresponds to input values between 66% and 88% of the estimated group I maximum. Thus it would seem that the highest threshold fibers in group I do not contribute to excitation of the monosynaptic reflex (cf. Rall, '51).

DISCUSSION

Group I-M compared with group I-A

Those group I fibers which contribute to excitation of the monosynaptic reflex constitute a functional sub-group conveniently designated as group I-M. The designation, group

I-A, has been purposely avoided because it applies already to a functional sub-group based upon a different experimental criterion, namely the behavior in response to stretch of the receptor organ to which the group I fiber is connected (Hunt and Kuffler, '51; Hunt, '54).

The reason for making this distinction may be stated briefly as follows: although it seems probable that all fibers belonging to group I-M belong also to group I-A, it is entirely possible that some of the smaller group I-A fibers do not have the same central connections as group I-M, but have instead central connections resembling those of the A-type afferent fibers which make up group II.

Evidence in favor of this suggestion is provided for gastrocnemius nerve by considering the results of Hunt ('54) together with the results of the present paper. He obtained, for the medial branch, the size distributions of afferent fibers belonging to groups A and B. Although these distributions indicate that a small group I volley might be expected to include more I-A fibers than I-B fibers, there is no support to the notion that I-A fibers might be missing in the size range which corresponds to the increase of a group I volley from 75% of maximum to maximum. In figure 5 above, the range from 75% to maximum corresponds to an increase in stimulus strength from about 1.4 to about 1.6 times group I threshold; using the inverse rule, this corresponds to fiber diameters of about 15 μ down to about 13 μ. It would seem, from the consideration of *effective input* in the previous section, that group I fibers having diameters less than about 15 μ do not belong to group I-M, and that most of group I-M consists of group I-A fibers having diameters greater than 17 μ. A corollary to this would be that group I-A fibers with diameters less than 15 μ (and some between 15 μ and 17 μ) should be regarded as functionally more like group II than like group I-M. This suggestion is not inconsistent with a sub-division of A-type afferent fibers into only two functional groups. It simply means that instead of sub-dividing A-type afferent fibers into the conventional size groups I and II (with an arbitrary dividing line at 12 μ), we consider two slightly overlapping functional groups: group I-M fibers distributed fairly symmetrically over the range from 15 μ to 21 μ diameter, and a large group (A-non-M) distributed unimodally over the full size range of group II and extending up to diameters of 17 μ. The size distribution of group I-B fibers has been found by Hunt ('54) to range from about 10 μ to 20 μ diameter.

The detailed size distribution of group I-M fibers must be regarded as unknown. One reason is that the relation between fiber size and the number of synaptic terminals (or the amount of synaptic excitation) distributed to the motoneuron pool per fiber is unknown. Another reason is that the possible decreased effectiveness of synaptic excitation delivered perhaps as much as one-half msec. later by the smaller fibers is not easily assessed; such late excitation might have to compete with the earliest disynaptic inhibition (Laporte and Lloyd, '51).

Relation of output to effective input

The family of experimental input-output relations in figure 2 has been reproduced in figure 6 A, together with the dashed-line curve relating estimated effective input to experimentally measured input. This family of curves becomes transformed as shown in figure 6 B, when the same output values are replotted with each experimental input value replaced by its estimated effective value.

Since the output values in figures 2 and 6 have already been scaled to represent a reasonable estimate of their fractional pool discharge values, the transformed family of input-output curves in figure 6 B represents the end-result toward which the present experiments were aimed, namely, the estimated relation of fractional pool discharge to effective input magnitude.

These curves show clearly that a very considerable degree of spatial summation is required to produce any reflex output. They indicate that as the effective input is increased above the threshold value, the increase of output with input has a decided upward curvature until the output corresponds to nearly 20% of the pool. With further increase in effective input, the increase of output with input is approximately linear until the output reaches about 80% of the pool.

The input-output curves in figure 6 B are quite similar in shape to that derived by Lloyd ('45) to relate the size of "discharge zone" to the size of "excited zone." This is not surprising because what Lloyd has designated as "excited zone" was measured as facilitation, and corresponds closely to what is here referred to as an estimate of effective input. It may be noted that in deriving this important curve by "eliminating the common variable," Lloyd ('45) actually eliminated two different variables by implicitly assuming them proportional; the monosynaptic excitation deliverd to the discharge zone motoneurons of S_1VR by an input volley in S_1DR, must be assumed proportional, for all relative

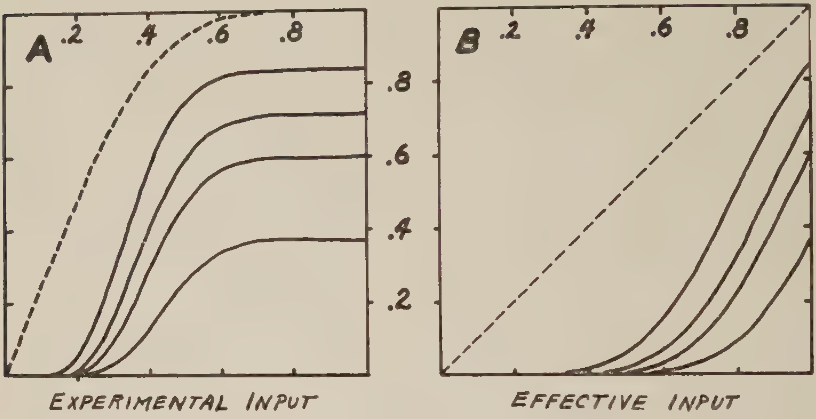

Fig. 6 Transformation of input-output family of curves. The curves in (A) are the same as those in figure 2. Abscissae in (A) represent relative size of diphasic input records. Abscissae in (B) represent relative size of estimated effective input. Ordinates of dashed-line in both (A) and (B) represent relative size of estimated effective input. Ordinates of the 4 input-output curves in both (A) and (B) represent estimated fractional pool discharge.

grades of dorsal root input, to the monosynaptic facilitatory excitation delivered to subliminal fringe motoneurons of S_1VR by an input volley in a filament of L_7DR.

Although the 4 curves in figure 6 B obviously resemble each other, they cannot be reduced to a single curve by rescaling each curve relative to its maximum output value. When Lloyd ('45) remarked that his segmental results from different preparations "superimpose one upon another" when scaled relative to maximum, this reflected a greater interest in the similarities than in the differences between such curves. Actually, his results (Lloyd, '43a, fig. 1) do show a case of significant difference. Also, the segmental reflex contains portions of many distinct monosynaptic pathways, and the overall averaging of input and output would be expected to obscure differences present in the component input-output relations. Finally, it may be noted that results for different levels of reflex excitability in a single preparation, and estimates of fractional pool discharge were not obtained at that time.

The 4 sets of input-output results in figure 2 were obtained by using two different experimental methods of changing the reflex excitability level of the pathway. The effect of nembutal anesthesia on the monosynaptic reflex has been attributed to a decrease in motoneuron excitability (Eccles, '46; Brooks and Eccles, '47); decreased background of facilitatory internuncial activity may also be a contributory factor. Tetanic conditioning, however, has been shown to enhance the synaptic excitatory effectiveness of the conditioned pathway rather than to increase the excitability of motoneurons (Lloyd, '49; Eccles and Rall, '51). However, as long as input volleys and tetanic conditioning are confined to the same afferent nerve, it seems reasonable that a general increase in synaptic excitatory effectiveness of the afferent pathway should produce a change in the input-output characteristics of the pathway which is equivalent to that produced by a general increase in motoneuron excitability.

When the 4 input-output curves in figure 6 B are viewed as 4 distinct members of a single family of curves, it may be seen that they differ from each other essentially by translation along the horizontal (input) axis. In other words, when the reflex threshold of the pathway is raised by increased depth of anesthesia, the entire input-output curve in figure 6 B is translated to the right; when the reflex threshold of the pathway is lowered by tetanic conditioning, the entire input-output curve in figure 6 B is translated to the left. This means that the members of this family of curves differ from each other in respect to a single parameter, which may be called ''level of reflex excitability of the pathway,'' and which may be characterized either by the fractional pool discharge obtained with a maximum input, or by the reflex threshold requirement in terms of estimated effective input.

This report of experimental input-output results may be concluded with a few remarks about the implications concerning spatial summation of synaptic excitation. The detailed presentation of simple theoretical models of a monosynaptic reflex pathway, and the prediction of input-output relations for such models is left for a separate paper. It has been found, contrary to previous expectations (Lloyd, '45), that theoretical prediction of input-output relations like those in figure 6 B is possible when motoneuron threshold is defined as the number of synaptic knobs required to be active over its surface at the same time, irrespective of their locations on its surface; this threshold definition implies that spatial summation may be regarded as simply additive over the motoneuron suface. The sufficiency of such simple assumptions does not disprove the *zonal* concept of spatial summation and motoneuron threshold (Lorente de Nó, '38; Lloyd, '45); the *zonal* definition can be shown to lead to prediction of similar theoretical input-output relations. It is concluded that experimental input-output results of the kind considered here do not provide a sufficiently critical test to force, by themselves, a choice between these alternative concepts of spatial summation and motoneuron threshold (cf. Rall, '55).

SUMMARY

1. The experimental relation between the size of a monosynaptic reflex output volley and the size of its causative afferent input volley has been obtained with single shock stimulation of gastrocnemius nerve. This has been done at 4 different levels of reflex excitability in a single preparation.

2. The fraction of the motoneuron pool discharged in producing a given output volley was estimated by comparison of reflex motor volleys with maximum antidromic motor volleys, and by observation of output potentiation obtained with brief tetanic conditioning.

3. Observations of monosynaptic facilitation and of ventral root synaptic potentials, as well as the input-output results themselves, all point to the conclusion that the higher threshold afferent fibers belonging to group I do not contribute effective input to the monosynaptic pathway. It is suggested in the *discussion* that the afferent fibers which are effective in the monosynaptic reflex constitute a functional subgroup (designated group I-M) with an estimated size range of from 15 μ to 21 μ in diameter.

4. When experimental input values are replaced by their estimated effective values, the input-output relations become transformed (fig. 6) to a characteristic shape resembling that derived by Lloyd ('45) for the relation between "discharge zone" and "excited zone."

5. The 4 members of the transformed family of input-output curves, relating estimated fractional pool discharge to estimated effective input, differ from each other essentially only by translation along the input axis. This difference corresponds to a difference in reflex excitability of the pathway obtained either by tetanic conditioning or by changed depth of nembutal anesthesia.

ACKNOWLEDGMENT

The author wishes to thank Professor A. K. McIntyre and Professor J. C. Eccles for advice and encouragement during the course of this research, Mr. K. Bradley for assisting with a number of the experiments, and the Medical Research Council of New Zealand for the provision of equipment, technical assistance and the costs of publication.

LITERATURE CITED

BROCK, L. G., J. C. ECCLES AND W. RALL 1951 Experimental investigations on the afferent fibres in muscle nerves. Proc. Roy. Soc. B, *138:* 453–475.

BROOKS, C., McC. AND J. C. ECCLES 1947 A study of the effects of anesthesia and asphyxia on the mono-synaptic pathway through the spinal cord. J. Neurophysiol., *10:* 349–360.

ECCLES, J. C. 1946 Synaptic potentials of motoneurons. J. Neurophysiol., *9:* 87–120.

ECCLES, J. C., AND W. RALL 1951 Effects induced in a monosynaptic reflex path by its activation. J. Neurophysiol., *14:* 353–376.

ECCLES, J. C., AND C. S. SHERRINGTON 1930 Numbers and contraction values of individual motor units examined in some muscles of the limb. Proc. Roy. Soc. B, *106:* 326–357.

ERLANGER, J., AND H. S. GASSER 1937 Electrical signs of nervous activity. Philadelphia, Univ. Penn. Press.

GASSER, H. S., AND H. GRUNDFEST 1939 Axon diameters in relation to the spike dimensions and the conduction velocity in mammalian A fibers. Am. J. Physiol., *127:* 393–414.

HENNEMAN, E. 1954 Maximal discharge of a motoneuron pool during potentiation. Fed. Proc., *13:* 69.

HUNT, C. C. 1954 Relation of function to diameter in afferent fibers of muscle nerves. J. Gen. Physiol., *38:* 117–131.

HUNT, C. C., AND S. W. KUFFLER 1951 Stretch receptor discharges during muscle contraction. J. Physiol., *113:* 298–315.

JEFFERSON, A., AND A. BENSON 1953 Some effects of post-tetanic potentiation of monosynaptic responses of spinal cord of cat. J. Neurophysiol., *16:* 381–396.

LAPORTE, Y., AND D. P. C. LLOYD 1951 Disynaptic reflex linkage between muscles of a myotatic unit. Fed. Proc., *10:* 78–79.

LLOYD, D. P. C. 1943a Reflex action in relation to pattern and peripheral source of afferent stimulation. J. Neurophysiol., *6:* 111–120.

——— 1943b Neuron patterns controlling transmission of ipsilateral hind limb reflexes of cat. J. Neurophysiol., *6:* 293–316.

——— 1945 On the relation between discharge zone and subliminal fringe in a motoneuron pool supplied by a homogeneous presynaptic pathway. Yale J. Biol. Med., *18:* 117–121.

——— 1949 Post-tetanic potentiation of response in monosynaptic reflex pathways of the spinal cord. J. Gen. Physiol., *33:* 147–170.

LLOYD, D. P. C., AND H. CHANG 1948 Afferent fibers in muscle nerves. J. Neurophysiol., *11:* 199–207.

LORENTE DE NÓ, R. 1938 Synaptic stimulation as a local process. J. Neurophysiol., *1:* 194–207.

O'LEARY, J., P. HEINBECKER AND G. H. BISHOP 1935 Analysis of function of a nerve to muscle. Am. J. Physiol., *110:* 636–658.

RALL, W. 1951 Input-output relation of a monosynaptic reflex. Proc. Univ. Otago Med. Sch., *29:* 17–18.

——— 1954 Monosynaptic reflex input-output analysis. J. Physiol., *125:* 30–31.

——— 1955 A statistical theory of monosynaptic input-output relations. J. Cell. and Comp. Physiol., *46:* 373–412.

REXED, B., AND P. THERMAN 1948 Calibre spectra of motor and sensory nerve fibres to flexor and extensor muscles. J. Neurophysiol., *11:* 133–139.

ROSENBLUETH, A., N. WIENER, W. PITTS AND J. GARCIA RAMOS 1949 A statistical analysis of synaptic excitation. J. Cell and Comp. Physiol., *34:* 173–205.

DEVIATIONS FROM ALL-OR-NONE BEHAVIOR IN A MOLLUSCAN UNSTRIATED MUSCLE: DECREMENTAL CONDUCTION AND AUGMENTATION OF ACTION POTENTIALS[1]

WERNER SCHMANDT AND WILLIAM SLEATOR, JR.
Department of Physiology, Washington University School of Medicine, St. Louis, Missouri

TEN FIGURES

INTRODUCTION

Recent investigations of less well-known excitable systems such as some invertebrate smooth muscles (Prosser, '54) motor end plates (Fatt and Katz, '51) and 'slow' skeletal muscle fibers of the frog (Kuffler and Vaughan Williams, '53), and dendrites and cell bodies in the mammalian central nervous system (Clare and Bishop, '55a) have shed some light on a variety of electrical responses which do not show all-or-none properties. Consideration of these and other facts has suggested that from a comprehensive viewpoint perhaps the all-or-none response and decrementless conduction should be regarded as special cases rather than the general rule for excitable tissues (Clare and Bishop, '55b).

Thus it seemed worth-while to make a fairly thorough study of the electrical properties of the byssal retractor muscle of Mytilus edulis when it became apparent, during studies of optical changes in the muscle, that it showed graded electrical responses and decremental conduction. Other systems demonstrating similar effects such as endplate regions

---

[1] This investigation was supported by a research grant (G2657) from the National Institutes of Health, Public Health Service.

of skeletal muscle fibers or nerve cell bodies cannot be studied so easily since the conduction distances are extremely short. Another reason for doing the work was that, because of the histological features of this smooth muscle, it has been frequently used in mechanical (Winton, '36; Nieuwenhoven, '47; Abbott and Lowry, '53), electrical (Prosser, Curtis and Travis, '51) and pharmacological (Twarog, '54) investigations. Current views of general behavior of the muscle are in large part based on the comprehensive papers of Fletcher ('37a, b, c), with some of whose important conclusions we disagree.

The ideal method for studying the electrical properties and behavior of the individual cells in a tissue is, of course, to record from an intracellular microelectrode. However, the relaxed fibers of this muscle have such small diameters (3–5 μ) that the probability of damage by the electrode would cast some doubt upon the results. Also the proof of decremental conduction would be indirect unless two electrodes were inserted at different places along the same fiber, an almost prohibitively difficult procedure. Methods yielding summed potentials of parallel elements were therefore considered suitable for this study.

METHODS

The experiments reported here were carried out on the anterior byssal retractor muscle of the common sea shore mussel Mytilus edulis. This is a white unstriated muscle, 3.5 to 5.5 cm long and 1 to 2 mm in diameter (nearly uniform cross section) in animals of more than 10 cm shell length.[2] According to Fletcher's ('37a) valuable histological description, which has been confirmed by Nieuwenhoven ('47) and Twarog ('54) the muscle consists of about 50,000 fibers, each 3 to 5 μ in diameter when relaxed, and each extending the whole length of the muscle. This was found by teasing the fresh fibers apart or macerating the muscle as well as by observing that a biphasic action potential may become monophasic when the muscle is crushed at one end. Despite careful examination no ending of fibers between origin and insertion of the muscle was ever observed by these authors. The great length as well as the nearly uniform diameter of each fiber was very advantageous to the present study. Further histological details may be found in Fletcher's article.

---

[2] The byssus is the glandular organ which produces threads by means of which the animal holds itself to rocks. The byssal retractor muscles move the shell with respect to the byssus and are thus responsible for changing the animal's position.

In order to remove the muscle without injuring any part of the fibers the dissection was done as follows: After the shell is opened, which is made possible by cutting the adductor muscles, byssal threads and foot are removed and the two halves of the animal are separated by a precise cut through the byssal organ between the origins of the byssal retractors. Usually this medial cut left both muscles uninjured. The surrounding soft tissues being carefully pulled off the muscle, the exact origin of the fibers in the byssal organ can be seen (fig. 1). A thread is tied around the byssus beyond this origin and the tissue is cut beyond the thread. Finally, a small piece of the shell containing the insertion of the muscle is sawed out, so that the muscle fibers are intact at both ends. The muscles are then submerged for at least one hour, while under a few grams tension, in continuously aerated artificial sea water (Hodgkin and Katz, '49). Prepared in this way, the muscles may remain excitable for one or sometimes several days. However, the best results were obtained within a few hours of dissection, after allowing a one hour rest for restoration of phosphagen compounds as suggested by the findings of Eggleton ('34). Before an experiment was started, the muscle was usually stimulated a few times tetanically to bring about more uniform conditions. Muscles still contracted after dissection were readily relaxed by this procedure.

The muscle was then mounted inside a plexiglass chamber, the details of which may be seen in figure 1, which also shows the arrangement of the silver-silver chloride electrodes, and of mechanical and electrical recording equipment. The resistance along the walls of the chamber between any two electrodes not touching the muscle was at least 1000 times that through the muscle. Rectangular shocks were used for stimuli, and the lead closer to the recording electrodes was usually made cathode and grounded, as shown in figure 1.

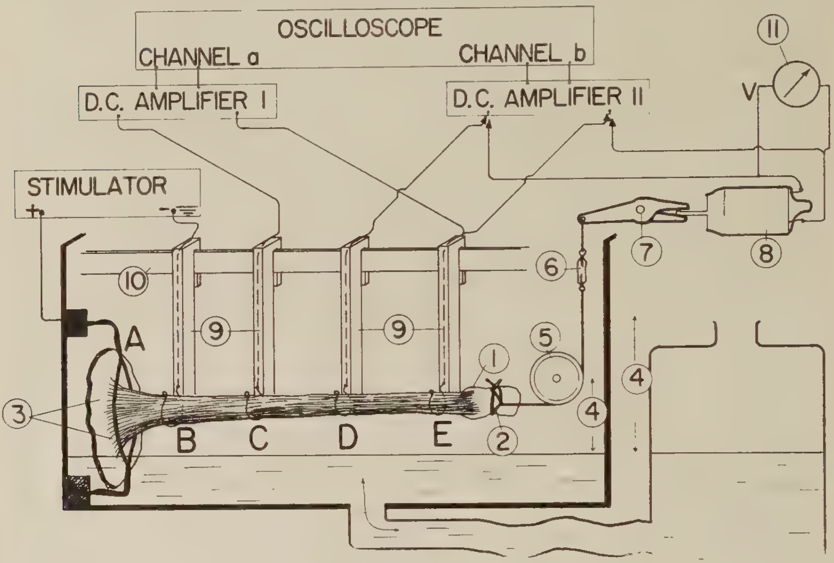

Fig. 1 (1) Origin of muscle fibers from byssal tissue; (2) thread on byssal tissue beyond muscle fibers; (3) insertion of muscle into shell piece which was sawed out from shell; (4) arrangement to submerge muscle in desired solution inside moist chamber; (5) pulley; (6) turnbuckle for tension adjustment (actually outside the chamber); (7) torsion rod; connected to (8) mechano-electronic transducer tube RCA 5734; (9) plexiglass supports for electrodes; sliding on (10) plexiglass bar; (A) fixed chloride coated silver wire loop; (B) (C) (D) (E) chloride coated silver wire electrodes, 0.25 mm thick, encircling the muscle about three-fourths of its circumference; (11) voltmeter to indicate tension on muscle.

The amplifiers were direct coupled differential ones which had a rise time (to 98%) of about 0.1 msec. However, a short but very large input signal could produce a sudden shift in the base line, which then moved back to its original level during the next half second or so. Tests showed that the amplifier sensitivity and time constant were normal during this interval. However, action potential magnitude had to be read from the new sloping base line in those records where the stimulus artifact was large enough to produce this effect (e.g., plate 1 c and fig. 4). The two beams of the cathode ray oscilloscope and their amplifying channels were entirely independent and could be used either for recording the same action potential from different points of the muscle or for simultaneous recording of an action potential and the essentially isometric contraction. Records were made by photographing the screen of the scope. In all cases an upward deflection of the record means increasing tension, or negativity of the electrode closer to the site of stimulation (C or D in fig. 1, for example) with respect to the distant one (E in fig. 1).

RESULTS

Dependence of action potentials on properties of the stimulus

The size of the electrical response of this muscle (peak voltage of action potential at a fixed point) was studied as a function of stimulus strength in order to establish a maximal or other standard stimulus. Representative examples for stimulus durations of 1 and 10 msec are shown in figure 2 for ''cathodal'' stimulation (electrode B in fig. 1 cathode and grounded). In similarity with Fletcher's curves, a definite plateau indicating maximal and supramaximal stimuli is missing, although his curves show somewhat less slope in the region where the plateau would be expected. Fletcher established his curves, however, by averaging responses to stimuli of stepwise increasing and later decreasing strength. As indicated by broken lines and arrows in figure 2, a repetition of the same (strong) stimulus after allowing sufficient time for the delayed relaxation in these cases no longer yields the same height of response. Plotting the means would result in less slope. With longer stimulus duration, the responses soon decline (fig. 2, curve b).

It seems important, therefore, to note that for both "anodal" and "cathodal" stimuli the response increases with stimulus strength to a peak, and then immediately starts to fall off with stronger stimuli.[3]

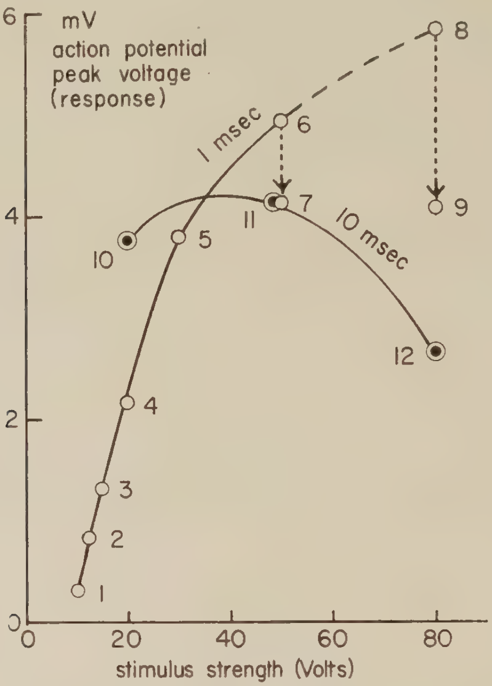

Fig. 2 Action potential peak voltage as function of stimulus strength. 12 successive "cathodal" stimuli; 1–9 (circles) 1 msec duration, 10–12 (dotted circles) 10 msec duration. Stimuli 1–6 applied at 2 min intervals, 7: 5 min, 8: 15 min, 9: 12 min, 10: 10 min, 11: 9 min, 12: 15 min after preceding stimulus.

Because of the lack of a maximal stimulus in the conventional sense, and because of the probability of damage by stimuli producing action potentials at or beyond the peak of the electrical response curve, a smaller "standard" stimulus was chosen with the help of mechanical records. The procedure consisted of stimulating the muscle tetanically with various rectangular pulses and recording the contractions isotonically or isometrically. Then the voltage, duration, and frequency of the pulses were varied and for each parameter the minimum value was determined which would still produce a nearly maximal contraction and not fatigue the muscle too soon. For any reasonably effective stimulation contraction was nearly complete in about 5 sec, and was independent of whether the individual pulses were all of the same polarity, or were alternated. In this way the optimum stimulus was found to be 20 V, the duration 1 msec and the frequency 10

---

[3] The larger response to weak stimuli and the earlier fall-off of the response curve with stronger stimuli of "anodal" polarity are probably due to greater current density under the cathode when it is at the extreme shell end of the fibers, and to some anodal polarization, which tends to increase the action potentials, nearer the recording electrode.

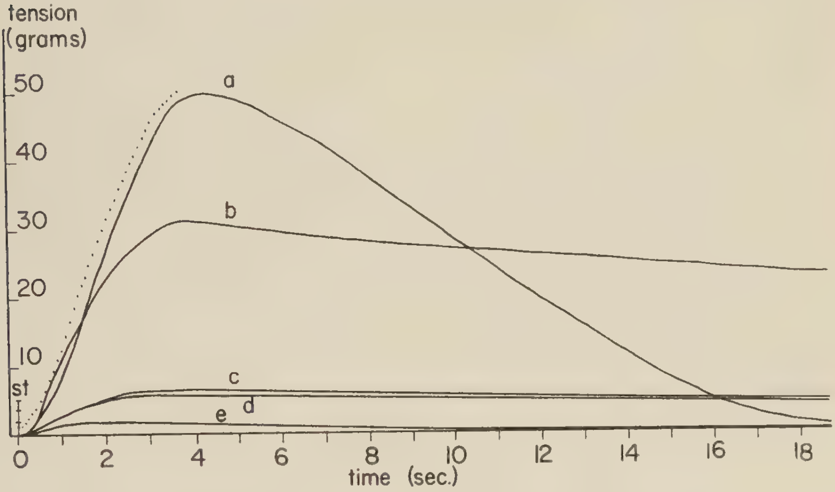

Fig. 3 Isometric contraction (tracings).

(a) Tetanic stimulation: 40 shocks of 20 V, 1 msec duration, 10/sec. Longer or stronger stimulation could increase the contraction by another 25 or 30%, which is apparently the maximal tension and cannot be surpassed even by use of multiple stimulating electrodes.

(b) Single stimulus 80 volts, 50 msec duration. Contraction is about 50% of maximal. Relaxation never became complete, apparently because of damage to the muscle.

(c) (d) (e) From records taken prior to (a) and (b).

(c) Single stimulus 30 V, 20 msec.
(d) Single stimulus 60 V, 5 msec.
(e) Single stimulus 30 V, 5 msec.

stim/sec. An isometric contraction due to such stimulation is shown in figure 3, curve a. Such contractions were followed by relatively fast relaxation, and could be repeated 30 to 60 times before fatigue appeared.

The mechanical response to such a single shock is very small but there is a marked "staircase effect" in this muscle (described below). The mechanical responses to single shocks increase with their strength and duration to a maximum near 50% of a tetanic contraction for a stimulus of 50 to 80 volts and 50 msec duration (fig. 3, curve b). However, at stimulus strengths already well below this, the muscles show signs of damage, such as very slow and incomplete relaxation, and rapid fatigue, leading to inexcitability after a few such stimuli. Thus a maximal single stimulus cannot be defined either with electrical or mechanical responses. Therefore the optimum pulse of 20 V and 1 msec duration was chosen as our standard stimulus, and used, except where otherwise stated, in the following.

Dependence of action potentials on distance from stimulating electrode

A typical action potential produced by a single stimulus (1 msec, 20 V) and recorded at two points 13 mm apart along the muscle is shown in figure 4. Since the amplification and other recording conditions for the two channels were made the same, it is apparent that the action potentials of this muscle decrease markedly in size as they are propagated down it. Fletcher ('37a) observed this effect (see DISCUSSION) but his explanation seems not to be satisfactory. Therefore, the first objective of the experiments reported here was to determine the cause of this decrease.

Any one, or combination, of the following factors could cause the recorded size of an action potential to decrease with distance from point of stimulation: (a) Decrease in the number of fully active fibers due to injury depolarization near the unstimulated end, or to some fibers ending between the recording electrodes. (b) Variation in conduction velocity (dispersion) among the fibers, causing their action potentials to get increasingly out of phase as they travel. (c) Arrival of the "front" of an action potential at the distal electrode (E in fig. 1) before arrival of the peak voltage at the proximal one. (d) "True" decremental conduction, i.e., decrease in the size of action potentials as they are propagated along individual uninjured fibers.

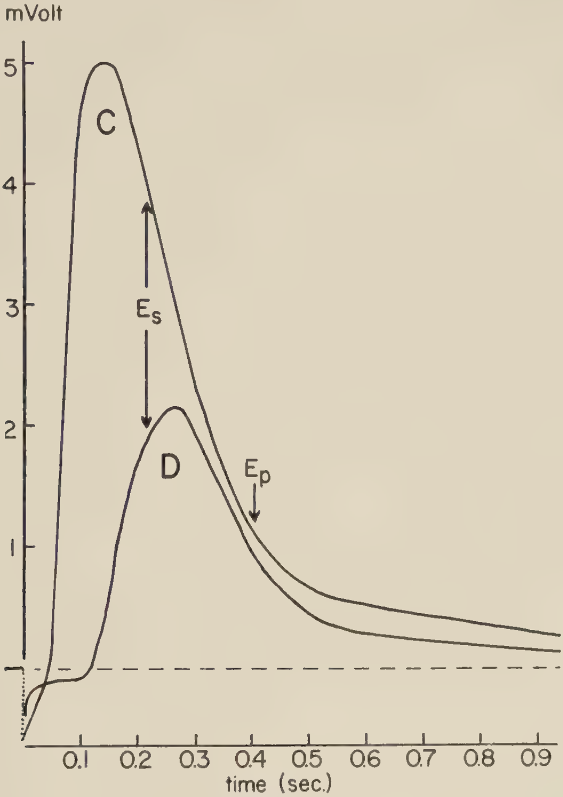

Fig. 4 Typical action potential recorded simultaneously at points C and D (fig. 1). Rectangular shock 20 V, 1 msec duration. Electrode distances in millimeters: A-B 6, B-C 6, C-D 13, D-E 16. E_s and E_p indicate at what time start and peak of the wave would occur at the distal electrode E, if the wave arrives there at all, as calculated from conduction velocity.

(a) The principal evidence against an injury current causing the observed action potential decrement is the fact that when the muscle is stimulated at the byssal end, nearly the same decrement is observed as when the action potential starts at the shell end. The byssal end was stimulated through electrodes E and D in figure 1, D being cathode and grounded, and channel I was connected to electrodes C and A, channel II to electrodes B and A. An injury near one end, if it allowed propagation at all, would cause an apparent increase in action potentials traveling away from it. Furthermore, the dissection technique described above, and the long survival in a steady state of the excised muscles, makes an injury which would depolarize this much very improbable. The strong decrement shown in figure 4 (reduction to about half in 13 mm) could be caused by fibers ending between the electrodes only if the *average* fiber length were about 18 mm, i.e., less than half the length of the muscle. This possibility can be ruled out by the careful histological work cited above.

(b) and (c) If the decrease in action potential size were due only to velocity dispersion among the fibers, we would find that the area under a true monophasic action potential (voltage-time integral) would remain constant due to increasing duration as peak voltage dropped. The usual method of obtaining monophasic action potentials by depolarizing the tissue under one electrode cannot, of course, be used when the full size of the potential must be observed. Another method is to place the distal electrode farther away from the proximal one than the length of the active locus. For example, in a muscle of 20 cm/sec propagation speed and 1 sec action potential duration the active locus will be 20 cm long and the electrode spacing should, therefore, be 4–5 times the length of the muscle. We could, however, obtain an accurate monophasic record of the rising phase of the action potential, which lasts e.g., 0.1 sec and thus occupies 2 cm of the muscle, by keeping the recording electrodes more than 2 cm apart.

The question then arises whether in a system with velocity dispersion, the area under just the rising phase of the action potential would remain constant during propagation. The answer to this is yes if the distribution curve of fiber velocities in the system shows a single maximum, i.e., if there are no separate groups of fibers such as the A, B and C fibers in a whole nerve. Experimental proof of this answer is provided by the data on frog sartorius muscle shown in figure 5. Evidence that the Mytilus muscle satisfies this condition is the uniformity of diameters of fully relaxed fibers and the fact that the action potentials showed no tendency toward more than one peak even after they had traversed the longest muscles.

(d) We may conclude, therefore, that in an uninjured muscle, if the area under the rising phase of the action potential recorded from any electrodes more than about 2 cm apart decreases with conduction distance, the individual fibers must show "true" decremental conduction rather than all-or-none behavior.

In 9 records on three different muscles in which an action potential was recorded simultaneously at two different points along the muscle as in figure 1, the distance between D and E being long enough to exclude any interference from deflection at E before the peak of the action potential at D was reached, the average decrease of area under the rising phase varied between 25.5% and as much as 61% per centimeter conduction distance.

In another series of experiments (125 records on 5 different muscles, conduction from shell to byssal end and 70 records on three different muscles, conduction in byssal-shell direction) a single proximal electrode was moved between stimuli, and the averages of several responses at each position were compared. In all cases the rising phase area decreased with distance already in the closest accessible region to the stimulating cathode, where any interference from negativity at the distal electrode could be excluded for the duration of the rising phase of the record. A representative group of such action potentials superimposed on each other is given in figure 5 a.

In figure 5 b the rising phase area is plotted against recording electrode position for a typical muscle conducting in both directions. The arrows indicate the point along the muscle where the front of the action potentials would be expected to arrive at the distal electrode. The absence of any visible increase at this point in the slope of the curves indicates that

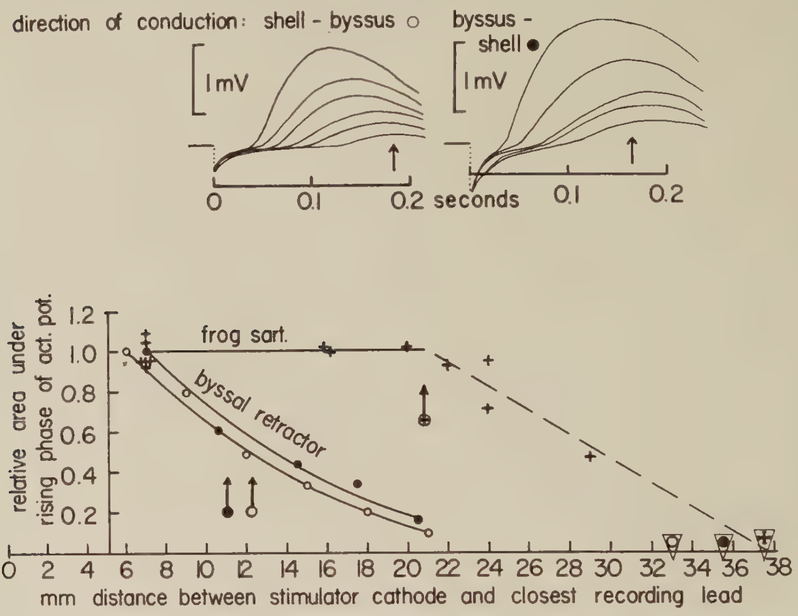

Fig. 5 (a) Upper part: Superimposed tracings of rising phases of Mytilus action potentials at different points along the muscle for both directions of conduction. Arrows indicate approximate time of arrival of the wave at the distal electrode.

(b) Lower part: Relative areas under rising phases of above action potentials are plotted as function of distance from stimulator cathode (abscissa). Hollow circles: Stimulated at shell end. Full circles: Stimulated at byssal end. Crosses: Results of similar experiments on frog sartorius. Arrows with symbol indicate earliest possible arrival of wave at distal electrode, triangles with symbol mark position of the respective distal electrodes. For frog sartorius, a straight line was drawn from this point to the point on the unit line where negativity at the distal recording electrode might start to interfere. The actual results scatter around this straight line.

in this case, as in several others, the decrement is so strong that no significant action potential reaches the distal electrode.

Also plotted in figure 5 b are the results of a similar analysis of the same kind of experiment carried out on that part of a frog sartorius muscle which is known to have parallel fibers. The velocity dispersion among these fibers is comparable with that in the Mytilus muscle, and the fact that the rising phase area stays nearly constant until the front of the action potential wave reaches E provides experimental proof of our argument above that this is what would happen in any system where the individual fibers showed decrementless (all-or-none) conduction. Whether the fall in the curve of frog sartorius may be due in part to fibers ending or tapering at these points has no bearing on the present consideration.

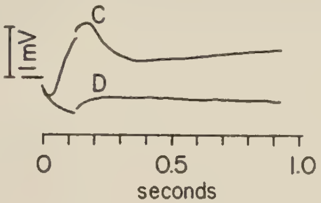

Fig. 6 Action potentials recorded at two points (C and D, fig. 1) along the muscle. Distances between electrodes in millimeters: A-B 6.8, B-C 6.8, C-D 8.5, D-E 14. Shock approximately 5.5 V, 125 msec duration (between gaps in record). The action potential fails to propagate through the 8.5 mm between C and D.

Further evidence of true decremental conduction in the Mytilus muscle is furnished more directly by the responses to ''small'' stimuli which frequently produce a distinct small action potential at the first of two proximal electrodes (C, nearest the stimulus) but not at the second (D). An example is shown in figure 6. Since the potential is invisible at D, its effect at E may be neglected, the area under the action potential is a true measure of total activity, and its disappearance at D is proof of decremental conduction in the active fibers.

A third kind of evidence bearing on this question may be obtained by measuring the maximum rate of rise of the action potentials. On the reasonable assumption that no fiber velocities increase with distance, the effect which velocity dispersion alone would have on this slope may be estimated by holding the area under the rising phase constant as its duration increases. For a representative series of records this procedure leads to an expected slope decrease of 3.5% per millimeter distance, while the actual slope decrease was 9.5% per millimeter. The only plausible cause of this difference is decremental conduction in the individual fibers.[4]

Electrical response to tetanic stimuli

Throughout this paper the expression "tetanic stimulus" will signify a series of short (1 or 2 msec) shocks separated by equal intervals less than 0.6 sec. Shocks repeated at constant intervals greater than this will be called a stimulus series. Since 0.6 sec is about the duration of the shortest single action potentials the fact that a tetanic contraction is maximal with a stimulus interval of about 0.1 sec suggests that the Mytilus muscle, in contrast to skeletal muscle, might still respond to stimuli spaced at intervals several times less than its action potential duration. This is confirmed by electrical records of such frequent stimulation as shown in figure 7.

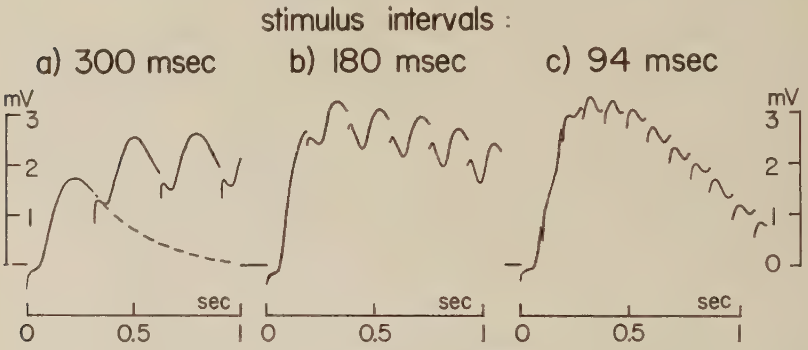

Fig. 7 Electrical responses to repetitive "tetanic" stimulation at intervals of (a) 300 msec, (b) 180 msec, (c) 94 msec.

---

[4] The influence of the decrement and of other factors on conduction velocity will be considered in a later paragraph.

Similar results are mentioned briefly by Fletcher ('37b) and by Prosser et al. ('51). Curve a in figure 7 gives the multiple action potential resulting from stimuli 0.3 sec apart.[5] The broken line indicates how the first action potential would have fallen off had the second stimulus not occurred. The contribution of the second stimulus is nearly equal to that of the first, and later ones maintain this peak voltage though they do not add to it. In curve b the stimulus intervals are 180 msec and each stimulus is again followed by a response. The reasons for the steeper rise of the first action potential will be discussed later. Curve c in figure 7 resulted from stimuli 94 msec apart and shows that a second stimulus can have a marked effect even when it falls within the rising phase of the first action potential. Here the third stimulus adds to the peak voltage, but the 4th does not, and the average voltage level drops off rapidly partly because the stimulus artifact is downward. Mainly for this reason records taken at 60 msec could not be interpreted. The amount of summation cannot be determined accurately because of such possible factors as increasing potential conducted to the distal electrode, steeper fall of the later potentials in a series as discussed later (augmentation) and possible changes in the shape of the stimulus artifact deflection. However, we can conclude that the absolutely refractory period, if there is one, is well under 90 msec, i.e., less than 15% of the shortest action potential duration.

One attempt was made to find out if simultaneous stimuli at different points on the muscle would lead to summation of separate action potentials conducted to a common point. No such summation could be observed at a point outside the stimulated region when the muscle was stimulated simultaneously at three cathodes (anodes between) about 50 msec conduction time apart.

---

[5] These responses are strikingly similar to those recorded by Kuffler and Vaughan Williams ('53) on repeated stimulation of nerves to 'slow' skeletal muscle fibers of frog.

Electrical responses to series of stimuli: Augmentation

When the muscle is given a series of standard stimuli with intervals less than about 30 sec, a new phenomenon occurs which we will call the ''augmentation effect.'' This is an increase in size of successive action potentials similar to the well known mechanical staircase effect in muscle.

Plate 1 a shows a typical series of 5 action potentials produced by equal rectangular stimuli (20 volts and 1 msec) given at intervals of 1 sec. During this series the oscilloscope beam was dimmed, so that fainter curves represent later action potentials. Except for the baseline of the first, all other action potentials start from the same level, which indicates that no significant summation was present. It will be noticed at once that, in comparison with the first, the subsequent action potentials increasingly become (a) higher, (b) steeper in their rising phase, reaching the peak earlier, and (c) steeper in falling phase and in some cases more biphasic. The phenomenon can be seen only in the first 7 to 10 action potentials from a series of stimuli, after which a steady state is reached. These changes were observed in every case, although they differed in magnitude from muscle to muscle.

From 50 records taken at various times during experiments on 20 different muscles, and at various distances from the stimulating electrodes, the results in table 1 were obtained. The stimuli used in this table were rectangular shocks of 20 to 40 volts and 1 msec duration and spaced at intervals of 0.8 to 5 sec. The augmentation effect has been investigated with series having intervals between standard individual shocks varying from 60 msec to 60 sec. The results are summarized in figure 8. Also the intervals between successive series of 5 stimuli (intervals between individual stimuli being in the optimal range of 1–4 sec) were varied from 2.5 sec to more than two minutes.

The results from these experiments may be condensed as follows: At shock intervals of about 30 sec or more, a response is no longer affected by its predecessor. Thirty seconds is also sufficient between any two series of 5 or so action potentials to secure almost the same increase in action potential voltage in the second series as in the first one. Both these results suggest that, at room temperature, a time near 30 sec

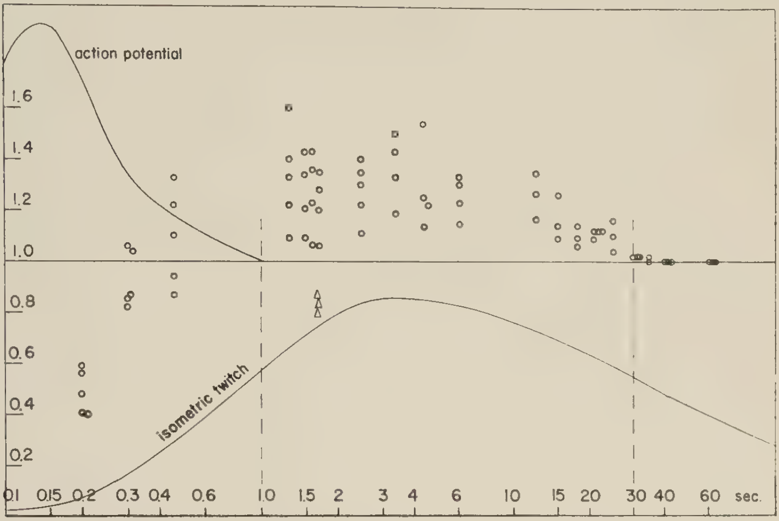

Fig. 8 Action potential voltage increase in the beginning of a series as function of stimulus interval. Ordinate: Voltage of action potentials in terms of the first of the series. Abscissa: Intervals between individual shocks in seconds, logarithmic. Circles: Averaged values from 100 series on 10 different muscles. The lowest circle in any vertical row of circles represents the relative size of the second, the next higher circle that of the third action potential with respect to the first. If two or more action potentials in a series have nearly the same voltage, they are marked as partly overlapping circles, shifted to the right as the series progresses. Triangles: Relative sizes of action potentials in a series subsequent to tetanic stimulation, averaged from 15 series on 6 different muscles. Time courses of a normal action potential and of an isometric twitch are added. The broken vertical lines at 1 and 30 sec separate the three groups referred to in the text.

is required for disappearance of measurable influence of previous activation of this type on an action potential, or, alternatively, for restoration of the conditions for a full scale increase in a stimulus series. Series following each other at shorter intervals, e.g., 10 sec, indicate partial persistence of the conditioning, i.e., the initial action potential of a second series is higher than that of the first, so that augmentation of the later members of a second series is less apparent. A 2.5 sec interval between two series merely continues the normal development from the level reached by the previous series.

Augmentation during tetanic stimulation

An augmentation effect also occurs in the responses to stimuli with intervals less than the duration of a single action potential (fig. 7). Because of the action potential "summation" which occurs here, the height of an individual action potential was measured from the potential level at which it started up to its particular peak. When analyzed this way, these records show typical augmentation from the second response on to about the 7th, but the second is smaller than the first. Later potentials may exceed the first at low but not at high tetanus frequencies. Averaged results from such experiments are plotted in figure 8 to the left of the dotted line at 1 sec. The relative positions of these three sets of points are reliable, though their absolute level (with respect to the horizontal line at 1.0) may be partly influenced by the long persisting effect of tetanic stimulation on the first subsequent action potentials, described in the following paragraph.

Action potential series following a tetanus

In addition to summation and augmentation effects, there is a third way in which repetitive stimulation of this muscle influences subsequent action potentials. A standard stimulus shortly after a tetanus produces an action potential with a higher voltage and usually a more rapid rise than normal. When a series of standard stimuli (interval 1 to 10 sec) is applied after a tetanus, the first action potential is substantially larger than the second and the later ones show augmentation with respect to the second, as illustrated in plate 1 b. The effect is also responsible for the difference in size between the first action potential in the tetanus shown in figure 7 b or c and that in 7 a which is the normal size, because 7 b and c were recorded soon after 7 a. As an average from 15 experiments on 6 different muscles, the peak voltage of the second action potential was 25% (range 10% to 60%) less than that of the first in a series subsequent to standard tetani (10 stim/sec for 5 sec). These cases are plotted as triangles in figure 8, where it can be seen that on the average the later action potentials did not reach the size of the first. If a tetanus involved fewer stimuli than standard, the first response in a succeeding series was nearer normal, and more augmentation occurred.

TABLE 1

	ACTION POTENTIAL VOLTAGE IN TERMS OF THE FIRST ACTION POTENTIAL IN THAT PARTICULAR SERIES					
	2nd	3rd	4th	5th	6th	7th act. pot.
Average of mean values from 20 different muscles	1.14	1.36	1.44	1.54		
Average of a total of 50 records from 20 different musc.	1.12	1.30	1.43	1.53	1.61[1]	1.74[2]
Lowest value	1.00	1.04	1.11	1.15	[1] average from 16 records	
Highest value	1.37	1.87	2.20	2.46	[2] average from 6 records	

The duration of this effect following a standard tetanus is several minutes (10 minutes following several tetani, plate 1 b). It is not "washed out" by activity during the period, for it may be seen to a smaller degree in a second and sometimes a third stimulus series following a tetanus. In 9 experiments the average decrease between first and second action potentials in such a second series was 14%.

This effect of a tetanus on succeeding action potentials was found to be qualitatively independent of all the factors considered below with regard to augmentation effect, i.e., strength and polarity of stimuli, direction of propagation, electrode position, and mechanical condition of muscle.

Influence of stimulus strength on augmentation effect

Increasing the stimulus in strength up to 80 volts and in duration to 10 msec does not affect the phenomenon qualitatively, though the relative and absolute increase in action potential height is somewhat less with strongest stimuli.

TABLE 2

STIM. DURATION	1 msec							10 msec		
Stimulus voltage V.	10	12.5	15	20	30	50	80	20	50	80
Voltage of 1st act. p.	0.33	0.83	1.31	2.16	3.79	4.12	5.82	3.76	4.11	2.65 [1]
Voltage of 4th act. p.	0.48	1.31	2.09	3.05	4.80	5.05	6.58	4.93	5.40	3.53 [1]
Increase in mV	0.15	0.48	0.78	0.89	1.01	0.93	0.76	1.17	1.29	0.88
Fourth a. p. relative to 1	1.44	1.58	1.60	1.41	1.27	1.23	1.13	1.31	1.31	1.33

[1] Muscle apparently hurt by previous stimulation of 50 V for 4 × 10 msec.

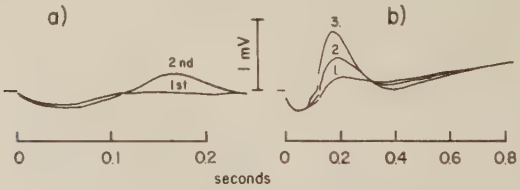

Fig. 9 Augmentation near threshold.

(a) Two equal stimuli (ca 5.5 V, 110 msec duration) given with 1.7 sec interval. Response recorded 8.5 mm away from cathode. No response to first, marked response to second stimulus.

(b) Three equal stimuli (ca 5.1 V, 110 msec duration.
- (1) Given prior to typical augmentation series (5 shocks of 20 V, 1 msec duration at intervals of 1.6 sec).
- (2) Given 1.6 sec after the 5th stimulus of the augmentation series.
- (3) Given 1.6 sec after a second such augmentation series which followed the first one after three minutes. For clarity, the augmentation series are not shown. They resembled closely that of plate 1 a.

Representative values from one muscle are given in table 2. Evidence given above indicates that stimuli of the strengths finally used in this example are damaging to the muscle. Augmentation also occurs when the individual shocks are near ''threshold'' in voltage and of long duration. Definite action potentials appeared later in some of these series even when the shocks were such that the first produced no observable response at the particular point of recording, figure 9 a. This was also true and even more marked, if a normal series of action potentials was placed in between two equal threshold stimuli. The response to the second small stimulus was then several times greater than that to the first, whenever the first was measurable, and it frequently led to a sizable second response even when the first could not be seen, figure 9 b.

Influence of some other factors on augmentation

The augmentation effects illustrated above were obtained with the stimulating cathode being closer to the recording leads. Very nearly the same changes occur when the closer electrode (B in fig. 1) is anode, and also when the polarity of the electrodes is alternated from shock to shock. An example of responses to stimuli of alternating polarity is shown in plate 1 c, where the levels of consecutive peaks increase regularly because the larger responses to ''anodal'' stimulation in this case happen to be compensated by the larger shift of base line (mentioned under METHODS), due to the ungrounded stimulus anode being closer to the recording lead.

When the direction of propagation along a muscle was reversed by stimulating near its byssal end, the relative increases in a series of responses were roughly the same as for the other conduction direction in that muscle.

The influence of position along the muscle, or distance between stimulus and recording electrodes on augmentation effect was also studied The augmentation is qualitatively the same wherever action potentials can be observed on the muscle. However, the relative increase between the first and a later action potential in a series, whether measured as peak height or as area under the rising phase, is greater for large conduction distances than for small, as shown for a representative case in table 3. This means that the later action potentials are propagated with relatively less decrement than the early ones in an augmentation series.

The mechanical condition (tension) of the muscle must be considered because, since tension increases with each stimulus, it is a possible source of augmentation. To investigate this, series of action potentials were recorded with the muscle at various initial tensions in the range 0 to 60 gm (about 2 kg/cm^2; more tension leads to irreversible "slip"). Except for small differences near the lower and upper limit of this range which may be attributed to different positions of the electrodes on the muscle, tension changes do not change augmentation effects significantly. Since 60 gm is much more than 5 standard stimuli can develop, this means that tension cannot play a significant part in causing the augmentation.

TABLE 3

MM DISTANCE FROM STIM. CATHODE	5	7	9	11	13	15	17
Relative peak voltage of 4th act. pot. in units of 1st	1.21	1.29	1.43	1.34	1.39	1.47	1.58
Relative area under rising phase of 4th act. pot. in units of 1st in its series	1.03	1.04	1.12	1.37	1.34	1.40	...

Conduction velocity under various conditions

The velocity of propagation of the action potentials (conduction velocity) was determined under standard conditions, and as a function of action potential size as influenced by stimulus strength, by distance from stimulus electrodes (decrement), and by previous stimulation (augmentation). Velocity was measured by recording from two points along the muscle (e.g., C and D in fig. 1), the separation of which was reasonably large and accurately known. Usually the time of arrival of an action potential at an electrode was taken as the intersection of the base line with the tangent to the inflection point of its rising phase. (This gave essentially the same results but more reproducibly than did use of the first measurable separation of trace from base line.)

The average conduction velocity in 14 muscles under standard conditions (stimulus 20–30 V, 1 msec, at shell end), was 22 cm/sec (range 17–29 cm/sec) at an average room temperature of 23°C. The two byssus-to-shell velocities measured also fell within this range.[6] The standard error in any one measurement was roughly 8%.

A comparison was made in several muscles between velocities of ''standard'' action potentials, and the larger ones produced by larger but unharmful stimuli (up to 50 V). Although in two cases the larger action potentials appeared to travel about 10% faster, there was in general no significant effect of stimulus strength on conduction velocity.

In order to estimate the effect of decremental conduction on velocity, data were used from a few suitable experiments in which successive action potentials were recorded at increasing known conduction distances. The time of arrival of the action potential at each position, measured from its stimulus artifact, was plotted as function of position, measured from the stimulus cathode. The conduction velocity of the segment of muscle between any two positions of the recording electrode is given by the slope of this curve between the two points.

These data do not show variations of velocity with conduction distance up to 20 mm which are significant in view of the size of the experimental errors. The accuracy is, however, sufficient to allow the conclusion that the rate of any decrease in velocity is several times smaller than the rate of decrement. Beyond 20 mm the action potentials were usually less than one-third original size and there was sometimes a significant drop in velocity. When these time-position lines are extrapolated toward the stimulated end of the muscle, most of them cross the cathode position at a time about 20 msec after the 1 msec stimulus. This effect, which was also reported by Fletcher, indicates either a delay of 20 msec (or slow propagation) as the action potential starts, or more likely a site of origin not at the cathode but nearer the end of the muscle (or the anode).

---

[6] Fletcher observed comparable variations and no preference for either direction of conduction, but his average velocity was somewhat lower (17.6 cm/sec), probably due to his lower temperatures of 12.5 to 18°C. Prosser et al., who submerged the muscle in mineral oil, found velocities of about 60 cm/sec. It is difficult to see how this difference in technique alone could account for such a large disagreement.

Special experiments were directed toward the question of whether conduction velocity changes accompanied the augmentation effect. Here each action potential was recorded 'simultaneously' at two points, with optimum separation and amplification, and the reproducibility of velocity measurements was the order of 3%. The average velocity difference between the first and 5th action potentials in 10 series on three different muscles was less than 2%, and therefore of no significance. Also, no significant velocity change associated with the first large action potential in a series following tetanic stimulation could be detected.

Effects of ionic changes in the medium

Another condition under which changes in action potential shape could be tested for influence on conduction velocity was provided by changing the composition of the medium (Hodgkin and Katz, '49). Results will be presented of about 150 records on 5 muscles exposed to a solution in which 50% of the sodium chloride was replaced by isotonic dextrose, all other components being present in the same concentration as in artificial sea water.[7]

---

[7] Replacement of NaCl by choline chloride led to a rapid irreversible inactivation and contracture of the muscle, as expected from the results of Twarog ('54) on acetylcholine.

In general the changes produced by low Na$^+$ are the opposite of those seen with augmentation except for conduction velocity, which decreases markedly as illustrated by figure 10. In this case the conduction velocity dropped within the first 4–6 minutes in the new medium to about two-thirds and after another 30 minutes to about one-half of its value in normal artificial sea water, the reapplication of which for 10 minutes resulted in regaining approximately 90% of the original conduction speed.

Table 4 provides a brief survey of the other effects of low sodium content of the bathing fluid together with the results

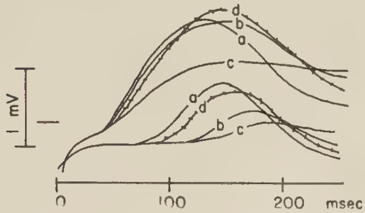

Fig. 10 Action potentials recorded at points C and D (fig. 1): (a) in normal sea water; (b) after 6 minutes; (c) after 36 minutes in solution with NaCl content half normal; (d) (crossed curve) after 8 minutes of reapplication of normal sea water. The total period of exposure to low sodium was 41 minutes. In this figure (d) is unusually small with respect to (a).

TABLE 4

	COMPARED WITH NORMAL	
	In low NaCl	Increased K$^+$
Mechanical response (isometric contraction)	Weaker, finally almost completely suppressed	Stronger
Action potential:		
Rising phase	Less steep	Steeper
Time of peak	Later	Earlier
Peak voltage	Decreased	Not much changed
Rate of repolarization	Smaller	Greater
Augmentation	Qualitatively always present	
Peak voltage after reapplication of normal sea water	Usually markedly higher for some time immediately after reapplication of normal sea water	

from K-enriched solutions in which the content of KCl was increased three- or 5-fold at the (relatively small) expense of NaCl, all other constituents unchanged.

Throughout these experiments the augmentation effect (increase in action potential height, rate of rise, and biphasic tendency) was always present, even when the individual responses were quite abnormal. The listed effects of change in ion content of the bathing fluid were reversible even after an hour or more.

Correlation of mechanical response and action potential

When single standard stimuli are used (20 V, 1 msec), the mechanical responses (isometric "twitches") show the same dependence on stimulus polarity as do action potentials, i.e., the contraction is larger when electrode B in figure 1 is anode than when it is cathode. This relation is reversed for very large stimuli, e.g., 60 V and 20 msec.

Single mechanical responses of an unfatigued muscle to a series of standard stimuli usually showed a clear staircase phenomenon accompanying augmentation of the action potentials, as seen in plate 1 d. The successive tension developments in such a series show a greater percentage increase over the first than do the action potentials. There is also a marked staircase effect of tetanic contractions produced by equal tetanic stimulation at intervals of one to several minutes.

However, with shocks that are stronger than standard or of longer duration or both, or with muscles not sufficiently relaxed since previous activation, the largest contraction step occurs earlier in the series and may even be the first (see plate 1 e). In such cases the action potentials show typical augmentation while the associated contraction steps are decreasing in size.

The converse situation may occur in a stimulus series just after a tetanus (plate 1 b) where the first action potential is the largest, but is associated with an extremely small contraction, whereas later smaller potentials lead to much larger contraction steps.

It may be summarized then that under some conditions there is a merely qualitative correlation between changes in the action potential size and the associated contraction increments, and that various special conditions can change either of the responses independently of the other.

DISCUSSION

In this section we propose to consider the arguments which lead us from the above experimental results to two major conclusions about the byssal retractor muscle.

1. Individual fibers do not respond, either electrically or mechanically, in an all-or-none way, and do conduct decrementally.
2. The responses of an individual fiber show the augmentation effect, i.e., vary with the interval since and frequency of previous stimulation.

Deviation from all-or-none behavior

Although several of the experimental findings presented here agree with Fletcher's, they suggest to us a different interpretation. Fletcher and subsequent workers concluded that this muscle conducts without decrement. However, if one examines in Fletcher's diagram ('37a, fig. 10) the areas under the reconstructed monophasic action potentials for proximal and distal electrodes, the proximal is roughly 20% larger than the distal. But even an increase in the area under the distally recorded action potential would not be surprising under his experimental conditions since he most certainly had some injury depolarization at the stimulated shell end where he cut and tied the muscle. His argument that after crushing the muscle decrease in action potential and increase in injury potential go parallel is irrelevant to this problem since, as Fletcher admits, the injury potential alone cannot account for the decrement in action potential. The increment in opposite direction, which would be expected if the decrement were only due to injury potential, is missing. From these quite correct observations Fletcher concludes that injury must cause some other unknown change in the tissue. However, the present studies combined with Fletcher's results, including his description of a local contraction unaccompanied by a fully conducted action potential, established quite conclusively that under the common experimental conditions conduction in this muscle is truly decremental.

This conclusion also fits in with the shape of the stimulus-strength response curves or stimulus-duration response curves. We apparently were not able to reach a maximal stimulus before damaging parts of the muscle, since up to such damaging stimulus strengths the action potential peak voltage increased and thereafter decreased progressively. The fact that no plateau of response over some range of stimulus strengths can be attained in these curves could be understood by assuming that stronger stimuli are noxious to some fibers which are exposed to the higher current densities, while other fibers farther inside the muscle or with high threshold are still not maximally stimulated. Thus it may be concluded from these strength-response curves that simultaneous maximal stimulation of all fibers is not possible. However they indicate an optimal stimulus range, namely where the steep initial rise of such curves begins to lessen. Our experiments were performed mainly in this optimal range and thus, for the muscle as a whole, were submaximal as those of Fletcher probably were also.

These results are in harmony with the findings from tetanic stimulation. An all-or-none response necessitates an absolutely refractory period of at least the length of the rising phase. However, since apparently only submaximal stimulation was possible, it might be argued that a first shock fired off only one set of fibers and the second a different set, each fiber, however, being strictly an all-or-none system. As Fletcher has pointed out, with sufficiently high frequencies this would require several sets of fibers which would be fired off in an alternating manner but otherwise have the same voltage output and time characteristics. This is an unlikely assumption, especially since these partial fusions of action potentials occur with different frequencies, which would require that the number of identical sets increases with increasing frequency. It also would require the assumption that a first shock of 1 msec duration after 100 or 600 times its duration would still be effective so that a previously subthreshold shock now fires off an action potential. Fletcher infers and we agree that a considerable amount of fusion occurs in single fibers. The results of tetanic stimulation show that the fibers can undergo partial depolarization, a property necessary for decremental conduction.

Combining then decremental conduction, lack of maximal stimulation, and lack or extremely short duration of absolutely refractory period, it is highly probable that contrary to previous belief, fibers of this muscle do not follow all-or-none behavior.

Augmentation

Experiments have ruled out all reasonable possibilities that the phenomenon described above as augmentation is an artifact: (1) it cannot be due to electrotonic polarization since it is present with millisecond shocks of alternating polarity, also with 25 sec intervals between shocks, and it is greater at greater distances from the stimulus. (2) The presence of the effect at 25 sec intervals rules out potential summation as cause since DC recordings show the potential always returning to the base line in less than 2 sec. (3) It cannot be due to contraction since the successive changes in electrical and mechanical records may vary independently of each other and it can be observed at all levels of passive tension. (4) All Mytilus muscles (some of which subsequently last 24 hours) show the effect, but in the same recording set up frog muscles do not.

The next question is whether it is logically possible to explain overall augmentation on the assumption that the individual fibers are all-or-none at a specific point for a fixed stimulus. The answer is yes *if* we suppose that a stimulus, subthreshold for a particular fiber, nevertheless lowers its threshold through a period many times longer than any polarization due to the stimulus (see Erlanger and Gasser, '37) so that the next stimulus of the same size activates the fiber. This hypothesis preserves the all-or-none character of the tissue only by endowing it with a new property (analogous to synaptic facilitation), but never established for all-or-none structures. Such behavior has been reported for olfactory nerve of pike by Garten ('03) and for frog muscle and nerve by Beritoff ('12), who describe a "Treppenphänomen" of action potentials from repetitive submaximal stimulation. Their observations were made with capillary electrometers or string galvanometers, and to our knowledge, have never been confirmed with modern equipment. These effects apparently only occurred within the duration of the negative after potential (supernormal phase) following a response and thus were probably due to the same group of fibers starting the same size action potential from a higher base line as clarified for nerve by Gasser ('35). The tendency of an all-or-none fiber to have a different threshold after a response is, of course, well known (see Graham, '34) but is not involved in explaining augmentation.

Our experiments also provide one piece of direct evidence against such persistent conditioning by subthreshold stimuli. This is the fact that we still observe augmentation with stimuli large enough to damage many of the fibers, and which would on the basis of the response to small stimuli and estimates of the final current densities throughout the muscle exceed the threshold of all fibers present (if they had a threshold). For this reason, and because of the implausibility of the required long persisting threshold change by subthreshold stimuli, it appears safe to abandon the idea that augmentation is caused by the later identical stimuli bringing in more all-or-none fibers.

We are therefore left with the conclusion that each individual fiber responding at the recording electrode gives a higher response to later stimuli in the series. This could happen either by higher response at the stimulating electrode conducted normally along the muscle, or by conduction of a standard response with less decrement, or both. The first possibility might correspond to the supernormal phase, usually expressed as lowered threshold to evoke the same all-or-none response, here, however, since it is not an all-or-none system, seen as greater response of the same elements to the same stimulus. Since we did not record exactly at the stimulating cathode, we cannot separate the two effects quantitatively. However, we do know that the observed augmentation is at least partly due to better conduction because (1) the factor of increase between the first and later action potentials in a series is greater at large conduction distances than at small (table 3 and related text), and (2) the later action potentials are more biphasic indicating more voltage at the distal electrode. Some information about mechanism of this decremental conduction would emerge from a study of any factors which would influence propagation speed. Therefore comparisons were made between the conduction velocities of the normal "first" action potentials and those of the larger and more rapidly rising action potentials late in an augmentation series. Neither these large action potentials nor those produced in other ways (i.e., first response after a tetanus, and the large ones which often occur when the muscle is returned to normal sea water after immersion in low sodium solutions) showed a conduction velocity more than 2% above normal (the probable error in velocity measurement). This is to be compared with the 50% increases in rate of rise of action potentials (volts/sec), and is difficult to explain, since membrane theories of conduction predict some connection between rate of rise and velocity. Such a connection appeared, on the other hand, when both velocity and rate of rise of action potential were depressed by immersing the muscle in a low sodium solution.

It may be worth while to mention one hypothetical mechanism which, on the assumption that Hodgkin's Na-ion theory (Hodgkin, '51) applies to this muscle, would explain how a change in action potential shape could lower velocity, but the opposite change would not raise it. Suppose that in this muscle under normal conditions the velocity were limited by a time constant inherent in turning on the inward sodium transport mechanism giving the action potential. Once the mechanism has been started it can transport Na^+ faster than normally (as it does later in a response series, or when internal Na^+ is low) but this does not cause the next element to be active any sooner because it is limited by its own time constant. However, when we sufficiently reduce the external Na^+, we can make the rate of rise of the action potential so small that depolarization of the membrane does determine the time of firing off the next element rather than its inherent time constant.

On this hypothesis, augmentation would be explained as an improvement in organization of the Na^+ transport as a series progresses, leading to a larger inward Na^+ current in each fiber during the action potential rising phase. This is in harmony with the facts that a low sodium solution around the muscle produces changes opposite to augmentation, and after the muscle is returned to normal sea water, the action potentials frequently are larger than normal.

It is important to compare the behavior of this muscle with that of the 'slow' skeletal muscle fibers of the frog described by Kuffler and Vaughan Williams ('53). They observed with intracellular electrodes the potential changes in these muscle fibers after nerve stimulation and interpreted them as a form of end plate or 'junctional' potential. These fibers show potential summation very similar to that in the Mytilus muscle (fig. 7) and also decremental conduction, but with a much stronger decrement(their potentials disappeared in a few millimeters, while in Mytilus it might take about 10 mm for a potential to drop to half). The 'slow' frog fibers did not show any augmentation effect and since all stimulation was through the nerves, variation of response size with stimulus strength had a different significance from that observed in the Mytilus muscle. The different decrement rate is probably responsible for the important difference that the 'slow' frog fibers depended on excitation at many points to produce maximal tension, whereas tetanic stimulation at one point of the Mytilus muscle could produce a "maximal" contraction (i.e., as strong as any produced by use of multiple stimulating electrodes). This does not imply, of course, that Mytilus fibers do not depend on multiple innervation for their normal function in the living animal.

This molluscan muscle may prove to be valuable for further studies into some still unsolved problems of impulse transmission, for instance, depolarization and Na-transport, since it apparently represents a primitive but widespread kind of conduction, possibly an intermediate form between protoplasmic irritability and conduction in vertebrate skeletal muscle and nerve.

SUMMARY

Electrical and mechanical records were taken from the unstriated anterior byssal retractor muscle of the mollusc Mytilus edulis. This muscle does not show all-or-none behavior: (a) there is no maximal stimulus, (b) conduction is decremental, (c) the absolutely refractory period, if any, is shorter than the rising phase of an action potential. Repetitive stimulation showed: (a) summation of action potentials if stimulus intervals are less than action potential duration ("tetanic" stimulation), (b) "augmentation," i.e., steeper rise, higher peak, and steeper fall of the first 7 to 10 action potentials, with stimulus intervals up to 30 seconds, (c) an unusually large first action potential even several minutes after tetanic stimulation. Augmentation was qualitatively independent of stimulus strength and polarity, direction of conduction, distance from stimulating electrode, and passive stretch. It was unaccompanied by conduction velocity increase, whereas Na deprivation, otherwise producing effects

opposite to augmentation, resulted in slowing conduction. Large mechanical staircase effects may occur independently of augmentation. Augmentation may be caused by an equivalent to "supernormality" in nerve, or by less decremental conduction after activity, or both. These results force us to abandon the previously accepted all-or-none concept for individual fibers of this muscle. Apparently they exhibit an intermediate behavior between general protoplasmatic irritability and the specialized conduction process in nerve and vertebrate striated muscle.

LITERATURE CITED

Abbott, B. C., and J. Lowy 1953 Mechanical properties of Mytilus muscle. J. Physiol., *120:* 50P.

Beritoff, J. S. 1912 Zur Kenntnis der Erregungsrhythmik des Nerven- und Muskelsystems. Zschr. f. Biol., *62:* 125–201.

Clare, M. H., and G. H. Bishop 1955a Dendritic circuits, the properties of cortical paths involving dendrites. Am. J. Psychiat., *111:* 811–825.

——— 1955b Properties of dendrites; apical dendrites of the cat cortex. EEG Clin. Neurophysiol., *7:* 85–98.

Eggleton, M. G. 1934 A physiological study of phosphagen in plain muscle. J. Physiol., *82:* 79–87.

Erlanger, J., and H. S. Gasser 1937 Electrical signs of nervous activity. University of Pennsylvania Press, Philadelphia.

Fatt, P., and B. Katz 1951 An analysis of the end-plate potential recorded with an intra-cellular electrode. J. Physiol., *115:* 320–370.

Fletcher, C. M. 1937a Action potentials recorded from an unstriated muscle of simple structure. J. Physiol., *90:* 233–253.

——— 1937b Excitation of the action potential of a molluscan unstriated muscle. J. Physiol., *90:* 415–428.

——— 1937c The relation between the mechanical and electrical activity of a molluscan unstriated muscle. J. Physiol., *91:* 172–185.

Garten, S. 1903 Beitrage z. Physiologie des marklosen Nerven. Fischer, Jena.

Gasser, H. S. 1935 Changes in nerve potentials produced by rapidly repeated stimuli and their relation to the responsiveness of nerve to stimulation. Am. J. Physiol., *111:* 35–50.

Graham, H. T. 1934 Supernormality, a modification of the recovery process in nerve. Am. J. Physiol., *110:* 225–242.

Hodgkin, A. L. 1951 The ionic basis of electrical activity in nerve and muscle. Biol. Reviews, *26:* 339–409.

Hodgkin, A. L., and B. Katz 1949 The effect of sodium ions on the electrical activity of the giant axon of the squid. J. Physiol., *108:* 37–77.

KUFFLER, S. W., AND E. M. VAUGHAN WILLIAMS 1953 Small-nerve junctional potentials. The distribution of small motor nerves to frog skeletal muscle, and the membrane characteristics of the fibres they innervate. J. Physiol., *121:* 289–317.

VAN NIEUWENHOVEN, L. M. 1947 An investigation into the structure and function of the anterior byssal retractor muscle of Mytilus edulis. (Thesis, Utrecht) Dekker en van de Vegt N. V. Nijmegen-Utrecht.

PROSSER, C. L. 1954 Activation of a nonpropagating muscle in thyone. J. Cell. and Comp. Physiol., *44:* 247–254.

PROSSER, C. L., H. J. CURTIS AND D. M. TRAVIS 1951 Action potentials from some invertebrate nonstriated muscle. J. Cell. and Comp. Physiol., *38:* 299–320.

TWAROG, B. M. 1954 Responses of a molluscan smooth muscle to acetylcholine and 5-hydroxytryptamine. J. Cell. and Comp. Physiol., *44:* 141–163.

WINTON, F. R. 1936 The changes in viscosity of an unstriated muscle (Mytilus edulis) during and after stimulation with alternating, interrupted and uninterrupted direct currents. J. Physiol., *88:* 492–511.

PLATE 1

EXPLANATION OF FIGURES

All records to be read from left to right. (a) Series of 5 action potentials. Duration of one sweep passage (width of record) 1 sec. First action potential 5.1 mV, 5th 6.35 mV. Stimuli 20 V, 1 msec duration, at intervals of 1 sec. Beam dimmed stepwise so that fainter curves represent later action potentials.

(b) Simultaneous mechanical and electrical records of a series of 4 action potentials, 10 minutes after last tetanic stimulation (12 tetani given within previous 34 minutes). Stimuli: 4 shocks 20 V, 1 msec, at intervals of 1.3 sec. Electrical record: Beam stepwise dimmed. Duration of one sweep passage 282 msec. Peak voltage of first (brightest) action potential 1.9 mV. Mechanical record: One passage 1.2 sec, on the scope all the time. (Stimulus artifacts in the last quarter.) Increasing tension produces upward deflection. Total tension increase on this record 3 gm.

(c) Series of action potentials produced by stimuli of alternating polarity. Shocks of 20 V, 1 msec at intervals of 2.5 sec. Beam progressively dimmed. Group with small stimulus artifact, containing the first (brightest) action potential: polarity as in figure 1, B cathode. Group with bigger, artifact, containing the second action potential: stimulating lead B in figure 1 anode, not grounded, A cathode and grounded. Total width of record 1 sec, peak voltage of first action potential 2.1 mV.

(d) Simultaneous electrical and mechanical responses to 6 shocks of 20 V, 1 msec duration, at intervals of 2.5 sec. Action potential record: beam stepwise dimmed. Peak voltage of first (brightest) action potential 1.9 mV. Tension increase from lowest to highest stimulus artifact on the record was 5.75 g. Same time scale for both records: Total width 1 sec.

(e) Simultaneous electrical and mechanical responses to 5 stimuli of 25 V, 5 msec duration, applied at intervals of 4.3 sec. Action potential record total width 1 sec, beam stepwise dimmed. Peak voltage of first action potential 0.67 mV. Mechanical record: total width of record 4.3 sec (beam always on scope). Tension increase from lowest to highest stimulus artifact 3.68 gm.

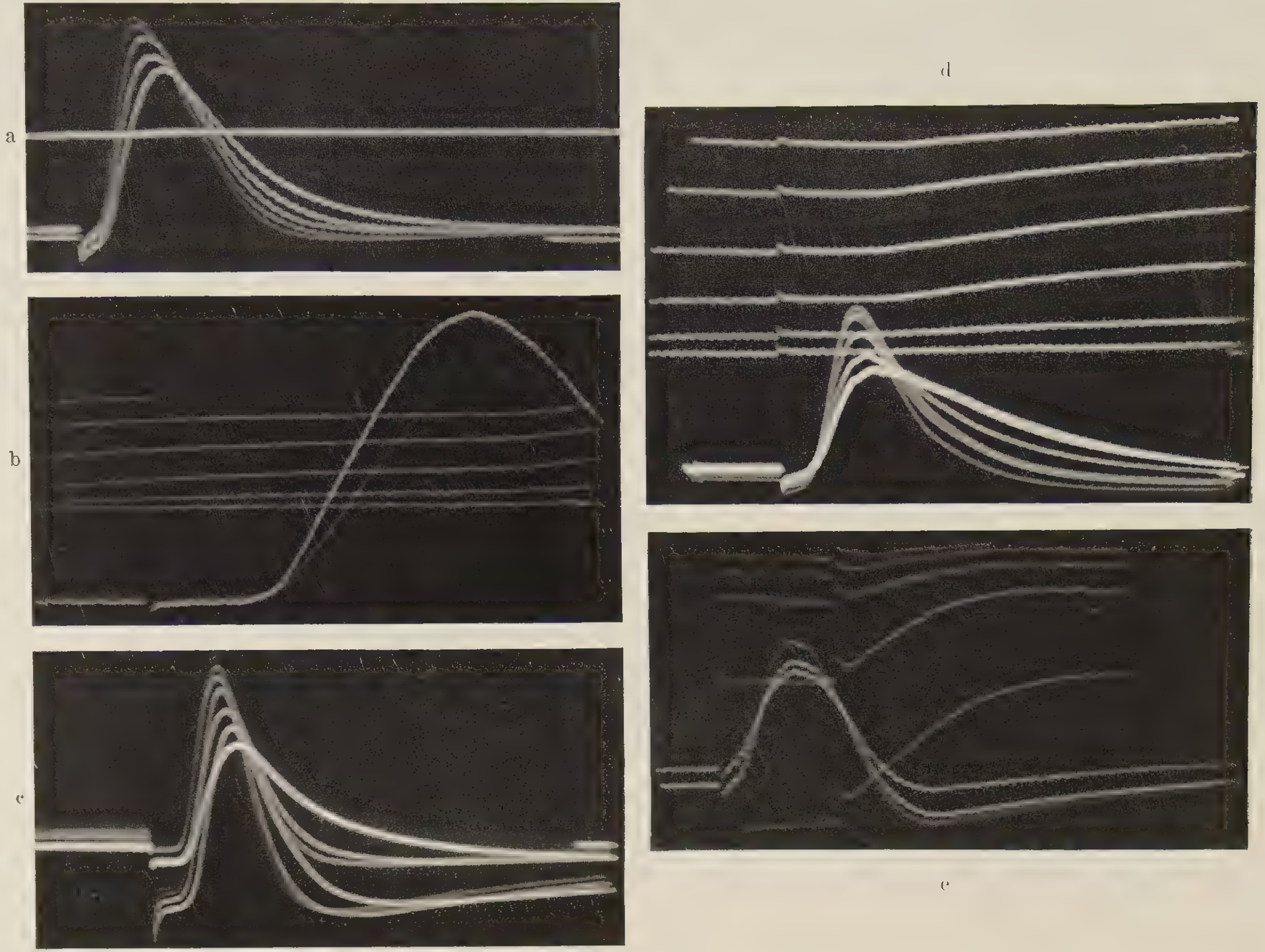
a
b
c
d
e

TISSUE SURVIVAL AFTER EXPOSURE TO LOW TEMPERATURES AND THE EFFECTIVENESS OF PROTECTIVE PRETREATMENTS

I. EVALUATION BY GROWTH IN TISSUE CULTURE [1]

A. CECIL TAYLOR AND ROBERT GERSTNER
Department of Anatomy, College of Dentistry and Graduate School of Arts and Science, New York University, New York, N. Y.

SEVEN FIGURES

A variety of mammalian tissues, both normal and malignant have been shown to survive exposure to extremely low temperatures. The literature also contains negative reports and there are unpublished failures to demonstrate evidence of life after freezing. The disparity between these results as well as considerable disagreement on the method of freezing most favorable for survival stem in large part from the use by different investigators of unlike tissues and of different treatments in freezing and from the failure to measure and define conditions with sufficient accuracy.

Survival of fresh skin frozen without pretreatment has been reported by Klinke ('39), Mider and Morton ('39), Briggs and Jund ('44) and by Billingham and Medawar ('52). Recently Polge, Smith and Parks ('49), and Smith and Parks ('51) have shown that pretreatment of spermatozoa and other tissues with glycerol or ethylene glycol solution protects

---

[1] Supported by a grant from the American Cancer Society upon recommendation of the Committee on Growth of the National Research Council to the Department of Anatomy, College of Dentistry, New York University, New York; and by a grant from the Atomic Energy Commission to the Plastic Surgery Unit, Department of Surgery, College of Medicine, New York University, New York.

against freezing injury. One of us had in the past repeatedly failed to obtain survival of unprotected mammalian (Taylor, '46, '49) and amphibian tissues after exposure to very low temperatures or after freeze drying (Weiss and Taylor, '43, '44). The results of these attempts have lead to the undertaking of a study to determine more exactly the effects of extremely low temperatures on living cells and the conditions under which tissues may remain alive after having been frozen. As a beginning for this work a series of tests has been made to determine the degree of survival which could be obtained in our laboratory under several conditions reported as favorable to survival. This paper presents these findings. They include a comparison of the effects of simple freezing and thawing with those of freezing and thawing after different pretreatments. A comparison is also made between the effects of these procedures upon normal skin and upon several malignant tissues.

Various methods are available for assaying the injury to cells and survival of tissues. Among them are observation of contractility or motility, observation of persistance and growth of grafts, application of vital stains, determination of enzyme activity, measurement of respiratory products, etc. Each has certain advantages and limitations. For this investigation an estimation of the amount of outgrowth from cultures *in vitro* of tissues previously treated has been used. Some advantages of the tissue culture method are the following. (1) It permits continuous microscopic observation of the treated tissue so that evidence of survival may be detected directly in cell behavior. (2) By the same observations, alterations in the cell morphology and behavior induced by the various treatments may be studied for clues to the nature and mechanism of the injury inflicted. (3) The treated tissue is completely isolated in a cell free medium. Thus there is no problem, as there often is with grafts *in vivo,* of distinguishing between the treated cells and untreated cells which may freely invade a graft from the surrounding host tissue.

Skin was selected as a test tissue because (1) on theoretical grounds, it should be more resistant to cold injury than other tissues, (2) because of clinical interest in the possibility of preserving it alive for grafts, (3) but especially because it would be a convenient tissue to use in correlated experiments on frozen autografts.

It has been well established that many transplantable tumors retain their infective capacity after frozen storage. Although questioned by Guy and his associates ('49) it is generally assumed that this capacity is evidence of survival of at least some of the frozen cells. For comparison with normal skin, three tumors of mice were subjected to the same freezing treatments. Two of these were rapidly growing mammary carcinomas and one a more slowly growing melanoma. A melanotic tumor was chosen because previous work (Taylor, '49; Billingham and Medawar, '52) had shown that normal melanocytes in the rat and rabbit are more susceptible to injury by freezing than other cells of the skin. It would be of interest to determine whether this susceptibility was shared also by the pathological pigment cells.

METHODS

Tissues

The tissues used in these tests were normal skin from laboratory stock rats and mice, and three types of mouse tumor. The skin was removed from the dorsum of the adults from which the hair had been shaved, or from new born animals after the surface had been swabbed with alcohol and ether to reduce contamination. Skin from near term fetuses obtained by Caesarian section was also used. The latter was preferred and more frequently used because it gave more rapid and luxuriant outgrowth in tissue culture. Since the normal skins obtained from these sources differed little in their response to the experimental treatment, the results have been here combined.

The tumors used were mammary adenocarcinomas from C3H and DBA strains of mice and Harding Passey melanoma. Growing tumors were removed and the active surface tissue dissected free under sterile conditions for use in the experiments.

All of these tissues, with the exception of those to be dehydrated as described below, were cut into strips measuring approximately 2 × 12 mm. These were then subjected to various pretreatments and freezing. After thawing, each strip was trimmed and cut into fragments for culturing.

Freezing and thawing

A wide range of rates of cooling and rewarming is now under investigation to determine the effects upon survival of tissues. The results will be reported elsewhere. For the present study an arbitrary rate was chosen on the basis of (a) the results of preliminary survival tests, (b) the ease of accurate repetition and (c) the applicability to tissues for grafting as well as for these *in vitro* experiments.

The procedure for freezing was to fold the moist strip of tissue over the test junction of a thermocouple or allow it to adhere to the surface of a fine wooden splint. In either case the tissue was then placed in a test tube (18 ×150 mm) so that it was suspended in air about 7 mm from the bottom and sides of the tube. The tube was then stoppered and immersed to within 2 cm of its top in liquid nitrogen for over three minutes. Rewarming was achieved by removing the splint or thermocouple from the test tube and plunging it, with the attached tissue, into Tyrode solution at room temperature until the tissue was thawed.

The actual temperature changes of the tissue were followed by means of a copper-constantin thermocouple embedded in the center of the tissue fragment or enfolded by it. To reduce error from heat conduction along the thermocouple, very fine wires (40 gauge) were used and these were heat insulated where they passed through the cooling tube. The reference junction was kept on ice at 0°C. Potential differences generated in the thermocouple actuated a Leeds and Northrop recording potentiometer which made a direct tracing of the temperature curve. Temperature recordings for each experiment were made repeatedly until the rate of temperature drop and rise with the exposure to freezing and thawing environments were reliably established. Subsequent freezings for the particular experiment were done on wooden splints without thermocouples.

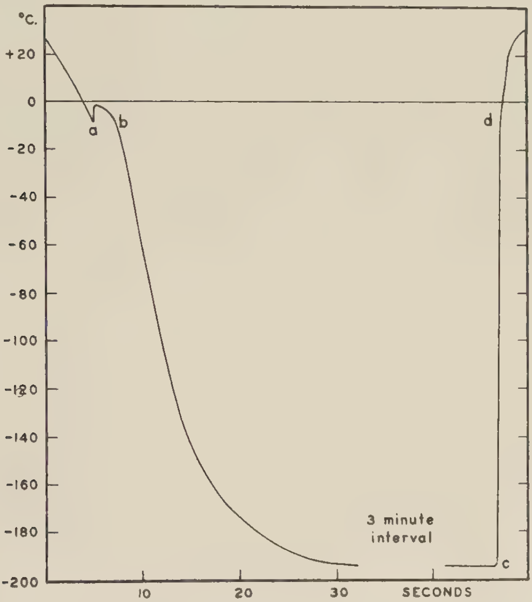

Fig. 1 Thermograph showing the temperature change within a fragment of untreated rat skin frozen and thawed by the method used in this study.

Figure 1 shows a typical thermograph obtained from chilling and rewarming a piece of rat skin according to the method described above. In this example the tissue was supercooled to — 8°C. by a steady drop in the temperature. At this point (a) ice crystal formation in the tissue caused a sudden rise in tissue temperature which reached about — 2.5°C. During the following two seconds (a-b) most of the water in the tissue was crystallized. Since ice is a better heat conductor than water the rate of heat dissipation from the tissue, and hence of its temperature drop, is more precipitous after freezing than before. Below — 150°C. the cooling rate slowed down as the tissue temperature approached that of its environment. To make certain of complete and thorough cooling, in all cases the tissue was left in liquid nitrogen for at least three minutes.

At (c) the tissue was plunged directly into warm Tyrode solution causing an abrupt temperature rise from — 190°C. to 0°C. in about one second. At the melting point a slight delay in warming can be detected due to the heat of fusion of ice. Although the latent heats causing the deflections at a-b and at d are equal the shorter time of the thawing deflection (d) is due to more rapid transfer of heat when the tissue is in contact with water.

Tissue culture

All tissues were cultured by the standard Maximow double cover slip method. Since the object of culturing was to determine the state of vitality of the tissue at the time of explanting it was not deemed necessary to carry cultures for more than 6 days. During this period the relative number of cells still alive and their activity in outgrowth could be estimated. Most of the cultures were, therefore, not washed or subcultured.

The medium used was commercially prepared lyophilized chick plasma, chick embryonic extract and horse serum in ratios of 1–1–2. To this was added penicillin at 1000 units per cubic centimeter, since complete sterility of skin fragments could not be assured.

Explanted tissues were incubated at + 36°C. and were examined daily. The state of vitality and the degree of outgrowth of all cultures were evaluated by comparison with control explants from the same tissue sample, cultured in the same medium under conditions identical to those of the experimental fragments.

An arbitrary system was adopted for evaluating outgrowth. The outgrowth from untreated controls was designated as grade 4. This grade does not represent an absolute quantitive measurement of outgrowth but varies with the length of incubation time. Grade O represents no outgrowth whatsoever. Grades 1, 2, and 3 stand for outgrowth approximately 25%, 50%, and 75%, respectively, as extensive as that of control samples of tissues incubated for the same length of time. Difficulty was encountered with this system in evaluating very poor outgrowth which exhibited only 1 to 20 cells. These were assigned fractional values for the protocols. In constructing tables and graphs these fractions were added and the integral sum placed in the category of grade 1.

Observations were made on the type of cells to emigrate from the explant and the time and order of their emergence. Deviations from the characteristic, or typical cell of each type were looked for and the history of cytological changes during the observation period was noted.

Experiment 1 — freezing without pretreatment

The basic experiment was the simple freezing and thawing of untreated tissue. The cultures of fragments thus frozen were compared for the amount of outgrowth with fresh unfrozen controls which had been cut from the same tissue sample.

The tissues in this experiment and in controls of the following experiments are referred to as untreated. In reality, however, all tissues (except those in experiment 4) both control and experimental, were routinely immersed in Tyrode solution to facilitate handling and to prevent undesirable dehydration during cutting and preparation for culturing or freezing. In order to ascertain whether this immersion in Tyrode would in itself act as a pretreatment and alter the response of tissues to freezing, a test was conducted to compare the survival of freshly removed and immediately frozen samples of skin with samples immersed first in Tyrode solution for 20 minutes before freezing. In these experiments no outgrowth was observed after freezing regardless of whether the tissues had been immersed in Tyrode solution or not. On the basis of these results and because both controls and experimental tissues received the same exposure to Tyrode solution, for the purpose of this study, tissues were not considered pretreated if they had been immersed only in Tyrode.

Experiment 2 — ethylene glycol pretreatment

This was the freezing and thawing of tissue strips which had previously been immersed for 20 minutes in concentrations of ethylene glycol in Tyrode solution varying from 10% to 80% by volume. Immediately after pretreatment the strips were frozen and thawed as described above. After thawing, the ethylene glycol was removed from the tissue strips before they were cut and cultured. This was done by washing for 10 minutes in each of 4 changes of Tyrode solution.

To serve as controls for each sample of tissue cultured in this experiment, fragments were taken from the same sample and cultured in the same medium under identical conditions after the following treatments: (a) without any experimental treatment, (b) after freezing and thawing but without ethylene glycol pretreatment, (c) after the ethylene glycol treatment alone but without freezing and thawing.

Experiment 3 — glycerol pretreatment

In a similar way tissues were pretreated with glycerol in Tyrode solution. Concentrations of from 10% to 100% by volume were used and the tissues were immersed for 20 minutes. Freezing and thawing was carried out as described above. The thawed tissue strips were washed in 4 changes of Tyrode solution for 10 minutes each before being placed in the culture medium. *In vitro* outgrowth was compared with that of (a) fragments which had received no treatment, (b) fragments which had been frozen and thawed without pretreatment, and (c) fragments which had received glycerol treatment but had not been frozen and thawed.

Experiment 4 — air dehydration pretreatment

Tissues were frozen and thawed after varying amounts of water had been allowed to evaporate from them. To facilitate handling and weighing of the tissues during the process of desiccation each of the skin samples, including the controls, was stretched over a paper frame made by cutting a window in a square of filter paper. Tumor samples were simply spread on paper squares. Each paper frame, or square was weighed before affixing the tissue and then the tissue and paper together were weighed. The wet weight of the tissue was calculated from these values. Tissues were desiccated by simply exposing them to dry air until the desired weight loss had been attained. The degrees of desiccation tested ranged from losses of 10% to 80% of the original wet weight.

In the dehydrated state the tissues were frozen and thawed in the same manner as were the chemically treated tissues. Following thawing, they were allowed to rehydrate in Tyrode solution and were then cut into fragments for culturing. Outgrowth from these dehydrated and frozen fragments was compared to that from untreated frozen controls and from dehydrated controls which had not been frozen.

Experiment 5 — sucrose pretreatment

Preceding their freezing and thawing the tissues of this experiment were placed for 20 minutes in a solution of sucrose. The concentrations used ranged from 15% to 90% of stock saturated sucrose solution (room temperature) in Tyrode. Controls for this experiment were fragments from the same tissue samples (a) receiving no treatment, (b) frozen and thawed without sucrose pretreatment, and (c) receiving sucrose treatment but not frozen and thawed.

The number of tissue fragments cultured and evaluated in each of these experiments to test the effects of pretreatment were:

1.	Unpretreated tissue	2300 fragments
2.	Ethylene Glycol-Tyrode	2738 fragments
3.	Glycerol-Tyrode	2414 fragments
4.	Air dehydration	2475 fragments
5.	Sucrose-Tyrode	640 fragments

Perfusion chamber observations

The visible effects upon cells growing in tissue culture of freezing alone and of each of the several steps in pretreatment, freezing and thawing were studied. This was done with phase contrast illumination by use of a special microscope stage tissue chamber. The upper compartment of this chamber permitted perfusion and washing of the culture during observation. Through the lower chamber a fluid could be circulated to serve as either a coolant or a thawing agent. With this device observations similar to those on red blood cells and amoeba by Smith, Polge and Smiles ('51) could be made on cultured mammalian cells. Still and motion picture photographic records were made of the changes observed.

RESULTS

1 — Freezing of untreated tissue

All experiments with both skin and tumor included control tissues which were frozen without pretreatment. The total number of such fragments cultured was well over 2300. In these cases cooling to the temperature of liquid nitrogen, under the conditions described before, followed by plunging into warm Tyrode solution completely prevented subsequent outgrowth in over 99% of the tissue fragments cultured. A small proportion (0.4%) of frozen fragments showed outgrowth of from 1 to 5 cells during the first 6 days. The experiment in which these apparently surviving cells were seen occurred early in the course of our investigation. A test experiment was later conducted specifically to check on the possibility of this survival. In this test particular care was taken to guard against contamination with non-frozen cells and against the possibility of accidental dehydration before freezing. No growth was seen in any of these cultures. The fate of the cells on this more careful check and in all subsequent control cultures has led us to assume that the living cells seen in the early experiment resulted from errors in technique.

2 — Ethylene glycol pretreated tissues

A. Pretreated controls. Immersion of skin and tumor tissues in ethylene glycol solution at concentrations less than 60% for 20 minutes before culturing caused only slight suppression of outgrowth. Treatments with concentrations higher than 60%, however, resulted in a sharp decrease in the subsequent outgrowth. At a concentration of 80% nearly all growth was prevented.

The harmful effect of ethylene glycol treatment alone was not the same in the 4 tissues tested. At concentrations below 60% its effect ranged from none at all on C3H carcinoma to about 30% suppression in the case of Harding Passey Melanoma. In the order of their increasing susceptibility to the toxic effects of ethylene glycol the tissues are: 1 — C3H carcinoma, 2 — normal skin, 3 — DBA carcinoma, and 4 — Harding Passey Melanoma.

B. Pretreated and frozen tissues. Pretreatment with ethylene glycol afforded all tissues some measure of protection against damage by freezing. The degree of the protective effect was not equal for all 4 tissues, and it varied with the concentration of glycol solution used. Figure 2 shows the average grade of outgrowth for each tissue after treatment with different concentrations of protective agent. The best protection against freezing in all these experiments resulted from the treatment of C3H carcinoma with 30 to 40% ethylene glycol. Among tissues thus treated no fragments were entirely killed by freezing and 62% gave outgrowth as good as, or better than the unfrozen controls.

Normal skin was next best. After treatment with concentrations of 20% and 30% all skin cultures showed some growth, 13% as good as the unfrozen controls and 80% at least half as good as the controls. In the case of skin, protection by ethylene glycol pretreatment was effective over a wider range of concentrations than with tumor tissues, some survival being apparent after pretreatment with all concentrations between 10% and 70%. With the two remaining tumors protections were less pronounced and were limited to treatments with glycol solutions of 20% concentrations. In the case of Harding Passey Melanoma only 31% of the treated fragments showed any outgrowth after freezing, and none of these gave outgrowth better than half as good as the controls.

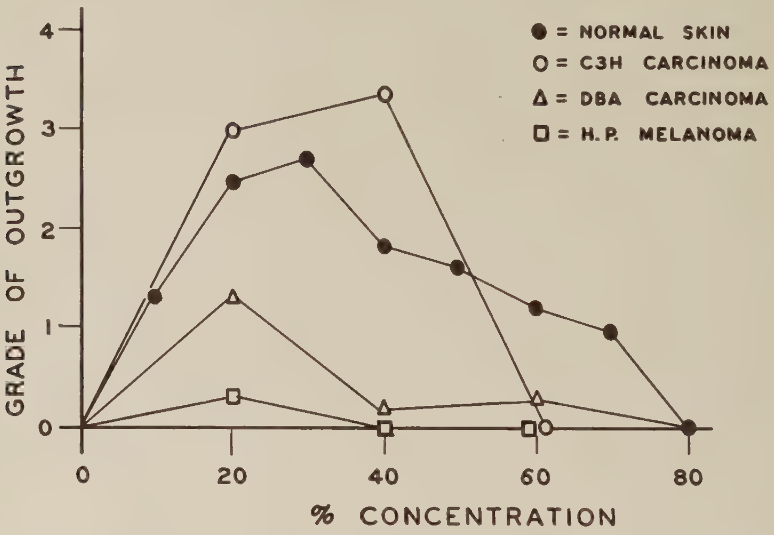

Fig. 2 Outgrowth from frozen tissues pretreated with ethylene glycol-Tyrode solution. Each point represents the average grade of outgrowth obtained from all cultures treated with the indicated concentration of protective agent.

3. *Glycerol pretreated tissues*

A. Pretreated controls. Tissues cultured after being treated with glycerol solutions for 20 minutes (without freezing) showed a decrease in average outgrowth that was roughly proportional to the concentration of the immersing solution. For normal skin and DBA carcinoma this was true only for the lower range. Immersion in 20%–30% solutions reduced outgrowth to an average value of grade 3 (25% reduction), and 50%–60% concentration to grade 2 (50% reduction). For these two tissues, treatment with higher concentrations did not further reduce the average of the grades of outgrowth but rather increased the spread of their distribution, so that in the case of skin treated with 90% glycerol, 14% of the fragments were without growth, while 13% were better than untreated controls. C3H carcinoma fared more poorly than DBA, whereas Harding Passey Melanoma gave no growth at all after treatment with solutions of 60% and higher.

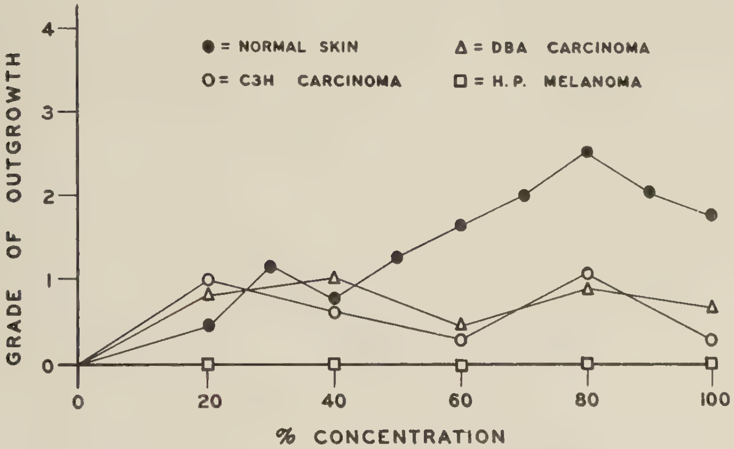

Fig. 3 Outgrowth from frozen tissues pretreated with glycerol-Tyrode solution. Each point represents the average grade of outgrowth obtained from all cultures treated with the indicated concentration of protective agent.

B. Pretreated and frozen tissues. The average outgrowth from the different tissues frozen after pretreatment with glycerol solutions are compared in figure 3. The highest grade of outgrowth was obtained from normal skin after pretreatment with 80% glycerol solution. Nineteen percent of the fragments so treated gave outgrowths as good as untreated controls and only 6% were without any outgrowth, the average grade of outgrowth being 2.5. With concentrations of glycerol above 50% the average grade of outgrowth obtained from tissues frozen after pretreatment was no lower than that from unfrozen tissues which had received the same glycerol treatment. Apparently, after pretreatment with these concentrations, all the tissue damage can be attributed to the glycerol treatment and none to the freezing.

This was not true for the two carcinomas where freezing consistently reduced the grade of outgrowth far below that for the unfrozen tissues with the same glycerol treatment. Although the protective effect of pretreatment in these two tumors was not as pronounced as in normal skin some of the fragments treated with each of the concentrations contained living cells.

No protection whatsoever was afforded to Melanoma tissues by glycerol pretreatment.

4. — Air dehydrated tissues

A. Dehydrated controls. Skin which was dried by evaporation of its water showed remarkable outgrowth when rehydrated and cultured. Seventy-three percent of the fragments which had lost 50% of their weight in evaporated water gave outgrowth as good as, or better than the undehydrated controls. Indeed it may be significant that in all tissues losing up to as much as 60% of their original weight in evaporated water some fragments grew better than the undehydrated controls maintained in Tyrode solution. After 70% weight loss, however, less than half of the fragments showed any outgrowth and none did after a weight loss of 80%.

It should be pointed out that samples of skin in these tests were not alike in their original water content. As calculated from weights before and after prolonged drying at 60°C. the adult skin contained from 60% to 70% of removable water while the fetal skin ran as high as 80%. This means that the amount of water removed, if expressed as a percentage of total free water in the tissue sample, would be a higher figure than the percentage based upon total tissue weight used in the graph. It is also obvious that those tissue samples indicated as having lost more than 70% of their original weight by desiccation were the fetal tissues which had a higher original water content than adult skin.

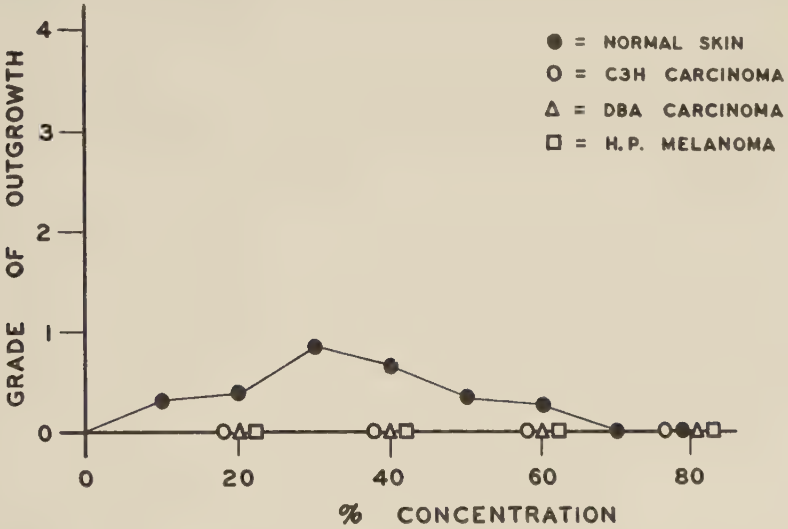

Fig. 4 Outgrowth from frozen tissues protected by dehydration. Each point represents the average grade of outgrowth obtained from all cultures losing the indicated percentage of weight through desiccation.

Dehydration without freezing affected the three tumors differently. In the case of C3H carcinoma weight losses by desiccation up to 60% improved the average outgrowth. The effects upon DBA were similar to those upon skin, while outgrowth from the Melanoma was more strongly suppressed.

B. Dehydrated and frozen tissues. In the case of skin, drying before freezing did offer some protection. The most effective pretreatment was 30% weight loss, figure 4. Even at its best, however, only 4% of the fragments exceeded grade 2, while over 60% of all fragments showed no outgrowth at all.

In none of the tumor tissues was there evidence of any protective action of dehydration pretreatment.

5. — *Sucrose pretreated tissues*

A. Pretreated controls. Normal outgrowth was obtained from skin treated with sucrose solution in concentrations up to 75%. No growth occurred after immersion in 90% solution. The two carcinomas were partially inhibited by treatment with 40% solution but still showed better than grade 2 outgrowth after immersion in 80% sucrose. Outgrowth from the Melanoma tissue was reduced to grade 2 after treatment with 20% sucrose and only 12% of the fragments showed any life after treatment with 60%.

B. Pretreated and frozen tissues. With the exception of a few cells observed in three of the DBA cultures, no outgrowth was seen in any tissues frozen after sucrose pretreatment. This was true even with skin, which showed excellent outgrowth after sucrose treatment alone.

In summary, a glance at the graphs makes several facts obvious.

1. The 4 treatments vary in the effectiveness of their protective action. Arranged in descending order of protection afforded they are: (1) ethylene glycol, (2) glycerol, (3) air dehydration, and (4) sucrose.

2. The 4 tissues vary from each other in their response to the treatment. C3H carcinoma and normal skin show the highest degree of survival and Harding Passey Melanoma shows the poorest. The malignant form of pigment cell thus exhibits the same vulnerability to freezing shown by the nonmalignant melanocytes as demonstrated in normal skin of the rat (Taylor, '49). These were shown to be killed by doses of cold which were sublethal for most of the other cutaneous cell types.

3. A tissue showing high survival rate with one pretreatment may show relatively poor survival with another (e.g., C3H tumors with ethylene glycol and with glycerol).

4. Air dehydration gives only partial protection to only one of the tissues tested (skin).
5. Sucrose was without effect in protecting against freezing damage.

6. *Retardation of outgrowth*

Cells which emigrate after the protective treatment alone or with freezing did not differ morphologically from cells emerging from untreated fragments. There was, however, a noticeable, consistent difference in the time of emergence and the rate of outgrowth of these cells. The retarding effect of glycerol and freezing treatment upon C3H tumor tissue is shown by the grades of outgrowth recorded for one experiment illustrated in figure 5. Here it is seen that the protective treatment alone delayed the outgrowth so that by the end of the first day of incubation a grade of only 2 or 3 was achieved. By the end of the second day, however, the difference between these explants and the controls had largely disappeared. The addition of freezing to glycerol pretreatment accentuated the retardation so that a grade of 1 was not obtained until the end of the first or second day. In

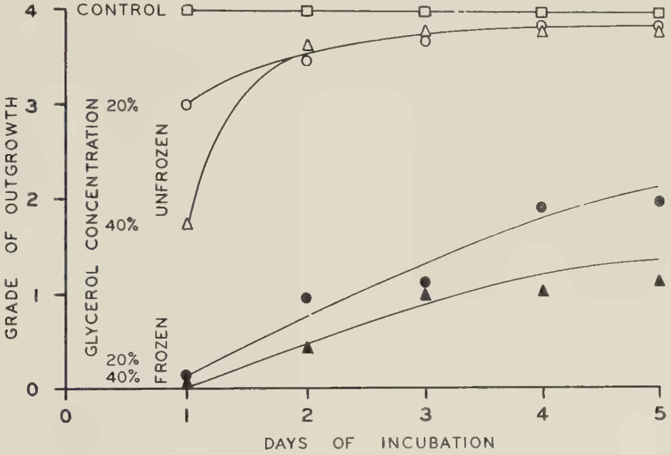

Fig. 5 The retarding effect of glycerol treatment and freezing upon the outgrowth from cultures of C3H tumor tissue.

the latter, although outgrowth consistently increased it did not catch up with the controls during the period of observation. The retarding effect was more pronounced after use of 40% concentrations of glycerol solution than after 20% concentration.

7. *Microscopic observation of cells during pretreatment and freezing*

By use of the perfusion chamber described above preliminary observations have been made on living cells during treatment. These observations have thrown some light on the response of isolated living cells to the experimental treatment employed and have suggested specific points for further study.

The gross damage done to a cell by freezing without pretreatment is illustrated in figure 6. The photograph at the left is of a cell in a culture being perfused with Tyrode solution before freezing. At the right is shown the same cell three minutes later after cooling to – 30°C. and rewarming to room temperature. Besides gross deformation of the cell there is obvious evidence of breakdown of the cell membrane. The optical properties of the cytoplasm and the size and distinctness of its granules are materially altered. Such cells were not observed to recover but invariably disintegrated.

The photographs of figure 7 show a group of cells at different stages in pretreatment with 30% ethylene glycol and freezing. In A are shown the cells in Tyrode solution before treatment. In B the same cells are seen about two minutes after perfusion with ethylene glycol solution. Slight retraction of the ends of the cytoplasmic processes can be detected. There is, however, little shrinkage to indicate loss of water from the protoplasm. In C are seen the cells after freezing to – 30°C. and thawing. Little morphological change is evident. Cell membranes appear intact and cytoplasmic processes remain extended. The optical contrast between hyaloplasm and granules is sometimes slightly increased. In picture C the cells are still in a perfusate of 30% ethylene glycol. Since prolonged immersion in this solution is lethal it was then washed out by gradual replacement with Tyrode solution. Picture D shows the effects of the return of the cells to saline solution. It is obvious that this is the most damaging step in the process. Large clear fluid filled vacuoles formed between the cell membrane and the cytoplasm. In some cells these were observed to subside with the recovery of the cell while in others they progressed to cause eventual rupture of the membranes.

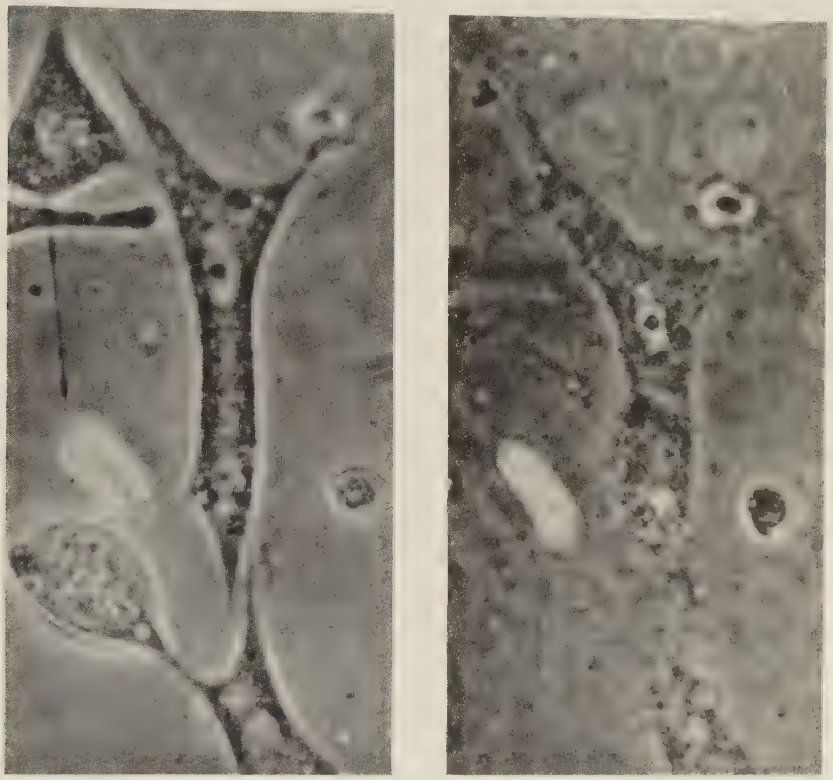

Fig. 6 Damage done to a cell by freezing without protective pretreatment. Left — Cultured cell perfused with Tyrode solution. Right — Three minutes after freezing to — 30°C. and thawing.

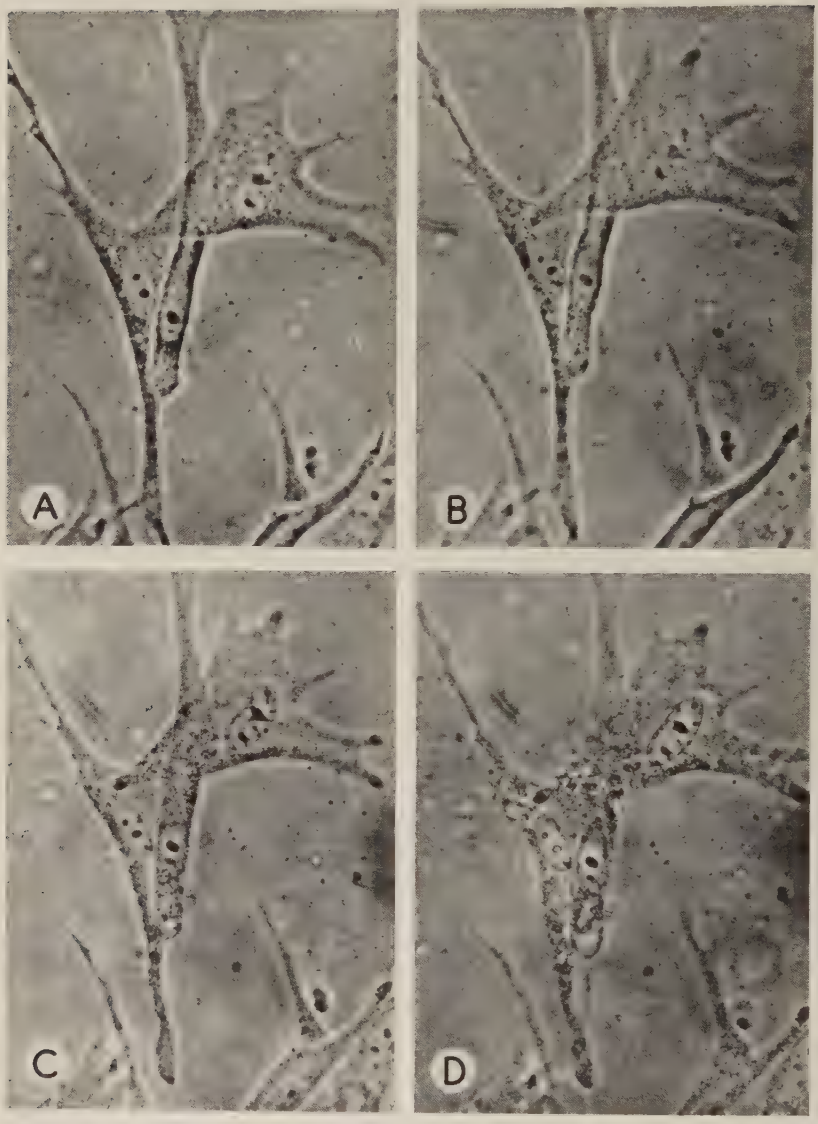

Fig. 7 Cells in the perfusion — freezing chamber photographed with phase contrast illumination. A. Perfused with Tyrode solution. B. Perfused with 30% ethylene glycol-Tyrode solution. C. After freezing to — 30°C. and thawing D. Ethylene glycol removed by continuous direct perfusion with Tyrode solution.

DISCUSSION

In this study cells chilled to — 195°C. without protective pretreatment failed to exhibit vital activity in subsequent culture. This result is in agreement with the studies of Smith ('52) on mouse ovarian tissue and of Pomerat ('53) on human skin when their tissues were cooled to similarly low temperatures. In both latter studies survival was judged by growth in tissue culture. On the other hand unprotected tissues frozen at low temperatures have been observed to survive if implanted back into the animal as autografts [Klinke ('39), Briggs and Jund ('44), Blumenthal and Walsh ('50), Billingham and Medawar ('52)].

From our recent grafting experiments to be reported elsewhere it is our experience that frozen skin which does not exhibit life when cultured in vitro may do so if grafted into the animal from which it was taken. This suggests that the environment in tissue culture is not sufficiently favorable for survival of cells which are damaged by freezing. While all cells of a tissue may not be killed by unprotected freezing those which do live must be severely damaged. Their inability to survive in culture, as do unfrozen cells, is evidence of this. So also is the relatively small numbers of surviving cells we have seen in frozen as compared to unfrozen grafts.

The degree of damage done to cells of a living intact tissue, such as skin, could not be directly visualized. However, in the case of cells in culture observed microscopically during freezing and thawing severe injury always resulted. In every case cell morphology was seen to be altered immediately after thawing and marked degenerative changes followed very quickly thereafter leading to eventual cellular breakdown. If the cells of an intact tissue are affected as are cells isolated in culture it is hard to see how any survival could occur. The recovery of some cells and tissues grafted after freezing suggest, therefore, that a degree of protection against low temperature damage may be afforded by the environment of the cell that is incorporated in an organized tissue which it lacks in growing in a culture medium. The failure of tissue fragments to survive in culture cannot be attributed to the small size of the piece of skin frozen, since fragments of identical size have been demonstrated to contain surviving cells when autografted.

Though tissue culture may not be a sufficiently sensitive method to detect signs of life in cells which have been severely damaged by freezing without protective treatment it is capable of clearly indicating the relative effectiveness of the different protective pretreatments that were tested and the difference in response of various types of tissues. Outgrowth from tissue explants which had received the various treatments before freezing ranged from none at all to luxuriant outgrowth which could not be distinguished from that of unfrozen controls.

The manner in which glycerol may effect its protection against freezing injury has been discussed by Lovelock ('53). He offers evidence to show that it acts as a buffer against damaging concentrations of salt in freezing. Luyet and Gehenio ('52) have emphasized the role of glycerol in binding some of the water of the tissue and thus reducing the amount of ice formed. The action of these protective agents is referred to as dehydration by Luyet and his colleagues. In the air dehydration experiment of this study, however, it is evident that loss of tissue water offers no protection to tumor tissues and only very slight protection to the skin. Both ethylene glycol and glycerol were far more effective in protecting all tissues. This would indicate that the protective action must be much more than simple dehydration. Furthermore, sucrose, considered to be a good dehydrator, was not at all effective, as used. Smith ('54) has argued that glycerol and ethylene glycol, since they rapidly penetrate into the cells, can produce only a transient dehydration of cells by osmosis.

From a study of the freezing characteristics of the protective solutions alone (Taylor — unpublished) it has been determined that a 40% concentration of glycerol or ethylene glycol in Tyrode solution, even when cooled at a relatively slow rate, may become an amorphous solid without the formation of ice crystals. Although tissues as a whole treated with these solutions were not found to be ice free, the amount of ice formed, as indicated by the liberated heat of crystallization, appeared to be greatly reduced and it may be possible that intracellular crystal formation is prevented.

Microscopic studies of the freezing and thawing process confirm the observations of Smith, Polge and Smiles ('51) that crystals formed in a medium of glycerol solution are small and granular as compared to the large spears or spikes which grow in saline solution alone. It was observed furthermore that gas bubbles of considerable size are left in the cytoplasm of cells upon melting of intracellular ice. The mechanical distortion of intracellular organization attendant upon phase changes from liquid to solid and back again and the violent redistribution of water and gas doubtless plays a part in cell damage along with the concentration of electrolytes and other physico-chemical changes.

A remarkable fact revealed by the microscopic studies of glycerol and ethylene glycol treated cultures is the lack of visible change in the cell as a result of freezing and thawing. This is in distinct contrast to the markedly altered morphology of the unpretreated cells after freezing. Far more damage resulted from too rapid application or removal of the protective solutions than from freezing and thawing. This latter damage was reduced by gradual changes of the perfusate or by interposing a cellophane membrane between the cultures and the perfusing solution as done by Polge ('51) for spermatozoa.

A word of comment concerning the toxicity of the protective treatments: except for extreme dehydration and the highest sucrose concentrations, dehydration treatment and sucrose solutions had no toxic effect on tissues. The proportion of glycerol treated fragments which exhibited inhibition of outgrowth increased with concentrations over 60%. However good survival followed immersion in 90%

concentrations. Skin treated in these higher concentrations for 20 minutes were hard and appeared glassy yet often gave good outgrowth upon culturing. Microscopic observation showed withdrawal of processes and contraction of cells during the first 8 to 10 minutes of perfusion with 30% glycerol. No further change was observed during the next hour of perfusion and the cells returned to normal appearance and activity when again placed in Tyrode. Irreversible changes set in after 8 minutes of direct exposure of the individual cells to 30% ethylene glycol. This interval could be extended to 15 minutes if a cellophane membrane were interposed. Longer treatment fixed the tissues. The toxicity of ethylene glycol probably accounts for the decline in the number of fragments showing outgrowth when freezing was preceded by immersion in concentrations above 40%.

SUMMARY

1. Normal rat and mouse skin and three tumors from mice were exposed to very low temperatures. Survival of these tissues and the degree of injury caused by the cooling treatment were checked by evaluating subsequent outgrowth in tissue culture and by direct microscopic observation.

2. The effects of freezing alone are compared with those of freezing preceded by protective treatment with glycerol-Tryode, ethylene glycol-Tyrode, and sucrose-Tyrode solutions and with simple air dehydration.

3. No vital activity was seen in cultured fragments of unprotected frozen and thawed tissue. Direct microscopic observation of cells thus treated revealed irreversible destructive changes.

4. Freezing and thawing caused the least injury to skin and tumor tissue when preceded by treatment with 30% ethylene glycol or 30%–80% glycerol in Tyrode solution.

5. Loss of up to 60% tissue weight by evaporation of its water offered only slight protection against freezing injury to skin and none at all to the tumors.

6. No protection from freezing injury resulted from treatment of tissues with any concentration of sucrose solution.

7. The bearing of these results on the mode of action of the protective agents is discussed.

LITERATURE CITED

BILLINGHAM, R. E., AND P. B. MEDAWAR 1952 The freezing, drying and storage of mammalian skin. J. Exp. Biol., *29:* 454–468.

BLUMENTHAL, H. T., AND L. B. WALSH 1950 Survival of guinea pig thyroid and parathyroid autotransplants previously subjected to extremely low temperatures. Proc. Soc. Exp. Biol. Med., *73:* 62–67.

BRIGGS, R., AND L. JUND 1944 Successful grafting of frozen and thawed mouse skin. Anat. Rec., *89:* 75–84.

GYE, W. E., A. M. BEGG, I. MANN AND J. CRAIGIE 1949 The survival of activity of mouse sarcoma tissue after freezing and drying. Brit. J. Cancer, *3:* 259–267.

KLINKE, J. 1939 Direct proof that cancer and normal cells live after freezing at temperature down to — 253°C. Growth, *3:* 169–172.

LOVELOCK, J. E. 1953 The mechanism of the protective action of glycerol against haemolysis by freezing and thawing. Biochem. et Biophys. Acta., *11:* 28–36.

LUYET, B. J., AND P. M. GEHENIO 1952 On the mode of action of glycerol in preventing injury by freezing in embryonic tissues of chick. Science, *11:* 526.

MIDER, G. B., AND J. J. MORTON 1939 Effect of freezing in vitro on some transplantable mammalian tumors and on normal rat skin. Am. J. Cancer, *35:* 502–509.

POLGE, C. 1951 Functional survival of fowl spermatozoa after freezing at — 79°C. Nature, *167:* 949–950.

POLGE, C., A. U. SMITH AND A. S. PARKS 1949 Revival of spermatozoa after vitrification and dehydration at low temperature. Nature, *164:* 666.

POMERAT, C. M., AND R. B. LEWIS 1953 The effect of rapid freezing and thawing on human newborn and adult skin. U.S.A.F. School of Aviation Medicine, Project no. 21-1202-0001 Report no. 5.

SMITH, A. U. 1952 Cultivation of ovarian granulosa cells after cooling to very low temperatures. Experimental Cell Research, *3:* 574–583.

—— ——— 1954 Biological applications of freezing and drying. I. Effects of low temperatures on living cells and tissues. Academic Press, New York.

SMITH, A. U., C. POLGE AND J. SMILES 1951 Microscopic studies of mammalian tissues during cooling to — 79°C. J. Roy. Microscopic Soc., *73:* 134–139.

SMITH, A. U., AND A. S. PARKS 1951 Preservation of ovarian tissue at low temperatures. Lancet, *2:* 570–572.

Taylor, A. C. 1946 Transparency of cornea after freezing in situ. Anat. Rec., *96:* 83.

———— 1949 Survival of rat skin and changes in hair pigmentation following freezing. J. Exp. Zool., *110:* 77–112.

Weiss, P., and A. C. Taylor 1943 Repair of peripheral nerves by grafts of frozen-dried nerve. Proc. Soc. Exp. Biol. Med., *52:* 326–328.

———— 1944 Transplantation of frozen dried cornea in the rat. Anat. Rec., *88:* (supp. 4) 99.

A STUDY OF THE PHOSPHORUS COMPOSITION AND P^{32} INCORPORATION IN IRRADIATED LYMPHATIC TISSUE [1]

HELEN HARRINGTON AND PAUL S. LAVIK

Atomic Energy Medical Research Project and the Department of Biochemistry, Western Reserve University, Cleveland, Ohio

Lymphatic tissue is one of the tissues most sensitive to ionizing radiation, and severe histological damage can be observed very soon after the administration of comparatively low radiation doses. On the other hand, such tissues as liver, kidney, and muscle show little damage after relatively large amounts of radiation (Hempelmann, Lisco and Hoffman, '52). The present investigation was based on the assumption that changes observed in the chemical composition and metabolic processes of the irradiated tissue might reveal information concerning the mechanism of radiation injury and the factors which determine the variation in the radiosensitivity of tissues to ionizing radiation. Accordingly, the phosphorus composition and the incorporation of radioactive phosphorus in thymus, spleen, and liver were compared at various intervals after the injection of a toxic dose of P^{32}.

EXPERIMENTAL

Wistar strain rats weighing approximately 200 gm were injected intraperitoneally with a toxic dose of P^{32} as sodium hydrogen phosphate (4.5 μc/gm body weight). This amount of P^{32} — the only radiation administered in these experiments

---

[1] The data in this paper were taken from the thesis submitted by Helen Harrington to the Graduate School, Western Reserve University, in partial fulfillment of the requirements for the degree of Doctor of Philosophy. Preliminary reports have been published previously (Lavik, Harrington and Buckaloo, '50; Harrington and Lavik, '51).

— was calculated to deliver about 500 roentgen equivalents to the thymus within 48 hours. At intervals after the injection, 4 or more animals were sacrificed and the desired tissue removed for analysis. In separating the acid-soluble, inorganic, phospholipid, ribonucleic acid (RNA), and desoxyribonucleic acid (DNA) fractions, a method was used which combined the main features of the procedures described by Schneider ('45) and Schmidt and Thannhauser ('45). Most extractions, however, were carried out in sintered-glass filter tubes, so that the tissue residue could be extracted exhaustively at each stage and thus avoid cross-contamination between phosphorus fractions of widely differing specific activities. The total phosphorus content of each fraction was determined by the method of Umbreit et al. ('49) except that the colorimetric procedure of Gomori ('42) was used. P^{32} was assayed in a liquid counter (Lavik, Harrington and Buckaloo, '51). The specific activity of each phosphorus fraction, corrected for radioactive decay, was then calculated as the per cent of the injected dose [2] per milligram of phosphorus in the isolated fraction. To provide a basis for comparison, control animals were given a tracer dose [3] (0.1 μc/gm body weight) of P^{32} and the tissues were removed, fractionated, and assayed as described above.

A modification of the methods of Dounce and Beyer ('48) and Euler et al. ('45), was employed in isolating cell nuclei from thymus tissue. At intervals after the injection, 4 animals given the toxic dose and 4 controls given the tracer dose were sacrificed and the thymus glands removed. The tissue was minced, squeezed through a small Délépine filter press to remove connective tissue, and homogenized in a small Waring Blendor in the presence of an equal mixture of 10% citric acid and cracked ice. The homogenate was filtered through one layer of lens paper, and the cytoplasmic debris was removed by centrifugation. Values for the DNA content per nucleus were obtained by dividing the concen-

---

[2] Doses were expressed as counts per gram body weight.

[3] The amount of carrier phosphorus injected was the same for the controls as for the irradiated rats, i.e., $0.1\,\gamma\,P^{31}$ injected per gram body weight.

TABLE 1

Effect of a toxic dose of P^{32} on the concentration of phosphorus in various fractions of rat tissues

DAYS AFTER P^{32} INJECTION	NO. ANIMALS	PHOSPHORUS CONTENT OF FRACTION, MG/GM FRESH TISSUE				
		Acid soluble		Phospholipid	RNA and Phosphoprotein	DNA
		Total	Inorganic			
		Thymus				
Tracer dose[4]	23	0.96 ± .04[1]	0.38 ± .04[1]	0.55 ± .03[1]	0.73 ± .04[1]	2.26 ± .13[1]
1/6	3	0.97 ± .03	0.30 ± .03	0.56 ± .03	0.77 ± .05	2.07 ± .19
1	4	0.98 ± .02	0.36 ± .02	0.62 ± .01	0.69 ± .05	2.08 ± .11
2	4	0.83 ± .03	0.36 ± .04	0.60 ± .02	0.46 ± .07	1.08 ± .21
3	4[2]	0.84 ± .03	0.41 ± .09	0.72 ± .04	0.59 ± .01	0.90 ± .05
6	8[3]	0.86 ± .04	0.36 ± .03	0.64 ± .02	0.52 ± .06	0.78 ± .09
8	8[3]	0.71 ± .08	0.37 ± .01	0.63 ± .08	0.50 ± .06	0.83 ± .21
		Spleen				
Tracer dose[4]	24	0.92 ± .06	0.32 ± .02	0.63 ± .04	0.51 ± .05	0.71 ± .12
1/6	4	0.92 ± .03	0.31 ± .02	0.57 ± .03	0.45 ± .05	0.58 ± .05
1	4	0.91 ± .04	0.35 ± .02	0.68 ± .08	0.45 ± .04	0.50 ± .04
2	4	0.92 ± .04	0.34 ± .04	0.69 ± .08	0.42 ± .04	0.41 ± .06
3	4	0.95 ± .03	0.36 ± .02	0.67 ± .05	0.44 ± .01	0.45 ± .05
4	4	0.89 ± .02	0.36 ± .02	0.65 ± .03	0.42 ± .03	0.40 ± .02
7	4	0.92 ± .05	0.35 ± .02	0.72 ± .05	0.48 ± .06	0.45 ± .09
		Liver				
Tracer dose[4]	20	1.09 ± .09	0.32 ± .01	1.35 ± .05	0.81 ± .03	0.14 ± .02
1/6	4	1.06 ± .06	0.33 ± .03	1.43 ± .09	0.83 ± .04	0.17 ± .01
1	4	1.10 ± .07	0.30 ± .05	1.45 ± .06	0.79 ± .04	0.16 ± .01
2	4	1.10 ± .03	0.34 ± .02	1.38 ± .05	0.82 ± .07	0.16 ± .02
3	4	0.92 ± .03	0.36 ± .03	1.17 ± .02	0.73 ± .04	0.12 ± .00
4	4	0.89 ± .03	0.39 ± .02	1.31 ± .12	0.77 ± .03	0.14 ± .01
7	4	0.98 ± .04	0.32 ± .02	1.35 ± .05	0.80 ± .10	0.14 ± .02

[1] Average deviation.

[2] Two thymus glands were used for each of two fractionations.

[3] Three, three, and two thymus glands were used for each of three fractionations.

[4] Accumulated data from controls, analyzed at same intervals as the experimental groups.

tration of DNA in a fresh suspension of nuclei by the number of nuclei.

RESULTS

Phosphorus composition

The effect of a toxic dose of P^{32} on the concentration of phosphorus in various fractions of thymus, spleen, and liver are shown in table 1. In thymus, a striking decrease was observed in the DNA phosphorus concentration between the first and second day after the injection of the toxic dose. Thus, the milligrams of DNA phosphorus per gram of fresh tissue decreased from a value of 2.08 on the first day to an average of 1.08 on the second day after injection and remained at a low value for the remaining 6 days of the experiment. The concentration of DNA phosphorus in the spleen also showed a decrease as early as 4 hours after P^{32} injection and remained about 60% of normal from the second through the 7th day. In contrast to the response of these radiosensitive lymphatic tissues, the concentration of DNA phosphorus in the liver was essentially unaffected by the toxic dose of P^{32}. The toxic dose was also without significant effect upon the concentration of other phosphorus fractions studied in all three tissues, except that the RNA plus protein phosphorus fraction of thymus and spleen showed a slight decrease.

TABLE 2

Effect of a toxic dose of P^{32} on the DNA phosphorus content of rat thymus nuclei

HOURS AFTER INJECTION	γ DNA PHOSPHORUS/NUCLEUS	
	Control[1]	Irradiated
17.5	6.2×10^{-7}	6.6×10^{-7}
20.0	6.6×10^{-7}	6.6×10^{-7}
43.5	6.5×10^{-7}	6.4×10^{-7}
48.0	7.2×10^{-7}	7.3×10^{-7}
72.0	7.0×10^{-7}	6.0×10^{-7}

[1] Standard deviation on the basis of 11 determinations with normal rats was 0.8×10^{-7}.

Despite the striking decrease in the concentration of thymus DNA, no change was found in the amount of DNA per nucleus in the irradiated thymus (table 2), nor was there a detectable accumulation of DNA in the extra-nuclear portion of the tissue.

Incorporation of P^{32}

The effect of irradiation on the incorporation of P^{32} into various phosphorus fractions in thymus and spleen is shown in figures 1 and 2. In thymus (fig. 1) the most striking effect of the toxic dose was on the incorporation into the DNA fraction. From the first to 6th day following the injection, the specific activity of this fraction was consistently less than one-half that of the corresponding control values. In the case of the RNA, the incorporation of P^{32} was essentially normal

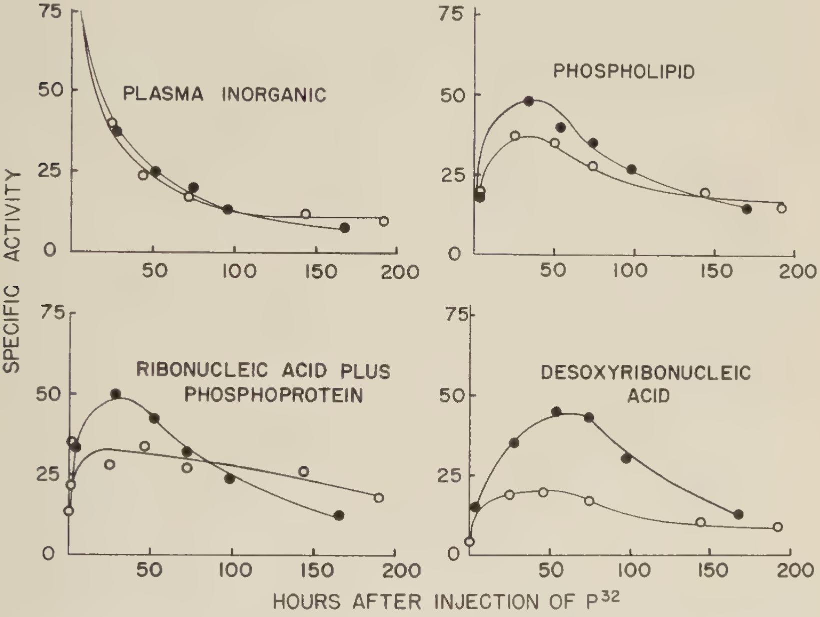

Fig. 1 Effect of a toxic dose of P^{32} on P^{32} uptake by phosphorus fractions of rat thymus. Solid circles represent tracer dose injected, open circles represent toxic dose.

during the first 4 hours but then slowed appreciably, as shown by the flattened curve during the balance of the experimental period. Although the specific activity of the phospholipid fraction rose to a somewhat lower maximum than normal, its relatively normal rate of decline after the second day suggests that inhibition of P^{32} incorporation in this fraction was quite limited in degree and duration.

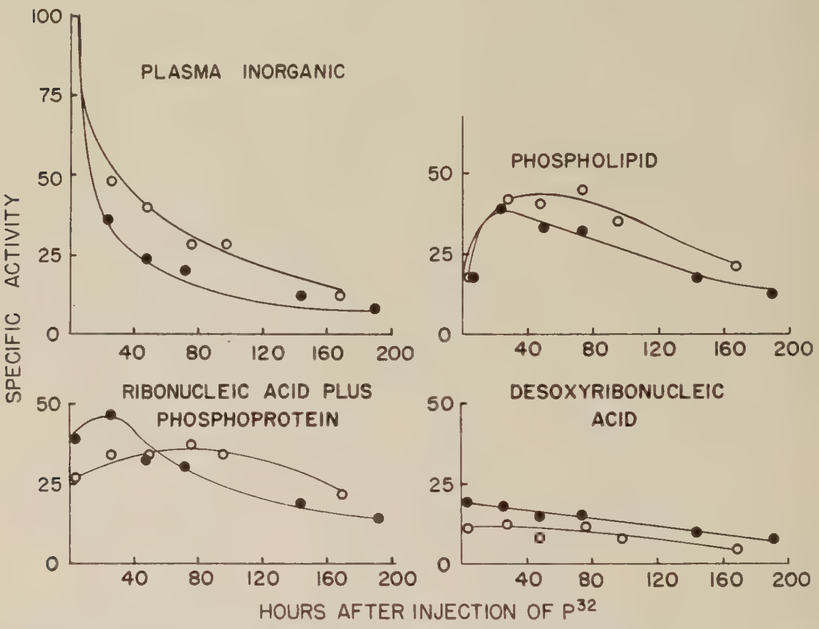

Fig. 2 Effect of a toxic dose of P^{32} on P^{32} uptake by phosphorus fractions of rat spleen. Solid circles represent tracer dose, injected; open circles represent toxic dose.

Figure 2 shows the specific activity data for spleen. The specific activity of the plasma inorganic phosphate and also of the total acid-soluble and inorganic phosphate fractions of the spleen in this experiment remained consistently higher in the animals given the toxic dose than in the controls. Because of this difference, which was greatest 24–72 hours after the injection of the isotope, it might be expected that the specific activities of the other phosphorus components in the irradiated spleen would also tend to be high. The inhibition of P^{32} incorporation into both RNA and DNA was undoubtedly more definite than indicated by the curves shown in figure 2, and, for the same reason, the apparent stimulation of the incorporation of P^{32} into the phospholipid fraction was probably not significant.

When the liver phosphorus fractions were examined in the same manner, the specific activity curves were found to be unaffected by the toxic dose of P^{32}. For example, 24 hours after the injection, the specific activity of the control DNA was 2.7, while the specific activity of the DNA from the irradiated animal was 3.1. The incorporation of P^{32} into the DNA fraction was so low, however, that only large changes would be detectable.[4]

DISCUSSION

The histological changes observed in spleen and thymus as a result of whole body x-irradiation, or irradiation from an internal source such as the P^{32} used in these experiments, consist of nuclear damage, an inhibition of cell division, and a cellular depletion. Thus, 2–3 days after irradiation, the thymus consists mainly of connective tissue, and the spleen is reduced to reticular and circulating blood cells (Murray, '48; Warren, MacMillan and Dixon, '50; Koletsky and Christie, '51). The biochemical effects of radiation have been reviewed recently by Ord and Stocken ('53), one of the most frequently observed effects being a specific decrease in the DNA concentration in radiosensitive lymphoid tissues. In the present investigation we have also observed a marked decrease in the concentration of DNA in thymus and spleen, which we believe is best explained on the basis of a change in the character of the cell population of these tissues.

---

[4] The effect of x-irradiation upon the incorporation of P^{32} into regenerating liver was also determined. It was found that 1000 r whole body x-irradiation did not affect the incorporation of P^{32} into the DNA fraction but that 3000 r caused a decrease of about 75%. One-half of each dose was given at two hours, and the remainder at 20 hours after hepatectomy.

The unusally high concentration of DNA in normal thymus is due to the great predominance of lymphocytes in this tissue. Although these cells contain the same amount of DNA per nucleus as do other types of diploid cells (Boivin, Vendrely and Vendrely, '48; Mirsky and Ris, '49), their small cytoplasmic volume results in a high DNA content per gram of tissue. The decrease in DNA concentration after irradiation (table 1) was therefore very probably due to a decrease in the relative number of the DNA rich lymphocytes, as indicated by the histological appearance of the tissue (Koletsky and Christie, '51). In normal thymus, nearly 50% of the phosphorus present was due to DNA (fig. 3, column I), but after the loss of DNA-rich lymphocytes, the proportion of DNA phosphorus decreased to a level more characteristic of the remaining connective tissue cells (fig. 3, column III). The phosphorus composition of the tissue lost from the thy-

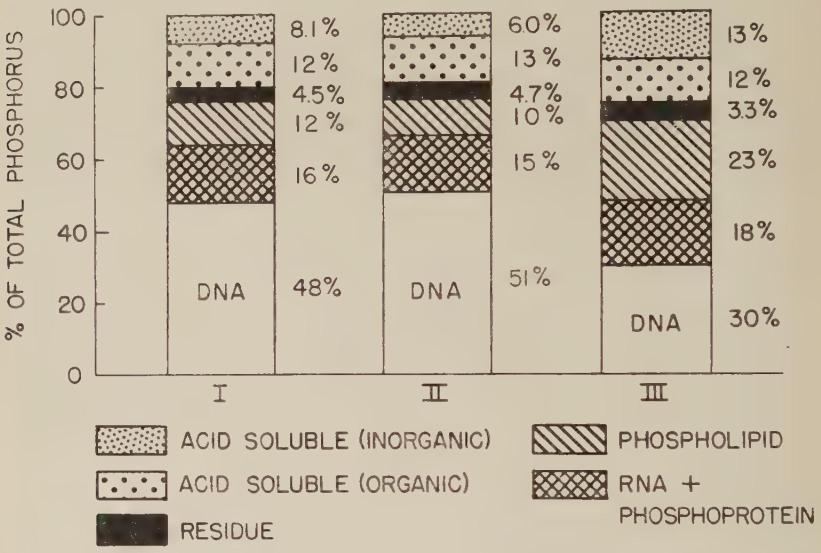

Fig. 3 Effect of a toxic dose of P^{32} on the phosphorus composition of rat thymus. Column I: Normal thymus composition. Column II: Composition of tissue calculated to be lost from thymus in 8 days after injection. Column III: Thymus composition 8 days after injection of a toxic dose of P^{32}.

mus during the same 8-day period was calculated from the analytical data. Figure 3, column II shows that this tissue also consisted chiefly of DNA-rich lymphocytes, since its composition closely resembled that of a normal thymus (column I).

The spleen is made up of a great variety of cells in which the DNA-rich cells are numerically less important than in thymus, as is reflected in the lower proportion of DNA phosphorus (fig. 4, column I). However, in spleen also, radiation apparently affects the DNA rich cells primarily, even though cells other than lymphocytes have been reported to be radiosensitive (Murray, '48). Thus, the proportion of DNA phosphorus in the tissue lost from the spleen (column II) was higher than in normal tissue (column I) and two times higher than in the radioresistant tissue remaining in the spleen after 6 days (column III).

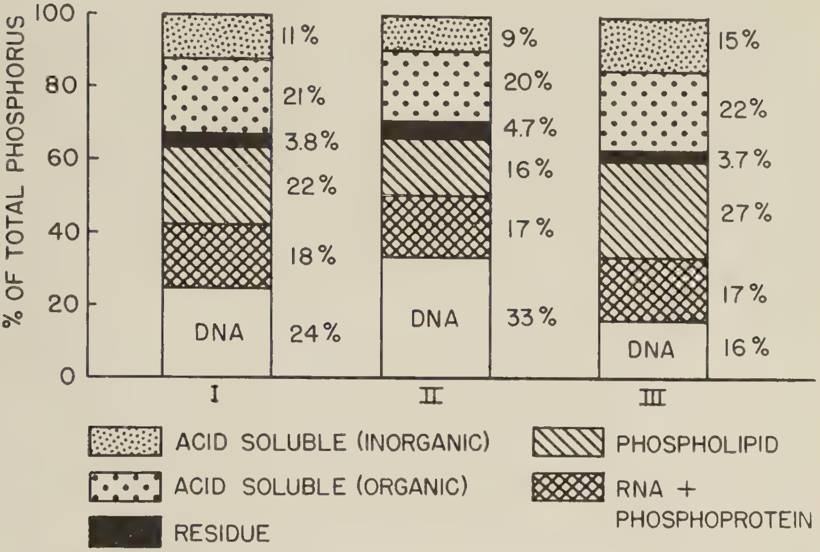

Fig. 4 Effect of a toxic dose of P^{32} on the phosphorus composition of rat spleen. Column I: Normal spleen composition. Column II: Composition of tissue calculated to be lost from spleen in 6 days after injection. Column III: Spleen composition 6 days after injection of a toxic dose of P^{32}.

Liver, which is known to be relatively radioresistant histologically (Hempelmann, Lisco and Hoffman, '52) was found to show no significant change in the concentration of DNA or other phosphorus fractions after the injection of the toxic dose of P^{32}. If radiosensitive cells are present in this tissue, they are apparently similar to the radioresistant cells in their chemical composition, and/or they make up only a small fraction of the total cell population.

Although the decreased DNA concentration can be explained on the basis of a change in cell population, another possible explanation might involve the destruction of DNA within the tissue cells, since irradiation has been shown to have a destructive action on DNA *in vitro* (literature reviewed by Ord and Stocken, '53). However, when the DNA content per nucleus in the thymus of rats given a toxic dose of P^{32} was determined in the present experiments, normal values were obtained even though the DNA concentration of the thymus decreased rapidly (table 2). A similar finding in irradiated bone marrow has been reported recently by Thomson, et al. ('53). Therefore, the decrease in the DNA concentration in these irradiated tissues is evidently not due to a progressive decrease in the DNA content of those cells which remain in the tissue at the time of analysis.[5]

The mechanism of cellular depletion is as yet undetermined. However, since the life-span of thymus lymphocytes is very short (Andreasen and Ottesen, '45), the decreased new cell formation — a known effect of radiation (Murray, '48) — could account for the cellular depletion in lymphatic tissues without necessarily involving a destructive action or even an increased removal of the cells. The mechanism by which radiation inhibits cell division is also as yet unknown, but it is possible that an impaired DNA synthesis may be involved. Many investigators have observed a decreased incorporation of precursors into the DNA of irradiated tissue (review, by Ord and Stocken, '53), and in the present experiments there was a marked decrease in the incorporation of P^{32} into the DNA of thymus and spleen. In thymus the decreased incorporation took place within 4 hours after the injection of the toxic dose of P^{32} — nearly 40 hours before the appearance of the changes in chemical composition. Therefore, alterations in the cellular composition of this tissue apparently were not responsible for the change in P^{32} incorporation. On the other hand, an early inhibition of DNA synthesis might account for histological and chemical changes, although such a possibility has not been definitely established experimentally. It is well known that tissues which are the most radiosensitive are those which have a high rate of cell division and DNA synthesis (McCarter and Steljes, '45). An interruption of DNA synthesis and/or new cell formation in such tissues would promptly lead to cellular depletion of the tissue, assuming that the normal process of cell removal was operative. Cell depletion in turn, could cause severe histologic and chemical changes in relatively short intervals. In slowly dividing tissues the rapid replacement of cells is not as necessary as in the radiosensitive lymphatic tissues, and an inhibition of new cell formation would therefore not be expected to result in marked histological and chemical changes. One of the principal effects of radiation, therefore, may be to inhibit DNA synthesis, the secondary effects of that inhibition becoming most noticeable in those tissues in which a rapid and continual synthesis of this essential compound is necessary.

---

[5] These results reveal nothing concerning the DNA per nucleus of cells lost from the thymus before analysis.

SUMMARY

The administration of a toxic dose of P^{32} to adult rats caused a striking decrease in the DNA phosphorus concentration in thymus and spleen and a smaller decrease in the RNA phosphorus concentration in thymus. No other phosphorus fraction of thymus and spleen nor any of the phosphorus fractions of liver were significantly affected by irradiation.

Since the decrease in the DNA concentration of irradiated thymus was not accompanied by a change in the DNA content

per nucleus, it apparently resulted from the removal of DNA rich cells.

The incorporation of P^{32} into DNA and RNA was reduced in the thymus and spleen of irradiated animals. However, the P^{32} uptake by the other phosphorus fractions of thymus and spleen and by the phosphorus fractions of liver was essentially normal.

The specific effect of irradiation on the DNA of lymphatic tissues suggests that the results may be due to an inhibition of DNA synthesis and/or new cell formation. Since the life span of lymphatic cells is very short, such an inhibition would promptly lead to cellular depletion and changes in chemical composition in these tissues.

LITERATURE CITED

ANDREASEN, E., AND J. OTTESEN 1945 Studies on lymphocyte production. Investigations on the nucleic acid turnover in the lymphoid organs. Acta Physiol. Scand., *10:* 258.

BOIVIN, A., R. VENDRELY AND C. VENDRELY 1948 Biochemistry of heredity. Compt. rend., *226:* 1061.

DOUNCE, A. L., AND G. T. BEYER 1948 The arginase activity of isolated cell nuclei. J. Biol. Chem., *174:* 859.

EULER, H. v., L. HAHN, H. HASSELQUIST, M. JAARMA AND M. LUNDIN 1945 Studies on the isolation and characterization of cell nuclei from calf thymus, hog liver, and rat Jensen sarcoma. Svensk Kem. Tid., *57:* 217.

GOMORI, G. 1942 A modification of the colorimetric phosphorus determination for use with the photoelectric colorimeter. J. Lab. Clin. Med., *27:* 955.

HARRINGTON, H., AND P. S. LAVIK 1951 Desoxyribonucleic acid content per nucleus in rat thymus damaged by β-radiation. Federation Proc., *10:* 194.

HEMPELMANN, L., H. LISCO AND J. G. HOFFMAN 1952 The acute radiation syndrome: A study of nine cases and a review of the problem. Ann. Internal Med., *36:* 279.

KOLETSKY, S., AND J. H. CHRISTIE 1951 Biologic effects of radioactive phosphorus poisoning in rats. Am. J. Path., *27:* 175.

LAVIK, P. S., H. HARRINGTON AND G. W. BUCKALOO 1950 *In vivo* effect of a toxic dose of P^{32} on phosphorus fractions of rat thymus. Federation Proc., *9:* 194.

——— 1951 Improved G-M counter for liquid samples. Nucleonics, *9:* December, 68.

McCarter, J. A., and E. L. Steljes 1948 Methods for the determination of the distribution of radioactive phosphorus among the phosphorus containing constitutents of tissues. Can. J. Research, *26E:* 333.

Mirsky, A. E., and H. Ris 1949 Variable and constant components of chromosomes. Nature, *163:* 666.

Murray, R. G. 1948 IN; Histopathology of Irradiation from External and Internal Sources. Ed. W. Bloom, chap. 8 and 9, McGraw-Hill, New York City.

Ord, M. G., and L. A. Stocken 1953 Biochemical aspects of the radiation syndrome. Physiol. Reviews, *33:* 356.

Schmidt, G., and S. J. Thannhauser 1945 A method for the determination of desoxyribonucleic acid, ribonucleic acid and phosphoprotein in animal tissues. J. Biol. Chem., *161:* 83.

Schneider, W. C. 1945 Phosphorus compounds in animal tissues. I. Extraction and estimation of desoxypentose nucleic acid and pentose nucleic acid. J. Biol. Chem., *161:* 293.

Thomson, J. F., W. W. Tourtelotte, M. S. Carttar and J. B. Storer 1953 Some observations on the effect of gamma irradiation on the biochemistry of rabbit bone marrow. Arch. Biochem, Biophys., *42:* 185.

Umbreit, W. W., R. H. Burris and J. F. Stauffer 1949 Manometric Techniques and Related Methods for Tissue Metabolism, 2nd ed., p. 190, Burgess, Minneapolis.

Warren, S., J. C. MacMillan and F. J. Dixon 1950 Effects of internal irradiation of mice with P^{32}. I. Spleen, lymph nodes, thymus, bone and bone marrow. Radiology, *55:* 375.

CHEMICAL INHIBITION OF REGENERATION IN STENTOR COERULEUS[1]

PAUL B. WEISZ
Department of Biology, Brown University, Providence, Rhode Island

ONE FIGURE

In recent years, antimetabolites and structural analogs of normal cell components have been used increasingly as tools in the study of morphogenesis. For example, Brachet ('46, '47) has explored the effect of acriflavin, barbituric acid, and benzimidazole on the development of amphibian eggs. More recently Bieber ('52, '54), in extensive investigations with a large variety of antipurines and antipyrimidines, has been able to show that particular developmental stages are specifically sensitive to inhibiting agents. Embryological work of this kind has come to supplement three earlier lines of experimentation with antimetabolites, all concerned in some fashion with the problem of growth: pathways in nucleic acid metabolism (e.g., Hitchings, '50); tumor growth and its inhibition (e.g., Kidder, '51); and nutrition and population growth in microorganisms (e.g., Lilly, '53).

Regenerating fragments of the ciliate *Stentor coeruleus* provide test systems in which differentiative events have been analyzed to substantial degree (cf. Weisz, '51, '54). Antimetabolite studies on such systems therefore give reasonable promise to be interpretable with some precision, thus adding to an understanding of morphogenesis derived from analogous work on eggs. Inhibition experiments on Stentor fragments are reported in this paper.

---

[1] This work was supported by a grant from the National Science Foundation, Division of Biological and Medical Sciences, Washington, D. C.

MATERIALS AND METHODS

Animals for experimentation were taken from mass cultures of *S. coeruleus,* maintained in this laboratory for a number of years. Test organisms were partially starved, i.e., until all visible food vacuoles had disappeared and the animals had become translucent. Then their oral apparatus was excised with steel needles, and the regenerants so produced were placed individually into given test solutions. After a specified length of stay, they were transferred singly to culture dishes for observations. No special attempt was made to keep cultures or test media sterile. Since the regenerants lacked ingestive structures, the results could not have been affected through feeding.

Normal fragment regeneration consists of a series of well-defined events (cf. fig. 1). Following the excision of the gullet, kinetosomes at the cut anterior terminal of kinety I reproduce repeatedly and produce an anarchic field of basal granules. The latter then become organized into a double row, and the granules in this row synthesize membranelles. This synthesis, beginning some 4 hours after the operation, represents the first visible phase of regeneration. The adoral band of membranelles so formed gradually lengthens longitudinally, then curves into a peristomial arc, and at its posterior terminus a new gullet differentiates. Form regulating shifts follow, which bring the newly developed oral system into correct anterior location. Structural regeneration is normally completed some 3 to 5 hours after the appearance of the primordium of membranelles, i.e., some 8 to 10 hours after gullet removal.

In extensive preliminary tests, more than 20 different compounds were screened for their effect on regeneration. These included substituted purines and pyrimidines, and a variety of other commercially available antimetabolites.[2] Three factors were found to limit usability of the drugs: pH, effective concentration, and non-specific toxicity. A "non-specific"

[2] Grateful acknowledgement is made to Dr. G. H. Hitchings and the Wellcome Research Laboratories for their generous gift of a number of compounds.

toxic reaction in *Stentor* consists, as long experience with this organism has shown, of excessive cytoplasmic vacuolation, depigmentation, ectoplasmic dedifferentiation, cytolysis, and death. These symptoms are produced to varying degree and with varying rapidity by many widely different irritants, including distilled water and buffer salts. Hence unbuffered autoclaved tap water was used as standard culture medium and solvent for test compounds. Also, only such compounds could be used that would, without buffer, give solutions within the pH tolerance for *Stentor* (approx. pH 6 to 8).

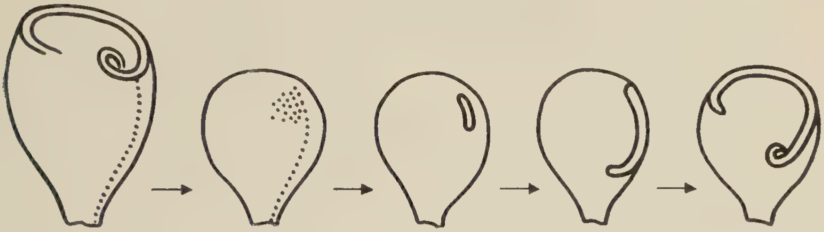

Fig. 1 Simplified diagram of regenerative events in cortex of *S. coeruleus.* From left to right: intact organism with anterior peristomial band of membranelles and gullet in left ventral position (dotted line indicates position of kinety I); after decapitation, development of anarchic field of kinetosomes at cut terminal of kinety I; subsequent formation of primordium of membranelles, followed by growth of membranellar band and establishment of new gullet.

Substances qualifying in this respect were then tested for biological activity. In some cases even saturated solutions were without effect (e.g. sulfanilamide, 8-azaguanine). In others, the inhibitions produced at non-toxic concentrations lasted only as long as the organisms were actually exposed to the test compound (e.g. 6-azathymine), or the effective concentration range was so narrow as to preclude extensive experimentation (e.g. 2-amino-4-methyl-pyrimidine). Such substances were not considered further. Four compounds, 2, 6-diaminopurine sulfate, benzimidazole, barbituric acid, and 5-nitro-uracil, produced good inhibition fairly consistently. However, these agents were mildly toxic, and even though pathological symptoms disappeared as soon as the test organisms were removed to water, too much reliance could not be placed on results.

Of the 20 or so agents considered initially, actually only one was found to be ideal in all respects: acriflavin.[3] It gave solutions of a fairly stable pH 7.6 without buffer, was highly effective at low concentrations and over a considerable range, and so far as could be determined was absolutely non-toxic. This substance was therefore used predominantly in the experiments. Parallel tests with diaminopurine and other mildly toxic compounds were found to yield qualitatively the same results. Since acriflavin acted much more consistently and could be better controlled, experiments with other inhibitors were confined to exploratory tests, and these will not be described specifically.

For regenerants, the effective concentration range was found to be 7 to 16 mg/l. Whole animals tolerated lower concentrations only, a disparity observed also for inhibitors other than acriflavin.

I. Inhibition of regeneration

Eighty experiments were carried out to determine how acriflavin affects regeneration, and how these effects varied with different concentrations and times of exposure. Four standard acriflavin concentrations were used, 8, 10, 13, and 16 mg/l. Durations of exposure were 1, 2, 3, and 4 hours, counted from the moment of gullet excision. Table 1 gives a qualitative summary of the results.

A few minutes after a regenerant was placed into a test solution, the first effects were observed. Depending on acriflavin concentration, greater or lesser ciliary and myonemal paralysis became manifest. Also, smaller or larger amounts of pellicular material peeled off the surface of the regenerants, and this material accumulated on the stationary cilia. In other respects, the regenerants remained perfectly normal.

---

[3] Acriflavin-Neutral, N. F. IX, Nutritional Biochemicals Co., Cleveland. This material is a mixture of 2,8-diamino-10-methyl-acridinium chloride and 2,8-diamino-acridine; it is used clinically as a bacteriostatic agent.

Very shortly after the organisms were removed from acriflavin, the ciliary beat returned, body contractility reappeared, and pellicular debris was swept off the body surface by ciliary action. In appearance and behavior, these regenerants could not be distinguished from normal ones. However, their morphogenetic machinery was clearly affected by acriflavin. This became apparent when, 4 hours after gullet removal, regeneration did not begin as it should.

TABLE 1

Inhibition of regeneration in relation to acriflavin concentration and duration of exposure

CONC. mg/l \ EXPOSURE, HOURS	1	2	3	4
8	+	++	++	+++
10	++	+++	+++	+++
13	+++	+++	++++	++++
16	+++	++++	*d*	*d*

Key:	Number of plus-signs denotes degree of inhibition.
+:	Delayed onset, often partial structural regeneration.
++:	Variously partial (and delayed) regeneration.
+++:	Sometimes strongly inhibited regeneration, more often total permanent inhibition.
++++:	Permanent total inhibition if fragment survives, or fragment death overnight.
d :	Fragment death within a few hours.

Table 1 indicates that the inhibitions were the more pronounced the higher the acriflavin concentration and the longer the exposure to acriflavin. Two classes of inhibitory effects were observed, one involving the timing of successive regenerative events, the other, the degree to which structural regeneration was completed. Time effects were of two kinds: (1) delay of onset of regeneration, from a barely significant delay of about one hour or a delay of several hours (followed by essentially normal regeneration), up to permanent delay (2 to 3 days or more), followed by the death of the nonregenerated fragment; (2) moderate delay of onset as above, plus slower-than-normal progress of succesive regenerative steps.

Structural inhibitions ranged between complete normal regeneration and complete non-regeneration. Three graded intermediate effects were obtained consistently, as if these represented critical unitary morphogenetic events, essentially all-or-none in nature and interconnected by acriflavin-sensitive transition reactions: (1) adoral band grows and curves, but a gullet is never formed; (2) adoral band grows, but does not curve into a peristomial arc and persists as a straight band without gullet; (3) adoral primordium appears but does not grow further and is soon resorbed (without subsequent resumption of regeneration). All such partially or abortively regenerated fragments died after 2 to 3 days.

Temporal and structural inhibitions occurred simultaneously, producing a graded range of results, from slightly delayed, normal regeneration (at low concentrations and short exposures), to permanent total inhibition (at either high concentrations or long exposures or both). In the course of these experiments it was found that two regenerants treated in absolutely identical fashion (in the same culture and test dishes) sometimes responded differently: one would be inhibited to a greater extent than the other. The differences could be appreciable, and such cases occurred often enough to suggest significance. Presumably, the physiological state of the responding organisms or the ease with which acriflavin penetrated into them could vary. This would clearly play a role in the production of inhibition effects (and would also account for the observation of more discrete degrees of inhibition than there were discrete degrees of inhibitor concentrations or spans of exposure).

A second group of 40 experiments was carried out to determine if inhibition effects could be correlated with specific exposure periods within the test interval, i.e., the 4 hours between gullet removal and the visible onset of regeneration. Preliminary tests here showed that the minimum effective exposure time was about 10 minutes (plus or minus about

5 minutes, depending on the acriflavin concentration used). Regenerants were therefore given 15-minute exposures at successive periods during the 4-hour test interval. However, the inhibition effects were the same, regardless of the specific exposure period chosen.

It may be reiterated that parallel tests with diaminopurine, benzimidazole, barbituric acid, and 5-nitro-uracil gave the same pattern of results as the experiments described above.

II. Reversal of inhibition

Preliminary experiments were carried out to determine qualitatively to what extent acriflavin inhibition could be reversed, and what agents would be effective here. Solutions of likely reversing agents were used as solvents for acriflavin, and regenerants were exposed to these mixtures for one hour.

Adenine, guanine, thymine, uracil, folic acid, and ribo- and desoxyribonucleates were found to be effective reversing agents. Xanthine and 5-methyl-cytosine were not effective, and guanylic acid in acriflavin was found to be lethal. That nucleates would be reversing could be inferred from McIlwain's ('41) work on bacteria, which indicated that both types of nucleic acids as well as nucleotides formed insoluble complexes with acriflavin. Brachet ('46) additionally found that adenylic acid, guanylic acid, and adenosine triphosphoric acid reversed acriflavin inhibition in developing frog eggs.

The experiments showed that, regardless of the particular agent used, any degree of reversal could be obtained by adjusting reverser concentrations. Thus normal, or temporary partial, or permanent partial regeneration could be obtained consistently in appropriate acriflavin-reverser mixtures. Acriflavin controls produced permanent total inhibition.

McIlwain (loc. cit.) found that when acriflavin and nucleic acids were mixed in solution, the fluorescence of acriflavin disappeared, suggesting *in vitro* complex formation. A similar disappearance of fluorescence was noted in present experiments with nucleates. Moreover, regenerants placed into such test solutions did not exhibit ciliary or myonemal paralysis, and were not inhibited subsequently. Evidently, acriflavin was prevented from affecting the organisms, probably as a result of *in vitro* complex formation with the nucleates. This would explain the "reversing" action of nucleates, but it also raised the question whether the analogous action of purines and pyrimidines was not equally due to *in vitro* complex formation (even though the fluorescence of acriflavin persisted in such test mixtures).

Experiments were therefore undertaken in which *in vitro* effects were obviated. Regenerants were first exposed to acriflavin alone, for one hour, then were transferred to reverser alone, for an equal length of time. In a parallel series of tests, the sequence of test solutions was reversed. In these experiments attention was given to inhibition ratios, to determine whether or not acriflavin acted competitively.

The action of adenine, thymine, and ribonucleate was studied most thoroughly, in over 200 individual experiments. Adenine data are summarized in table 2. All reversing agents used yielded the same qualitative pattern of results, as follows:—

1. When exposure to acriflavin was followed by exposure to a reversing agent, then the latter did not diminish or otherwise alter the inhibition produced by acriflavin.

2. When exposure to a reversing agent was followed by exposure to acriflavin, then the result depended on the relative concentrations of the test agents. At high reverser and low acriflavin concentrations, normal regeneration occurred. At somewhat lower reverser or higher acriflavin concentrations, a "protective" action of the reverser was still in evidence, but it was less effective: regeneration was variously delayed, partial, or abortive. To this extent the reversing agent still minimized the subsequent action of the inhibitor. At relatively low reverser or high acriflavin concentrations, the reverser was no longer effective. Inhibition occurred as if only acriflavin had been used.

3. When the inhibitor/reverser ratio remained constant, but the absolute concentration levels were increased, then the pattern of results changed (regardless of whether inhibitor and reverser were used simultaneously or not). Where inhibitions were completely reversed at low absolute acriflavin concentrations, they became total and permanent when concentrations were raised. Such changes in results, despite fixed inhibitor/reverser ratios, are evidence for non-competitive inhibition.

TABLE 2

The reversing action of adenine: data summary

ACRIFLAVIN/REVERSER RATIO FINAL ACRIFLAVIN CONC., mg/l	0.02	0.03	0.04	0.08
8	+ + —	+ ± —	+ — —	+ — —
10	+ ± —	+ — —	+ — —	+ — —
13	+ — —	— — —	— — —	— — —
16	— — —	— — —	— — —	— — —

Key: In each square, *left top* symbol: acriflavin plus adenine together.
middle symbol: adenine followed by acriflavin.
right bottom symbol: acriflavin followed by adenine.

+: Normal regeneration.
±: Delayed and/or partial regeneration.
—: No regeneration.

4. On a weight basis, nucleates proved to be almost 100 times more effective as reversing agents than purines or pyrimidines. As a group, the latter ceased to be effective when the inhibitior/reverser ratio was in the order of one part acriflavin to 15 parts reverser. With nucleates on the other

hand, reversing action ceased only at a ratio of about one part acriflavin to 0.2 parts reverser.

CONCLUSIONS AND SUMMARY

The data support the following interpretation:—

1. *Stentor coeruleus* possesses body components which may combine with molecules of acriflavin or other inhibitors. Such combinations may interfere with the functioning of these ''targets,'' leading directly or indirectly to a given degree of morphogenetic inhibition. Inhibitions consistently occur at specific points in the sequence of regenerative events, suggesting the existence of successive unitary developmental steps, interconnected by acriflavin-susceptible reactions. This parallels the similar finding of Bieber ('54), in inhibition studies on developing frog eggs.

2. Target structures may also combine with a variety of reversing agents, provided the organelles have not previously combined with inhibitors. Combination with reversers to a greater or lesser extent prevents a subsequent combination with inhibitors, resulting in a functional ''protection'' of the targets.

3. The inhibition produced by acriflavin is non-competitive. In view of this, and in view of the lack of specificity of the reversing agents, little can be inferred about the chemical nature of the acriflavin-sensitive targets. A structure at least partly related to nucleic acids or their derivatives seems to be indicated broadly, but beyond this, both the inhibitions and the reversals could be explained quite well on a physical basis.

4. Previous work (Weisz, loc. cit.) has shown that development of adoral membranelles, hence regeneration as a whole, depends on the morphogenetic activity of the anarchic kinetosomes produced by kinety I. Directly or indirectly, acriflavin evidently affects these kinetosomes. At low concentrations, acriflavin appears to interfere with the membranelle-synthesizing activity of the granules, and at higher

concentrations, their reproduction and formative migrations into a longitudinal row seem to be blocked as well.

5. This interpretation is strongly supported by the observations on ciliary paralysis. Clearly, all basal granules of the organism are rapidly affected by acriflavin. But it is probably significant that inhibition of ciliary motility ceases as soon as exposure to acriflavin ceases, whereas morphogenetic inhibition lasts much longer and may even be permanent. This suggest that different kinetosomal functions may be affected via acriflavin.

LITERATURE CITED

Bieber, S. 1954 Analogues of nucleic acid derivatives and the growth and development of Rana pipiens. J. Cell. and Comp. Physiol., *44:* 11–32.

Bieber, S., R. F. Nigrelli and G. H. Hitchings 1952 Effects of purine and pyrimidine analogues on development of Rana pipiens. Proc. Soc. Exp. Biol. and Med., *79:* 430–432.

Brachet, J. 1946 Action de l'acriflavine sur le developpement des oeufs de Batraciens. C. R. Soc. Biol. Paris, *140:* 893–894.

——— 1947 Nucleic acids in the cell and the embryo. Symp. Soc. Exp. Biol., *1:* 207–224.

Hitchings, G. H. and others 1950 Studies on analogs of purines and pyrimidines. N. Y. Acad. Sci. Annals, *52:* 1318–1335.

Kidder, G. W. and others 1951 Further evidence on the mode of action of 8-azaguanine in tumor inhibition. Cancer Res., *11:* 204–211.

Lilly, D. M. and others 1953 Growth promotion in carnivorous protozoa by substituted purines. Proc. Soc. Exp. Biol. and Med., *83:* 434–438.

McIlwain, H. 1941 A nutritional investigation of the anti-bacterial action of acriflavine. Biochem. J., *35:* 1311–1319.

Weisz, P. B. 1951 An experimental analysis of morphogenesis in Stentor coeruleus. J. Exp. Zool., *116:* 231–258.

——— 1954 Morphogenesis in protozoa. Quart. Rev. Biol., *29:* 207–229.

THE INFLUENCE OF ESTROGEN ON NUCLEAR VOLUMES AND CHEMICAL COMPOSITION[1]

SEYMOUR GELFANT[2] AND JACKSON J. CLEMMONS
Department of Pathology, University of Wisconsin Medical School,
Madison, Wisconsin

INTRODUCTION

Using karyometric methods for the determination of nuclear volumes, Salvatore ('48, '50) has shown that estrogen causes a doubling of nuclear volumes in the cells of the rat uterus. Salvatore interprets these volume increases to be "interphasic growth of nuclei (nuclear hypertrophy)" accompanied by a "multiplication of the nuclear genome," and he concludes that estrogen acts upon the genes by "inducing their reproduction." This interpretation of the physiological significance associated with estrogen-induced nuclear volume increase has been challenged by Alfert and Bern ('51). By the use of cytophotometric methods for measuring amounts of desoxyribonucleic acid (DNA) and intranuclear proteins, these workers have shown that the interphasic doubling in nuclear volume in the gland cells of the estrogen stimulated rat uterus is accompanied by an increase in protein and that the DNA content remains constant. Since the amount of DNA is associated with the number of chromosome sets in a nucleus, they concluded that the interphasic doubling in nuclear volume was not due to the action of estrogen on chromosomal or genic duplication. Recent evidence in support of this latter interpretation has been presented by Gelfant, Meyer and Ris

---

[1] This investigation was supported by a grant from the U. S. Atomic Energy Commission (AT-11-1-64 Proj. 8).

[2] Present address: Department of Zoology, Syracuse University, Syracuse, N. Y.

('55), who have shown that estrogen-induced nuclear volume increases in the rat uterus occur even when DNA synthesis and mitosis have been inhibited.

Recent advances in x-ray methods (historadiography) have made it possible to quantitate the mass of a structure a few microns in diameter and thereby to determine the water and protein content of a single cell or part of a cell "in situ" (Engstrom and Lindstrom, '50; Clemmons and Aprison, '53). In the present investigation the historadiographic method was employed to aid in the study of nuclear volume changes. Three aspects of the problem were studied. Karyometric measurements were made to determine changes in nuclear volumes. Cytophotometric measurements of desoxyribonucleic acid (DNA) were made to determine the role of DNA in nuclear volume changes and to establish the interphasic or mitotic condition of the nuclei involved in these changes. Historadiographic measurements of total organic matter (mass) were made, and by knowing the DNA content, the role of the protein and hydration in nuclear volume changes could be determined. It was hoped that by relating the changes in nuclear volumes to the changes in chemical composition, some of the physiological mechanisms involved in estrogen-induced nuclear volume increase might be elucidated.

MATERIALS AND METHODS

Twelve female rats of the Holtzman-Rolfmeyer strain were ovariectomized on the 21st day of age. After a 4-day rest period, 6 animals were injected subcutaneously with a 0.1 μg of estradiol in 0.1 ml oil daily for three days. Six animals served as castrate controls. Twenty-four hours after the last injection all animals were killed by cervical dislocation. The uteri were removed and weighed to determine the effectiveness of castration and estrogen administration. Pieces of uteri were fixed in 1 : 3 acetic alcohol. In order that microtome cuttings of treated and untreated uteri would be of equal thickness, castrate and estrogen treated uteri were embedded in paraffin in pairs (lying in close parallel apposition). Cross sections of double-embedded uteri were cut at 5 and 10 μ.

Determination of nuclear volumes. Nuclear volumes were determined on Feulgen stained sections cut at 10 μ. The major and minor axes of nuclei were measured, using an ocular micrometer calibrated in microns. Nuclear volume was calculated according to the formula $\frac{a^2b}{1.91}$, where "a" is the major axis and "b" the minor axis of an oblate sphere. Data were obtained on 100 nuclei each in the surface epithelium and glands of estrogen stimulated and castrate control uteri.

Determination of DNA content of individual nuclei. Sections cut at 10 μ were terated with the Feulgen reagent according to the method of Ris and Mirsky ('49). The absorption of colored substance in Feulgen stained nuclei was determined by a photometric apparatus similar to that described by Pollister and Ris ('47). Measurements of central areas of nuclei, using a constant plug size of 3.38 μ, were made according to the method devised by Swift ('50). The final calculation of total amount of absorbing substance in arbitrary units per nucleus was made using the formula E·a·b, where "E" is the extinction, "a" the diameter of the long axis, and "b" the diameter of the short axis of a nucleus. Data were obtained on 100 nuclei each in the glands and surface epithelium of estrogen stimulated uteri and on 80 nuclei each in the glands and the surface epithelium of castrate control uteri.

Determination of total organic matter (mass) of individual nuclei. Procedures for the historadiographic determination of mass have been described in a previous publication (Clemmons, Lalich and Angevine, '54). Each preparation of double embedded uteri cut at 5 μ was mounted on a metal disc along with a nitrocellulose reference wedge consisting of three steps ranging in thickness from 0.4–1.3 μ. Gevaert-Lippman film was used with an exposure of 90 seconds at 2 kv. and 50 ma. Calibration curves of foil thickness ($L_2\mu$) vs. transmittance of the historadiographic image of the reference foils were constructed. A structure in the tissue section absorbs x-rays to the same extent as some thickness of the reference foils. This thickness may be defined as the absorption equivalent ($L_2\mu$). Transmittance values of the historadiographic image of the unknown were measured, and from the calibration curve the equivalent $L_2\mu$ values were obtained. The microdensitometer was adjusted to read a fixed circular area 3 μ in diameter. The $L_2\mu$ values for the unknown were converted to mass per cubic micron (m_p/μ^3) by using equation (1)

$$m_p/\mu^3 = \frac{L_2\mu \cdot B \cdot 1.59 \cdot 10^{-13}}{L_s} \qquad (1)$$

"B" is the ratio of the absorption constants for the nitrocellulose reference material (parlodion) to that of an average protein (albumin). Both of these constants were determined experimentally and "B" was found to have the value of 1.13. The density of the reference material expressed in grams per cubic micron is 1.59×10^{-12}. "L_s" is the section thickness, 5 μ (determined by microscopic focusing). Data were obtained on 100 nuclei each in the surface epithelium, and on 50 nuclei each in the glands of estrogen stimulated and castrate control uteri.

RESULTS

The data on nuclear volumes (in cubic microns), on DNA content per individual nucleus (in arbitrary units), and on equivalent absorption thickness (L_2) of individual nuclei (in microns) were arranged in classes, and frequency histograms of volume and absorption equivalent were constructed (figs. 1 and 2). Modal values were computed according to the method described by Arkin and Colton ('50), and the modal value class is indicated in each histogram. The data on DNA content per individual nucleus were not expressed in a separate histogram, but were included as modal value classes in figure 1.

Figure 1 shows the changes in nuclear volumes that occur in the glands and surface epithelium of the uterus after estrogen treatment. The basic nuclear volume in the untreated uterus is the same in both the glands and surface epithelium. Estrogen causes a doubling in nuclear volume in the gland cell nuclei, and a tripling in volume in the nuclei of the

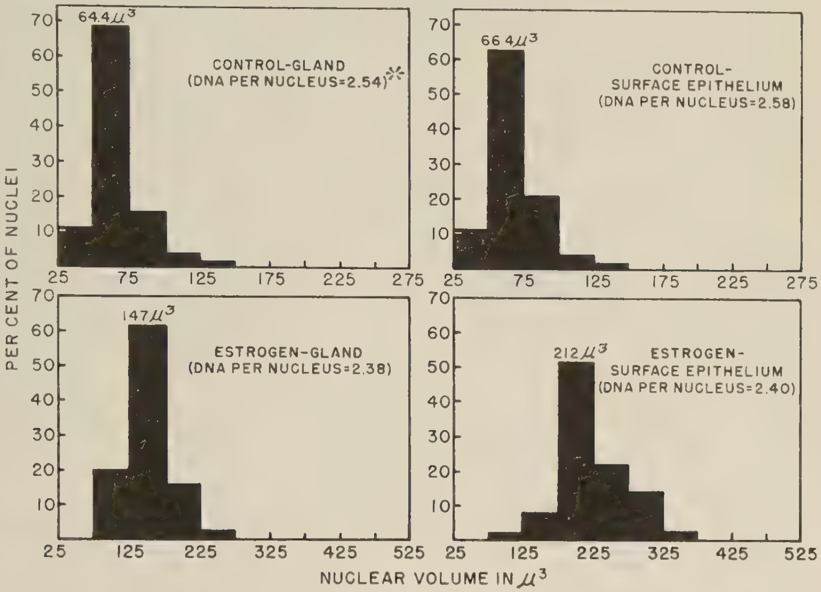

Fig. 1 Frequency histograms showing changes in nuclear volume. *DNA content per nucleus in arbitrary units.

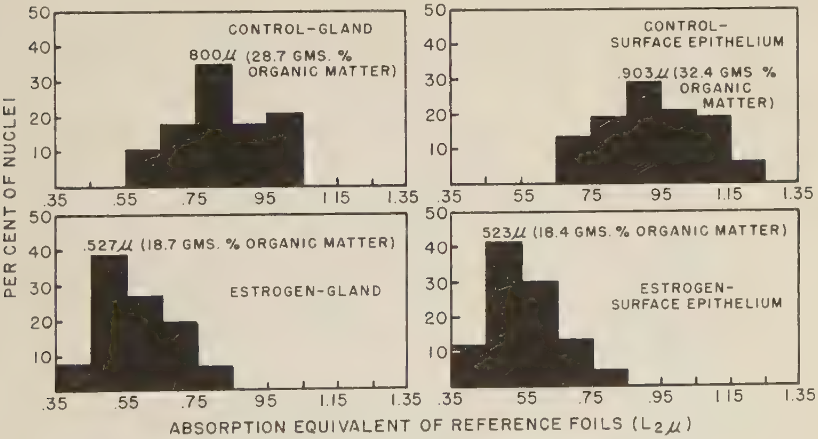

Fig. 2 Frequency histograms showing changes in absorption equivalent (thickness) and in concentration of organic matter per nucleus.

surface epithelium. The DNA content per nucleus remains constant in all nuclei. The amount of DNA is essentially the same in the gland cell nuclei and surface epithelium nuclei in both the control and estrogen treated uteri.

Figure 2 shows the changes in equivalent absorption thickness ($L_2\mu$) of individual gland and surface epithelium cell nuclei. The modal class $L_2\mu$ values were converted into grams per cent organic matter by using equation (1) in the text, and these values are presented along with the thickness values. In the untreated uterus the basic thickness values (absorption equivalent) for the surface epithelium nuclei are slightly higher than for the gland nuclei. Thus the concentration of organic matter in grams per cent is also slightly higher in the surface epithelium nuclei. Estrogen administration causes a decrease in absorption equivalent in both gland and surface epithelium cell nuclei. The concentration of organic matter is decreased to approximately 18.5 gm % in both.

Table 1 summarizes the data presented in figures 1 and 2 and shows the relationship that exists between nuclear volume change and chemical composition in individual gland and surface epithelium nuclei. The values for the concentration of organic matter/μ^3 were obtained by converting the equivalent absorption ($L_2\mu$) values according to equation (1). The content of total organic matter per nucleus was obtained by multiplying nuclear volume by concentration of organic matter/μ^3. The data in table 1 express changes in concentration and content of three nuclear components, DNA, proteins, and water, in relation to estrogen induced nuclear volume increase. Increased nuclear volume is accompanied by a decrease in the concentration of DNA and by a decrease in the concentration of organic matter/μ^3. However, the content of DNA per nucleus (concentration of absorbing material × volume) remains constant in nuclei that have either doubled or tripled in volume, and the total content of organic matter per nucleus has increased, with an increase in volume. Since the DNA content per nucleus remains constant, changes in total organic matter (mass) can be assumed to be due to changes in protein content. Thus, the total organic matter per nucleus (protein) has increased 48.8% in the gland nuclei, with a doubling in nuclear volume. And the total organic matter per nucleus (protein) has increased 81% in the surface epithelium with a tripling in nuclear volume. The significance of increased protein content in terms of histone and non-histone protein in relation to nuclear volume increase will be alluded to in the discussion.

TABLE 1

The effects of estrogen on nuclear volume, DNA content and total organic matter (mass) of individual gland and surface epithelium nuclei in the rat uterus

MEASUREMENT	CONTROL GLAND	ESTROGEN GLAND	CONTROL S. EPITHELIUM	ESTROGEN S. EPITHELIUM
Nuclear volume (μ^3)	64.4	147.0	66.4	212.0
DNA (arbitrary units)	2.54	2.38	2.58	2.40
Equivalent absorption thickness ($L_2\mu$)	.800	.527	.903	.523
Organic matter (mass) gm/μ^3 ($\times 10^{12}$)	.287	.187	.324	.184
Gm % organic matter (mass)	28.7	18.7	32.4	18.4
Total organic matter (mass) gm/nucleus ($\times 10^{12}$)	18.5	27.5	21.5	39.0

See text for explanation.

DISCUSSION

Our results on nuclear volume changes confirm the reports of Salvatore ('48, '50) and of Alfert and Bern ('51) that estrogen causes a doubling in nuclear volume in uterine gland cells. In addition, we note a tripling in nuclear volume in the surface epithelium cells of the estrogen stimulated uterus. The determinations of DNA content per nucleus, of total organic matter (mass) per nucleus, and of water content per nucleus, provide a basis for interpreting nuclear volume increases in terms of chemical composition and physiological mechanisms.

The basic question of whether estrogen-induced nuclear volume increase involves multiplication of chromosome sets has previously been answered by Alfert and Bern ('51). The present investigation confirms and extends the results obtained by these workers. Examination of large numbers of nuclei showed that nuclear volume increase is not related to increase in DNA content. The DNA content per nucleus remained constant both in the gland nuclei that doubled in volume, and in the surface epithelium nuclei that tripled in volume. Therefore, it can be concluded that estrogen-induced nuclear volume increase is not a result of chromosome multiplication. The increases in nuclear volume that occur are interphasic (non-mitotic) changes, and the DNA content does not contribute to these changes. It should be pointed out that these results do not indicate an absence of mitosis in the estrogen stimulated uterus, for dividing nuclei were observed in both the glands and surface epithelium. The results merely indicate that the nuclei studied were nondividing nuclei undergoing functional hypertrophy.

An increase in nuclear volume can be associated with three factors — chromosome multiplication, hydration, or an increase in certain chemical constituents. In the present problem, the first factor has been eliminated as being the causal agent. The second factor, hydration, has been shown to play a minor role in estrogen-induced functional nuclear hypertrophy. There is an increase in water per nucleus, associated with increased volume, but hydration *per se* is not responsible for the total increase in nuclear volume. It would appear, then, that the third factor, an increase in certain chemical constituents, is responsible for nuclear volume increase. Our results demonstrate this to be true. We note that increased nuclear volume is accompanied by an increase in total organic matter (mass), and by showing that the DNA content does not increase, we conclude that the changes in mass reflect changes in protein content. A similar observation and conclusion has been made by Alfert and Bern ('51), using quantitative staining reactions for DNA and total proteins.

One problem of particular interest in nuclear physiology is concerned with the quantitative determination of changes in chemical constituents in relation to changes in nuclear volume. In the present study, the data on total organic matter (mass) per nucleus in relation to nuclear volume changes offer a means of estimating quantitatively the part played by several nuclear components in volume changes. According to Mirsky and Ris ('51), the three most important constituents of chromosomes are DNA and two protein fractions, histone and non-histone protein. If we assume that 40% of the total organic matter of the inactive castrate control nucleus is non-histone protein, we then can calculate the relative amounts of the three constituents and establish their roles in nuclear volume changes. The assumption that 40% of the total mass of the inactive control nucleus is non-histone protein is based upon the work of Allfrey et al. ('52) and refers to the non-histone protein content of inactive calf thymus nuclei. (Unpublished work in our laboratory indicated that these nuclei have about the same DNA content and volume as the control rat uterine gland nuclei.) Thus, if we use the 40% value as an indication of the amount of non-histone protein in the inactive control nuclei of the uterus, the following calculations can be made. Using the gland nuclei as an example (table 1), 40% of the total organic matter per nucleus (18.5×10^{-12} gm) of the control nucleus is 7.4×10^{-12} gm. This value subtracted from the total organic matter gives the value for DNA plus histone (11.1×10^{-12} gm). Since both the DNA content (table 1) and the histone content exhibit a quantitative constancy with increased nuclear volume (Alfert, Bern and Kahn, '53), the value of 11.1×10^{-12} gm (DNA plus histone) can be used to calculate the amount of non-histone protein in the estrogen gland nuclei. By substracting the constant fraction, 11.1×10^{-12} gm from the total organic matter (27.5×10^{-12} gm), the amount of non-histone protein can be derived (16.4×10^{-12} gm). Thus, in the gland nuclei, the non-histone fraction doubles ($7.4–16.4 \times 10^{-12}$ gm) with a corresponding doubling in nuclear volume ($64.4–147\ \mu^3$). The same calculations applied to the nuclei of the surface epithelium reveal a tripling in non-histone protein ($8.6–26.1 \times 10^{-12}$ gm) corresponding to a tripling in nuclear volume ($66.4–212\ \mu^3$).

The above calculations determining the role of non-histone protein in estrogen-induced nuclear volume changes in the rat uterus are supported by the evidence recently presented by Alfert, Bern and Kahn ('53). These workers have shown that increased nuclear volume in the rat thyroid is accompanied by an increase in non-histone protein. It thus appears that hormonally-induced nuclear hypertrophy is primarily a result of an increase in the non-histone protein fraction of the nucleus (hydration plays a minor role). It is highly probable that the close correlation between non-histone protein and nuclear volume indicates a functional relationship between this chemical fraction of the nucleus and the metabolic activity of the cell.

SUMMARY

1. Estrogen-induced changes in nuclear volume and chemical composition of rat uterine gland and surface epithelium cells were studied. Determinations were made of nuclear volumes (karyometric measurements), of DNA content per nucleus (cytophotometric measurements), and of total organic matter (mass) per nucleus (historadiographic measurements).

2. Estrogen caused a doubling in nuclear volume in the gland cell, and a tripling in volume in the surface epithelium cell nuclei.

3. The DNA content per nucleus remained constant and was not associated with increased nuclear volume.

4. There was a slight increase in water content per nucleus, and a substantial increase in total organic matter (mass) per nucleus accompanying volume increase.

5. Quantitative calculations revealed that the non-histone protein fraction of the nucleus was mainly responsible for estrogen-induced functional nuclear hypertrophy. The non-

histone protein fraction doubled with a doubling in nuclear volume, and tripled with a tripling in nuclear volume.

ACKNOWLEDGMENTS

We wish to express our appreciation to Dr. D. Murray Angevine and Dr. Joseph L. Lalich for their helpful comments during the course of this investigation.

LITERATURE CITED

ALFERT, M., AND H. A. BERN 1951 Hormonal influence on nuclear synthesis. I. Estrogen and uterine gland nuclei. Proc. Nat'l. Acad. Sic., *37:* 202–205.

ALFERT, M., H. A. BERN AND R. KAHN 1953 Karyometric and cytochemical studies on the rat thyroid gland. Anat. Rec., *117:* 585–586.

ALLFREY, V., H. STERN, A. E. MIRSKY AND H. SAETREN 1952 The isolation of cell nuclei in non-aqueous media. J. Gen. Physiol., *35:* 529–554.

ARKIN, H., AND R. COLTON 1950 *Outline of Statistical Methods.* Barnes and Noble Inc., New York.

CLEMMONS, J. J., AND M. H. APRISON 1953 An improved historadiographic apparatus. Rev. Sci. Instr., *24:* 444–454.

CLEMMONS, J. J., J. J. LALICH AND D. M. ANGEVINE 1954 The technic of quantitative historadiography. Lab. Investigation, *3:* 19–32.

ENGSTROM, A., AND B. LINDSTROM 1950 A method of determining mass of small biological objects. Biochem. et Biophys. Acta., *4:* 351–373.

GELFANT, S., R. K. MEYER AND H. RIS 1955 Effect of estrogen, Aminopterin, citrovorum factor and nitrogen mustard on the rat uterus. J. Exp. Zool., *128:* 219–257.

MIRSKY, A. E., AND H. RIS 1951 The composition and structure of isolated chromosomes. J. Gen. Physiol., *34:* 475–492.

POLLISTER, A. W., AND H. RIS 1947 Nucleoprotein determination in cyltological preparations. Cold Spring Harbor Symp. Quant. Biol., *12:* 147–157.

RIS, H., AND A. E. MIRSKY 1949 Quantitative cytochemical determination of desoxyribonucleic acid with the Feulgen nucleal reaction. J. Gen. Physiol., *33:* 125–145.

SALVATORE, C. A. 1948 A cytological examination of uterine growth during the estrous cycle and artifically induced estrus. Rev. Brasil. Biol., *8:* 505–523.

——— 1950 Action of estrone and progesterone on nuclear volume (studied by applying the karyometric-statistical method). Biol. Bull., *99:* 112–119.

SWIFT, H. H. 1950 The desoxyribose nuclei acid content of animal nuclei. Physiol. Zool., *23:* 169–198.

NOTICE TO CONTRIBUTORS

THE JOURNAL OF CELLULAR AND COMPARATIVE PHYSIOLOGY, appearing bimonthly, is intended as a medium for the publication of papers which embody the results of original research of a quantitative or analytical nature in general and comparative physiology, including both their physical and chemical aspects. Short preliminary notices are not desired and papers will not be accepted for simultaneous publication or which have been previously published elsewhere. While not specifically excluding any particular branch of physiology, contributors should recognize that excellent journals already exist for publication in the field of experimental and physiological zoology, dealing particularly with genetics, growth, behavior, developmental mechanics, sex determination, and hormonal interrelationships, and also for pure mammalian functional physiology and the physical chemistry of non-living systems. Preference will be given to analyses of fundamental physiological phenomena whether the material is vertebrate or invertebrate, plant or animal. Since the journal is restricted, it is not possible to publish more than a limited number of papers which must be short and concise.

It is recognized that prompt publication is essential, and the aim will be to issue papers within three months of acceptance.

Manuscripts and drawings should be sent to the Managing Editor, DR. ARTHUR K. PARPART, Princeton University, Princeton, New Jersey.

The paper must be accompanied by an author's abstract **not to exceed 225 words in length,** which will appear on the advance abstract cards of the Bibliographic Service of The Wistar Institute in advance of complete publication. Nothing can be done with the manuscript until the abstract is received.

Manuscripts should be typewritten in double spacing on one side of paper 8½ × 11 inches, and should be packed flat — not rolled or folded. The original, not carbon, copy should be sent. The original drawings, not photographs of drawings, should accompany the manuscript. Authors should indicate on the manuscript the approximate position of text figures.

Manuscripts and drawings should be submitted in complete and finished form with the author's complete address. All drawings should be marked with the author's name. The Wistar Institute reserves the privilege of returning to the author for revision approved manuscript and illustrations which are not in proper finished form for the printer. **When the amount of tabular and illustrative material is judged to be excessive, or unusually expensive, authors may be requested to pay the excess cost.**

The tables, quotations (extracts of over five lines), and all other subsidiary matter usually set in type smaller than the text, should be typewritten on separate sheets and placed with the text in correct sequence. Footnotes should not be in with the text (reference numbers only), but typewritten continuously on separate sheets, and numbered consecutively. Explanations of figures should be treated in the same manner, and, like footnotes, should be put at the end of the text copy. **A condensed title for running page headlines, not to exceed thirty-five letters and spaces, should be given.**

Figures should be drawn for reproduction as line or halftone engravings, unless the author is prepared to defray the additional cost of a more expensive form of illustration. All colored plates are printed separately and cost extra. In grouping the drawings it should be borne in mind that, after the reduction has been made, text figures are not to exceed the dimensions of the printed matter on the page, 4¼ × 6¾ inches. Single plates may be 5 × 7½ inches, or less, and double plates (folded in the middle), 11½ × 7½ inches. Avoid placing figures across the fold, if possible.

Figures should be numbered from 1 up, beginning with the text figures and continuing through the plates. **The reduction desired should be clearly indicated on the margin of the drawing.**

All drawings intended for photographic reproduction either as line engravings (black-ink pen lines and dots) or halftone plates (wash and brush work) should be made on white or blue-white paper or bristol board — not on cream-white or yellow-tone. Photographs intended for halftone reproduction should be securely mounted with colorless paste — never with glue, which discolors the photograph.

Galley proofs and engraver's proofs of figures are sent to the author. All corrections should be clearly marked thereon.

The journal furnishes the author fifty reprints, with covers, of the paper gratis. Additional copies may be obtained according to rates which will be sent the author as soon as the manuscript has been examined at The Wistar Institute, after acceptance.

THIS NUMBER COMPLETES VOLUME 46

JOURNAL OF CELLULAR AND COMPARATIVE PHYSIOLOGY

Vol. 46 DECEMBER 1955 No. 3

CONTENTS

Wilfrid Rall. A statistical theory of monosynaptic input-output relations. Eight figures 373

Wilfrid Rall. Experimental monosynaptic input-output relations in the mammalian spinal cord 413

Werner Schmandt and William Sleator, Jr. Deviations from all-or-none behavior in a molluscan unstriated muscle: Decremental conduction and augmentation of action potentials. Ten figures 439

A. Cecil Taylor and Robert Gerstner. Tissue survival after exposure to low temperatures and the effectiveness of protective pretreatments. I. Evaluation by growth in tissue culture. Seven figures 477

Helen Harrington and Paul S. Lavik. A study of the phosphorus composition and P^{32} incorporation in irradiated lymphatic tissue 503

Paul B. Weisz. Chemical inhibition of regeneration in Stentor coeruleus. One figure 517

Seymour Gelfant and Jackson J. Clemmons. The influence of estrogen on nuclear volumes and chemical composition 529

PRESS OF
THE WISTAR INSTITUTE
OF ANATOMY AND BIOLOGY
PHILADELPHIA

Printed in the United States of America